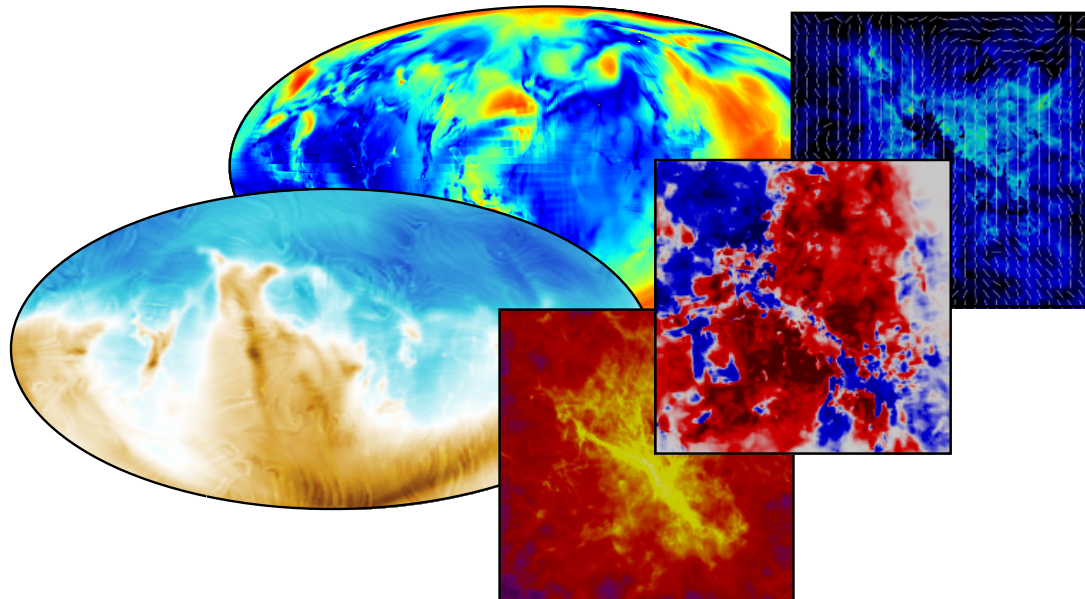


POLARIS

(Polarized Radiation Simulator)

User manual for POLARIS v4.03*



Stefan Reissl^{1,3} and Robert Brauer^{2,3}

¹Heidelberg University, Institute for Theoretical Physics,
Albert-Überle-Str. 2, 69120 Heidelberg, Germany
reissl@uni-heidelberg.de

²CEA Saclay, DRF / IRFU / Service d'Astrophysique,
Orme des Merisiers, 91191 Gif sur Yvette, France
robert.brauer@cea.fr

³University of Kiel, Institute of Theoretical Physics and Astrophysics,
Leibnizstraße 15, 24118 Kiel, Germany

*See Chapter 9 for the changelog of recent updates

Front page images

Oval panels: All-sky maps of intensity and degree of linear polarization of a post-processed SILCC simulation provided by Philipp Girichidis.

Squared panels: Degree of linear and circular polarization as well as line of sight magnetic field strength of a post-processed MHD collapse simulation provided by Daniel Seifried.



Figure: Institutes that were or are still involved in the development of POLARIS. From left to right: Institute of Theoretical Physics and Astrophysics at the CAU Kiel (ITAP), the Center for Astronomy at the University Heidelberg (ZAH), and the Institute of research into the fundamental laws of the Universe at CEA Saclay (IRFU).

1 Introduction

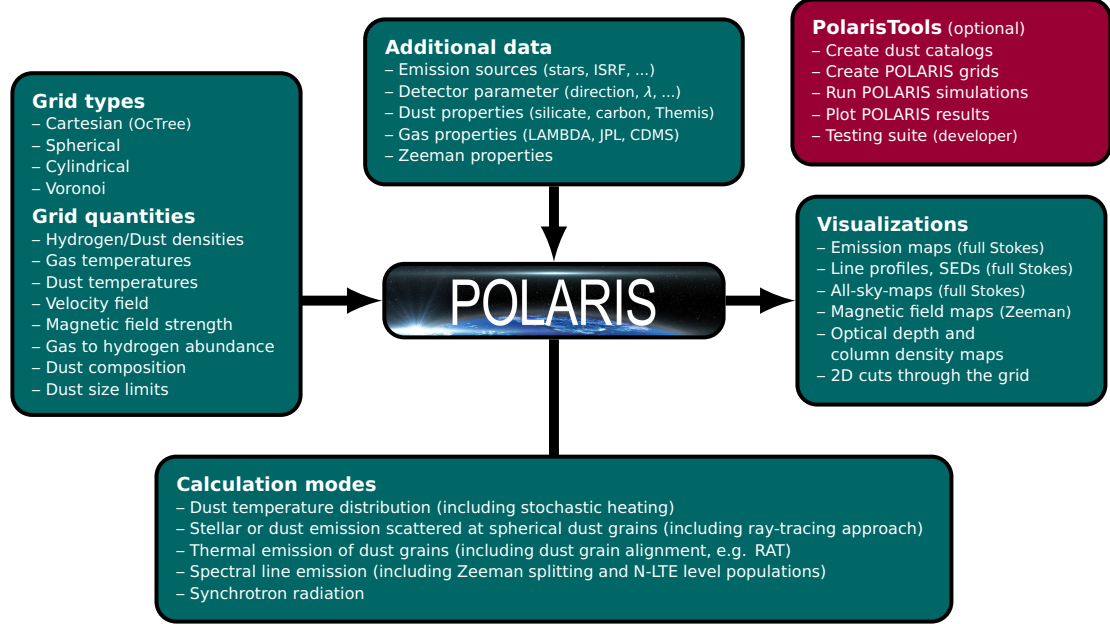
Table 1: *History of POLARIS and related publications*

Apr., 1999	• <i>Development:</i> MC3D in version 1 (basis for POLARIS, Wolf et al. 1999)
Feb., 2003	• <i>Development:</i> MC3D in version 2 (basis for POLARIS, Wolf 2003)
2010	• <i>Development:</i> MC3D in version 4 (basis for POLARIS)
2014	• <i>Development:</i> Start of POLARIS development
June, 2014	• <i>Publication:</i> Reissl et al. (2014)
July, 2015	• <i>Development:</i> Mol3D (basis for line RT in POLARIS, Ober et al. 2015)
Apr., 2016	• <i>Publication:</i> Brauer et al. (2016)
Sept., 2016	• <i>Publication:</i> Reissl et al. (2016)
2017	• <i>Development:</i> Final merge of MC3D and Mol3D into POLARIS
Sept., 2017	• First POLARIS workshop in Heidelberg (website)
May, 2017	• <i>Publication:</i> Brauer et al. (2017b)
July, 2017	• <i>Publication:</i> Reissl et al. (2017)
Nov., 2017	• <i>Publication:</i> Brauer et al. (2017a)
Mai, 2018	• <i>Publication:</i> Reissl et al. (2018)
Aug., 2018	• First public release of POLARIS

Legend: - *Cite this paper when using POLARIS in general*
- *Cite this paper when using the line transfer / Zeeman splitting*

POLARIS is a three dimensional (3D) Monte-Carlo (MC) continuum and line radiative transfer (RT) code. The aim of POLARIS is to provide a tool to investigate the observability of characteristic physical quantities of analytical astrophysical models as well as complex magneto-hydrodynamic (MHD) simulations. Hence, POLARIS is capable of simulating the direct and scattered thermal emission of dust grains, the direct and scattered emission of stars, the emission of spectral lines of various gas species, and synchrotron radiation of cosmic ray electrons and thermal electrons. Resulting from these simulations, POLARIS provides synthetic intensity and polarization maps, spectral energy distributions (SED) and line spectra. One of the key features of POLARIS is the consideration of the magnetic field. Via dust grain alignment and Zeeman splitting, POLARIS is capable of providing predictions for investigations of magnetic fields based on the dust and the gas phase. To achieve this, the code makes use of a full set of physical quantities as input to the simulate synthetic observational data (density, temperature, velocity, magnetic field, dust grain properties, spectroscopy databases, and different sources of radiation). This combination of features makes POLARIS a unique radiative transfer code with various applications not only related to magnetic fields. So far, POLARIS consists of the work of three PhD students (Stefan Reissl, Robert Brauer, Florian Ober) which were supervised by Sebastian Wolf at Kiel university. After their PhD, Stefan Reissl and Robert Brauer are still developing, improving, and using POLARIS in their positions as postdoctoral researchers. In Table 1, an overview of the history of POLARIS is shown. In addition, the table includes papers whose results were fully or partially obtained by POLARIS. Most of these studies needed the unique capabilities of POLARIS to obtain their results.

Figure 1.1: Illustration how POLARIS works and which kind of simulations can be performed.



Special thanks

Without the generous help of many people that give comments or find bugs, POLARIS would not be in its great shape. Therefore, Stefan and Robert want to say thank you to the following people:

- Robi Banerjee
- Robert Brunngräber
- Vincent Guillet
- Ralf Klessen
- Bastian Körtgen
- Florian Ober
- Eric Pellegrini
- Daniel Seifried
- Valeska Validivia
- Steffi Walch
- Sebastian Wolf

Thank You!

Copyright

The code is free of charge for any scientific purpose. This software is provided in the hope that it will be useful but without any warranty of ability or fitness of a particular purpose. We also reject any responsibility for incorrect result that may be result from this code. Any publication that makes use of the software package (completely or in part) must mention the name of the POLARIS code and cite the POLARIS paper(-s) as shown in Table 1.

Contents

1	Introduction	3
2	Installation	3
2.1	Installation (Linux, MacOS)	3
2.2	Installation (Windows)	5
3	Input files	7
3.1	The command file	7
3.2	Changed feature with respect to older versions	9
3.3	Grid files	9
3.3.1	Multiple dust compositions	10
3.3.2	Spherical grid	10
3.3.3	Cylindrical grid	14
3.3.4	Octree grid	15
3.3.5	Voronoi grid	17
3.3.6	Unit conversion	18
3.4	Dust properties	18
3.4.1	Dust cross sections	18
3.4.2	Scattering matrices	19
3.4.3	Dust refractive index	20
3.4.4	Heat capacities / Enthalpies	21
3.5	The gas species parameters	21
3.5.1	LAMDA molecular database	21
3.5.2	Zeeman parameters files	22
4	POLARIS pipeline	29
4.1	Photon propagation	29
4.1.1	The Stokes vector	29
4.1.2	General radiative transfer equation	30
4.1.3	Monte-Carlo (MC) photon transfer	31
4.1.4	MC noise estimation	32
4.1.5	Ray-tracing	32
4.2	Photon emitting sources	33
4.3	Optimization techniques	35
4.3.1	Sub-pixeling	35
4.3.2	Enforced first scattering	36
4.3.3	Peel-off technique	36
4.3.4	Wavelength range selection	37
4.4	Grid rotation	37
4.5	Detector parameters	38
4.6	Dust continuum radiative transfer	40
4.6.1	Phase functions	40
4.6.2	Dust heating	41
4.6.3	Grain alignment theories	42
4.6.4	The grain alignment radius a_{alg}	47
4.6.5	Dust Intensity and polarization maps	48
4.7	Line radiative transfer (LRT)	53
4.7.1	Level population approximations	55

4.7.2 LRT with Zeeman effect	56
4.8 Synchrotron RT	60
4.8.1 CR electrons	62
4.8.2 Thermal electrons	63
4.8.3 Synchrotron run with both electrons species	63
5 Output data	65
5.1 Output grids	65
5.2 Detector files	65
5.3 Gnuplot	71
5.4 AMIRA	75
6 Quickstart guide	77
6.0.1 Unpack the examples	77
6.0.2 Dust temperature distribution	77
6.0.3 Dust thermal emission	79
6.0.4 Dust thermal emission (with grain alignment)	79
6.0.5 Scattered stellar emission	79
6.0.6 Thermal emission and scattered stellar emission	79
6.0.7 Spectral line emission	79
6.0.8 Spectral line emission (with Zeeman splitting)	80
7 PolarisTools	81
7.1 Introduction	81
7.2 The command polaris-gen	82
7.3 The command polaris-run	82
7.4 The command polaris-plot	85
7.5 The command polaris-remote	93
7.6 The command polaris-extra	93
7.7 Available choices	96
7.8 Create your own project	101
7.8.1 Creating a model	101
7.8.2 Creating a gas species	101
7.8.3 Creating a dust component	101
7.8.4 Creating a detector	105
7.8.5 Creating a stellar radiation source	105
7.8.6 Creating a background radiation source	105
7.8.7 Creating a custom plot routine	105
7.8.8 Adding a server/cluster	112
7.8.9 Creating an external input	112
7.9 Quickstart guide	114
7.9.1 Create a grid	114
7.9.2 Dust temperature distribution	114
7.9.3 Dust thermal emission	114
7.9.4 Dust thermal emission (with grain alignment)	117
7.9.5 Scattered stellar emission	117
7.9.6 Thermal emission and scattered stellar emission	117
7.9.7 Spectral line emission	119
7.9.8 Spectral line emission (with Zeeman splitting)	119
8 Files and directories	121
9 Changelog	123
Index	124

2 Installation

2.1 Installation (Linux, MacOS)

Download

The POLARIS installation package can be downloaded from [\[here\]](#).

Requirements

The following packages are required for the installation:

- autoconf
- automake
- GNU Compiler Collection (gcc) with OpenMP support

(*Linux server/cluster user only*) Some linux servers have not a recent version of gcc with OpenMP support installed. However, most server/cluster systems offer the use of environment modules to update to a recent version of gcc or OpenMP. Information about the usage can be found [online](#).

(*Mac user only*) The installation of gcc with OpenMP support can be done by using Homebrew and entering the following command:

```
brew install gcc --without-multilib
```

The then installed gcc compiler can usually be found as gcc-X, where X is the version number. To use this compiler for the POLARIS installation on your Mac, the alias function can be used as follows:

```
alias gcc=gcc-X
```

Installation

To install POLARIS on your computer, open a terminal/console and go into the directory where you downloaded '[polaris.run](#)'. Then, by entering the following command, POLARIS will be installed in the current directory:

```
./polaris.run
```

If the package is not executable, enter the following command in advance:

```
chmod +x polaris.run
```

The POLARIS package will extract itself into a newly created [polaris/](#) directory and the terminal messages of the installation should look like Listing 2.1. POLARIS and PolarisTools (if chosen) can now be executed from any newly opened terminal/console. However, to use it in already open terminals/consoles, execute the following command to update the environmental paths:

```
source ~/bashrc
```

(*PolarisTools only*) If Python needs to be installed by the install script, the subsequent installation might quit with an error. In this case, execute the source command as described above and execute the install script again by entering the following command:

```
./polaris/install_polaris.sh
```

Listing 2.1: Terminal messages of the POLARIS installation.

```
Creating directory polaris
Verifying archive integrity... 100% All good.
Uncompressing the radiative transfer code POLARIS 100%
--- Installer for the radiative transfer code POLARIS ---
-- Additional features --
Do you want to enable PolarisTools [y/N]? (Python scripts collection)
y
-- Install required libraries for fits support --
Install cfitsio
- Configuring cfitsio [done]
- Compiling cfitsio [done]
Install CCfits
- Configuring CCfits [done]
- Compiling CCfits [done]
- Updating bashrc [done]
-- Install POLARIS --
- Configuring POLARIS [done]
- Compiling POLARIS [done]
- Installing POLARIS [done]
- Updating bashrc [done]
-- Install PolarisTools --
Checking for Python installation [found]
Looking for required Python packages
- Required python package pandas [found]
- Required python package numpy [found]
- Required python package scipy [found]
- Required python package matplotlib [found]
- Required python package astropy [found]
- Required python package os [found]
- Required python package array [found]
- Required python package struct [found]
- Required python package argparse [found]
Creating links to Python packages [done]
Setting up PolarisTools [done]
-> Installation of POLARIS [done]
```

→ If you want perform your first simulations as quickly as possible, go directly to Sect. 6 (using command files) or Sect. 7.9 (using PolarisTools).

→ If you already worked with a previous version of POLARIS by using command files, go directly to Sect. 3.2 to see how to adapt your command files to the current version of POLARIS.

Options of the installation script

The installation script '`install_polaris.sh`' in the `polaris/` directory can be used for the following purposes:

- **Recompiling the code**

Enter the following command to recompile the POLARIS source code (and PolarisTools if installed):

```
./install_polaris.sh -u
```

This is required to take advantage of any changes that are made to the source files.

- **Change the compiling mode**

Enter one of the following commands to recompile the POLARIS source code in release (-r, default) or debug (-d) mode:

```
./install_polaris.sh -r  
./install_polaris.sh -d
```

As an example, the debug mode is required to properly use programs like valgrind.

- **Deleting the POLARIS installation**

Enter the following command to properly remove POLARIS from your PC:

```
./install_polaris.sh -D
```

- **Overview of available options**

Enter the following command to see an overview of all available options:

```
./install_polaris.sh -h
```

2.2 Installation (Windows)

→ An installer to use POLARIS with Windows is currently under development.

3 Input files

3.1 The command file

A simulation with POLARIS can be executed by providing the path to a command file as a single argument:

```
polaris PATH/TO/THE/command_file
```

Predefined commands in a pseudo XML style are implemented in the code and allow the user to create a script with sequences of simulations. The structure of the command file is intended to be simple and suggestive. A complete list of commands is provided in Tables 3.4 to 3.7 at the end of this section.

The POLARIS parser does not distinguish between tab and whitespace nor does it care about the number of tabs and whitespaces between each command. Lines marked with a # or a ! are ignored and can be used as comments. The command file consists of an arbitrary number of tasks. Each task block has the following form:

```
<task> 0/1  
  # commands ...  
</task>
```

The number 1 is optional. Task blocks with a 0 will be skipped completely. Commands that are common to all tasks can be defined in an extra block in the beginning as the first block of the command file with:

```
<common> 0/1  
  # commands ...  
</common>
```

When identical commands appear in both the common-block and in a task-block the command written in the task-block has priority. The order of commands inside each task block is mostly irrelevant. Exceptions are gas species (see Sect. 4.7.2), background sources (see Sect. 4.2), and detectors (see Sect. 4.5) which are numbered in the order of theirs appearance. Each task-block needs a command that defines the pipeline ID (simulation type). A detailed description of each simulation type is provided in Chapt. 4.

A command file example to perform the calculation of the dust temperature can be found in Listing 3.1

In this example, the command CMD_TEMP runs a simulation for heating the dust by considering different photon emitting sources (see Sect. 4.2). In this case, a single star and the interstellar radiation field (ISRF) are considered as sources. The ISRF source requires an external file for the spectral energy distribution (SED). In contrast to dust polarization and emission, the LRT (see Sect. 4.7) and the synchrotron runs do not require a dust model (see Sect. 4.8).

A dust model consists of a arbitrary number of grain material, mass fraction, size distribution, and size ranges. In the above example the dust model is defined in the common block. In this particular case a dust grain model mixture of 62.5% silicate and 37.5% graphite is used with an size distribution of $n_d(a) \propto a^{-3.5}$. The values 0.005×10^{-6} and 0.25×10^{-6} are the minimal and maximal dust grain radii in meters. The available grain size range can be found in the dust parameters file (see Sect. 3.4). With <path_grid>, the path to the input grid is defined. Each simulation of a POLARIS pipeline requires a grid with a set of physical input parameters in a predefined geometry. The units of the grid quantities need to be in SI units or in cgs units, if <path_grid_cgs> is used. The creation of such a grid is described in Sect 3.3 in greater detail. With <path_out>, the path to the resulting output files is defined.

POLARIS can plot the input and output 3D distributions of the physical parameters of a particular grid as gnuplot files. The next optional lines define the number of data points and vectors as well as the step for the grid lines to be plotted. Additionally, the values of the xy-, xz-, and yz - midplane files can be written as fits files in a regular raster.

Listing 3.1: Example command file.

```
<common>
  #parameters of the optical properties of the dust
  <dust_component> "PATH/TO/POLARIS/input/dust/silicate_oblake.dat" 0.625 -3.5 0.005e-6
    ↪ 0.25e-6
  <dust_component> "PATH/TO/POLARIS/input/dust/graphite_oblake.dat" 0.375 -3.5 0.005e-6
    ↪ 0.25e-6
</common>

<task> 1
  #pipeline ID for dust heating
  <cmd> CMD_TEMP

  #A star as radiation source
  <source_star nr_photons = "1e6"> 1.15e2 4.16e2 1.8e1 7 9e3

  #ISRF as radiation source
  <source_isrf nr_photons = "500000"> "PATH/TO/POLARIS/input/
    ↪ interstellar_radiation_field.dat"

  #path of the input grid file
  <path_grid> "PATH/TO/YOUR/grid.dat"

  #parameters files for all output data
  <path_out> "PATH/WHERE/THE/RESULTS/SHOULD/BE/SAVED/"

  #Nr. of gnuplot points and maximal grid level to be plotted
  <nr_gnu_points> 4000 # optional
  <nr_gnu_vectors> 4000 # optional

  <max_lines> 3 # optional

  #Nr. of bins of the input and output mid-plane plots
  <write_out_midplanes> 256 # optional

  #Nr. of threads used for parallel computing
  <nr_threads> 8

  #conversion factor from cgs in SI units
  <conv_dens> 0.01 # optional

  #dust to gas ratio
  <mass_fraction> 0.01 # optional
</task>
```

Hence, the command `<write_out_midplanes>` defines the resolution of the mid-plane files with pre-defined number of bins (e.g. 256). In POLARIS the problem of radiative transfer is solved in a parallelized way using the OpenMP library. The number of processors can be defined with the command `<nr_threads>`. POLARIS works internally strictly in SI units for all input parameters. Physical quantities predefined in the grid need possibly to be converted (see Sect. 3.3.6 for details). With `<conv_dens> 0.01`, the grid density is converted from cgs in SI. Finally, the dust-to-gas mass ratio is defined by `<mass_fraction>`.

This sample script is just a general overview. A detailed description of the manifold features of POLARIS and the corresponding commands to control them is provided in the following sections.

HINTS:

- No extra directory needs to be created in advance. POLARIS creates automatically all the necessary directories defined by the output path.
- All paths have to be written in quotation marks.

3.2 Changed feature with respect to older versions

The version 4.00 is the first public release of the POLARIS code. In order to keep consistency we renamed some of the commands. However, people used previous versions for their projects and publications (versions less than 4.00). Hence, we give a short list of changed commands in Tab. 3.1.

Table 3.1: List of commands that changed compared to previous versions

previously	current version
CMD_RAYTRACING	CMD_DUST_EMISSION
CMD_MCPOL	CMD_DUST_SCATTERING
CMD_LINETRANSFER	CMD_LINE_EMISSION
<code><plot_inp_midplanes></code>	no longer exists
<code><plot_out_midplanes></code>	no longer exists
all of the detector commands	see Sect. 4.5
<code><gas_species vel_channels = ></code>	max_vel and vel_channels moved to detector
wavelengths & grain sizes	moved from indices to physical values in SI

3.3 Grid files

In POLARIS RT simulations can be performed with four different grid geometries so far. The available grid types are spherical, cylindrical, octree, and Voronoi. All the grids have in common that they start with a standardized header followed by a grid specific data section. All quantities are stored in a binary format.

The grid type itself is characterized by ID_{grid} (unsigned short, 2 bytes) which is the very first number in each grid file is shown in Table 3.2. After the grid ID_{grid} follows a number N_{phys} (unsigned short, 2 bytes) that defines the amount of physical quantities for each grid cell and a list of IDs (unsigned short, 2 bytes) to identify each quantity (see Tab 3.3). With exception of n_g/ρ_g , n_d/ρ_d , T_d , and n_{mol} all identifiers can only appear once in the header. POLARIS RT simulations require at least a gas density n_g/ρ_g as physical quantity in each grid cell. All other quantities are optional and depend on the kind of chosen simulation pipeline (see Chapt. 4). Instead of number densities n , mass densities ρ of the gas and dust can be defined as well. However, a grid cannot be used, if densities of both units are defined.

Table 3.2: IDs for the implemented POLARIS grid types.

type	octree	spherical	cylindrical	voronoi
ID _{grid}	20	30	40	50

3.3.1 Multiple dust compositions

There are two different methods to define the distribution of multiple dust compositions inside of the grid. Either the dust mixture index ID_{dust} is set for each grid cell or multiple dust density distributions (or gas densities via gas-to-dust mass ratio) are defined. With the first method, the radiative transfer is performed by using in each cell the dust composition related to the set ID_{dust} (see 4.6.5 for defining multiple dust compositions). This is the suggested method for grids based on MHD/HD simulations, since they usually are only supporting one density distribution and adding an additional value to each cell is easily realized. A more sophisticated approach is the usage of multiple density distributions (n_d/ρ_d or n_g/ρ_g). For this method, the user needs to define as much dust compositions as there are density distributions. With this, the radiative transfer is performed by using in each cell a mixture of the dust compositions that depends on the ratio between all density distributions. This method is well suited for grids based on analytical models since multiple density distributions can easily be created analytically.

HINTS:

- If you want a specific cell to be skipped in a RT simulation set its density to zero.
- POLARIS shifts the center of the grid to be in the center of the external coordinate system. The coordinates of the radiating sources (see Sect. 4.2) have possibly to be adapted accordingly!

3.3.2 Spherical grid

After defining the header, the spherical grid can be defined by an additional sequence of 8 numbers R_{\min} , R_{\max} , N_r , N_φ , N_θ , f_r , f_φ , f_θ . Here, the first two, R_{\min} and R_{\max} , respectively, define the inner and outer radius of the sphere followed by the number of cells in r-direction N_r , φ -direction N_φ , and θ -direction N_θ , respectively. The boundary of the grid is a sphere with a radius of R_{\max} . The shape parameter f_r , f_φ , and f_θ determine the distribution of steps along the r-direction and the ϑ -direction with:

Radial direction

- $f_r = 0$
The header has to be followed by $N_r - 1$ values (double, 8 bytes) that define the location of each i -th radial cell border with $r_2 < \dots < r_{i-1} < r_i < r_{i+1} < \dots < r_{N_r}$ whereas $r_1 = R_{\min}$ and $r_{N_r+1} = R_{\max}$, respectively.
- $f_r < 0$
The cell borders along the r-direction are equally distributed to create N_r cells.
- $f_r = 1$
The i -th cell border in the r-direction is calculated according to:

$$r_i = R_{\min} + (R_{\max} - R_{\min}) \sin\left(\frac{i\pi}{N_r}\right). \quad (3.1)$$

- $f_r > 1$
The i -th cell border in the r-direction is calculated according to:

$$r_i = R_{\max} + \frac{(f_r^i - 1)(R_{\max} - R_{\min})}{f_r^{N_r} - 1}. \quad (3.2)$$

Table 3.3: Identifier of the physical quantities in a POLARIS grid. (not yet fully supported or anticipated for a future version of POLARIS; only used internally and not designed to be set by user)

physical quantity	description	ID
n_g [m^{-3}]	gas number density	0
n_d [m^{-3}]	dust number density	1
T_d [K]	dust temperature	2
T_g [K]	gas temperature	3
B_x [T]	magnetic field in x-direction	4
B_y [T]	magnetic field in y-direction	5
B_z [T]	magnetic field in z-direction	6
$v_{g,x}$ [m/s]	gas velocity in x-direction	7
$v_{g,y}$ [m/s]	gas velocity in y-direction	8
$v_{g,z}$ [m/s]	gas velocity in z-direction	9
p_x [$\text{kg m}^{-2} \text{s}^{-1}$]	radiative pressure in x-direction	10
p_y [$\text{kg m}^{-2} \text{s}^{-1}$]	radiative pressure in y-direction	11
p_z [$\text{kg m}^{-2} \text{s}^{-1}$]	radiative pressure in z-direction	12
a_{alg} [m]	dust grain alignment radius	13
a_{\min} [m]	minimal dust grain radius	14
a_{\max} [m]	maximal dust grain radius	15
q	exponent of the grain size distribution	16
n_{mol}	number density of a molecular species	17
v_{turb} [m/s]	turbulent gas velocity	18
PDA	PDA photon count	19
ID_O	ID for the opiate database	20
ID_{dust}	ID for an individual dust component	21
n_{th} [m^{-3}]	number density of thermal electrons	22
T_e [K]	temperature thermal electrons	23
n_{CR} [m^{-3}]	number density of cosmic ray electrons	24
γ_{\min}	minimal Lorentz-factor	25
γ_{\max}	maximal Lorentz-factor	26
p	power-law index of cosmic ray electrons	27
ρ_g [kg m^{-3}]	gas mass density	28
ρ_d [kg m^{-3}]*	dust mass density	29
E_x [W/m/m^2]	radiation field density in x-direction	30
E_y [W/m/m^2]	radiation field density in y-direction	31
E_z [W/m/m^2]	radiation field density in z-direction	32
E [W/m/m^2]	total radiation field density	33

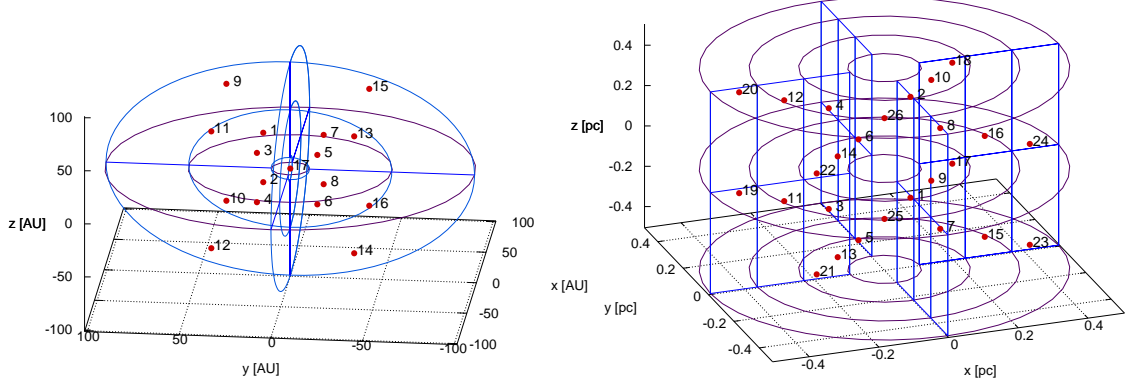


Figure 3.1: Exemplary representations of the POLARIS supported spherical grid (left) and cylindrical grid (right). The numbers represent the order of cells characteristic for each type of grid.

Phi direction

- $f_\varphi = 0$
The header has to be followed by $N_\varphi - 1$ values (double, 8 bytes) that define the location of each i -th phi cell border with $\varphi_2 < \dots < \varphi_{i-1} < \varphi_i < \varphi_{i+1} < \dots < \varphi_{N_\varphi}$ whereas $\varphi_1 = 0$ and $\varphi_{N_\varphi+1} = 2\pi$, respectively.
- $f_\varphi \neq 0$
The cell borders along the φ -direction are equally distributed to create N_φ cells.

Theta direction

- $f_\theta = 0$
The header has to be followed by $N_\theta - 1$ values (double, 8 bytes) that define the location of each i -th theta cell border with $\theta_2 < \dots < \theta_{i-1} < \theta_i < \theta_{i+1} < \dots < \theta_{N_\theta}$ whereas $\theta_1 = 0$ and $r_{N_\theta+1} = \pi$, respectively.
- $f_\theta < 0$
The cell borders along the θ -direction are equally distributed to create N_θ cells.
- $f_\theta = 1$
The i -th cell border in the θ -direction is calculated according to:

$$\begin{cases} \theta_i = \frac{\pi}{2} \sin\left(\frac{i\pi}{N_\theta-1}\right), & \text{if } i < \frac{N_\theta}{2} \\ \theta_i = \frac{\pi}{2} \left(1 - \sin\left(\frac{i\pi}{N_\theta-1}\right)\right), & \text{if } i \geq \frac{N_\theta}{2} \end{cases} \quad (3.3)$$

- $f_\theta > 1$

The i -th cell border in the θ -direction is calculated according to:

$$\left\{ \begin{array}{ll} \theta_i = \frac{\pi}{2} - \frac{(f_{\theta} \frac{N_{\theta}}{2} - i) \frac{\pi}{2}}{f_{\theta} \frac{N_{\theta}}{2} - 1}, & \text{if } i < \frac{N_{\theta}}{2} \\ \theta_i = \frac{\pi}{2} + \frac{(f_{\theta} \frac{N_{\theta}}{2} - i - 1) \frac{\pi}{2}}{f_{\theta} \frac{N_{\theta}}{2} - 1}, & \text{if } i \geq \frac{N_{\theta}}{2} \end{array} \right. \quad (3.4)$$

If multiple shape parameters f are zero, the lists of cell borders have to be in the same order as the shape parameters itself. As for the order of cells the grid runs over θ , φ , and r . Hence the position of each cell within the grid is defined by its order of appearance in the grid file. The cell at the center is the last cell in the list leading to a total amount of $N_c = N_r \times N_{\varphi} \times N_{\theta} + 1$ cells. This gives for the spherical grid file the following form:

```
IDgrid (unsigned short, 2 bytes, 30 = spherical)
Nphys (unsigned short, 2 bytes, maximal 21 possible physical quantities in each cell)
IDng ... IDp (unsigned short, 2 bytes, optionally and in arbitrary order)
Rmin Rmax (double, 8 bytes)
Nr Nphi Ntheta (unsigned short, 2 bytes)
fr fphi ftheta (double, 8 bytes)
ng ... p (double, 8 bytes, in the same order as in the header, 1st cell)
...
ng ... p (double, 8 bytes, last outer cell,  $N_c - 1 - th$  cell)
ng ... p (double, 8 bytes, center cell,  $N_c - th$  cell)
```

The spherical grid geometry as shown in Fig. 3.1 on the left hand side would result from the following sequence of values:

```
30 4 0 7 8 9
1.496e+11 1.496e+12
2 4 2
1.005 -1 -1
1.72e6 -1.647e+04 1.647e+04 0.0
1.72e6 -1.647e+04 1.647e+04 0.0
1.72e6 -1.647e+04 -1.647e+04 0.0
1.72e6 -1.647e+04 -1.647e+04 0.0
1.72e6 1.647e+04 -1.647e+04 0.0
1.72e6 1.647e+04 -1.647e+04 0.0
1.72e6 1.647e+04 1.647e+04 0.0
1.72e6 1.647e+04 1.647e+04 0.0
1.72e6 -3.897e+04 3.897e+04 0.0
1.72e6 -3.897e+04 3.897e+04 0.0
1.72e6 -3.897e+04 -3.897e+04 0.0
1.72e6 -3.897e+04 -3.897e+04 0.0
1.72e6 3.897e+04 -3.897e+04 0.0
1.72e6 3.897e+04 -3.897e+04 0.0
1.72e6 3.897e+04 3.897e+04 0.0
1.72e6 3.897e+04 3.897e+04 0.0
1.72e6 0.0 0.0 0.0
```

This example is a spherical grid containing four physical quantities, a constant gas number density of $n_g = 1.72 \times 10^6 \text{ m}^{-3}$ and a toroidal gas velocity component ($v_{g,x}$, $v_{g,y}$, and $v_{g,z}$) rotation around the z-axis. The geometry is defined by an inner radius of $R_{\min} = 10 \text{ AU}$ and an outer radius of $R_{\max} = 100 \text{ AU}$ and a number of cells of $N_r = 2$, $N_{\varphi} = 4$, $N_{\theta} = 2$ cells in r -, φ -, and θ -direction with the shape parameters $f_r = 1.005$, $f_{\varphi} = -1$, and $f_{\theta} = -1$.

3.3.3 Cylindrical grid

The structure of the cylindrical grid is quite similar to the spherical one. The header is followed by R_{\min} , R_{\max} , Z_{\max} , N_r , N_φ , N_z , f_r , f_φ , f_z . For the cylindrical grid R_{\min} and R_{\max} define the inner and outer radius followed by the number of cells in r-direction N_r , φ -direction N_φ , and z-direction N_z , respectively. The boundary of the grid is a cylinder with a radius of R_{\max} and the z-direction extends from $-Z_{\max}$ to Z_{\max} . The factors f_r , f_φ , and f_z serve the same function as introduced in Sect. 3.3.2 with the following modifications:

Radial direction

- The options of the radial direction of the spherical grid

Phi direction

- The options of the φ -direction of the spherical grid
- $f_\varphi = -1$
The header has to be followed by N_r values (double, 8 bytes) that define the number of phi cells $N_{\varphi,i}$ in the radial ring i . The value N_φ will be ignored in this case.

Z direction

- The options of the θ -direction of the spherical grid (replace θ with z)
- $f_z = -1$
The header has to be followed by N_r values (double, 8 bytes) that define the vertical width of each cylindrical cell $d_{z,i}$ in the radial ring i . After distributing N_z cells centered around the midplane, the leftover space to Z_{\max} will be ignored (set to be empty).

The grid cells run over z , φ , and r . The innermost cylinder cells start at $-Z_{\max}$ and run to Z_{\max} resulting in a total amount of $N_c = N_z(N_r \times N_\varphi + 1)$ cells. Hence the position of each cell within the grid is defined by its order of appearance in the grid file. The quantities in the cylindrical grid file appear in the following order:

ID_{grid} (unsigned short, 2 bytes, 40 = cylindrical)
 N_{phys} (unsigned short, 2 bytes, maximal 21 possible physical quantities in each cell)
 $ID_{\text{ng}} \dots ID_p$ (unsigned short, 2 bytes, optionally and in arbitrary order)
 $R_{\min} R_{\max} Z_{\max}$ (double, 8 bytes)
 $N_r N_\varphi N_z$ (8 bytes)
 $f_r f_\varphi f_z$ (double, 8 bytes)
 $n_g \dots v_{d,z}$ (double, 8 bytes, in the same order as in the header, 1st cell)
...
 $n_g \dots v_{d,z}$ (double, 8 bytes, last outer cell)
 $n_g \dots v_{d,z}$ (double, 8 bytes, first center cell at $-Z_{\max}$)
 $n_g \dots v_{d,z}$ (double, 8 bytes, last center cell at Z_{\max} , $N_c - th$ cell)

The following sequence of values grid is as shown in Fig. 3.1 on the right hand side:

```

40 4 0 4 5 6
3.086E+018 1.543E+019
3 4 2
1.001 -2 -2
7.36e2 0.0e+0 0.0e+0 1.0e-7

```

```
7.36e2 0.0e+0 0.0e+0 1.0e-7
```

This is an example of a cylindrical grid that contains four physical quantities, a constant gas number density of $n_g = 7.36 \times 10^2 \text{ m}^{-3}$ and a magnetic field with a constant magnitude of $1.0 \times 10^{-7} \text{ T}$ in the z-direction. The geometry is defined by an inner radius of $R_{\min} = 0.1 \text{ pc}$ and an outer radius of $R_{\max} = 0.5 \text{ pc}$. The number of cells are $N_r = 3$, $N_\varphi = 4$, $N_z = 2$ cells in r-, φ - and z-direction with the shape parameters $f_r = 1.005$, $f_\varphi = -2$ and $f_z = -2$.

3.3.4 Octree grid

For the octree grid one number (double, 8 bytes) follows after the header defining the dimension (l_{\max}) of the entire cube. Finally, the grid refinement has to be represented by a sequence of numbers where the first number (unsigned short, 2 bytes) defines whether the cell is a leaf (1) or a branch (0). The second number (unsigned short, 2 bytes) is the grid level. In case of a leaf it follows a data section with numbers (4 bytes) which must match the exact order of identifies of the physical quantities defined in the header. The boundary of the grid is a cube with a side length of l_{\max} . Hence the position of each cell within the grid is defined by its order of appearance in the grid file. In general the octree data format has the following form:

```
IDgrid (unsigned short, 2 bytes, 20 = octree)
Nphys (unsigned short, 2 bytes, maximal 21 possible physical quantities in each cell)
IDng ... IDP (unsigned short, 2 bytes, optionally and in arbitrary order)
lmax (double, 8 bytes, dimension of the cube at level 0)
0/1 (unsigned short, 2 bytes, 0 = branch, 1 = leaf)/(unsigned short, 2 bytes, level 0 = entire cube)
ng ... vd,z (float, 4 bytes, in the same order as in the header)
...
0/1 (unsigned short, 2 bytes) level (unsigned short, 2 bytes)
ng ... vd,z (float, 4 bytes, last cell)
```

The grid refinement as shown in Fig. 3.2 would result from following sequence of values:

```
20 2 0 3
1.892e16
0 0
1 1 1.43e5 25
1 0
2 1 5.56e7 31
2 1 5.56e7 31
2 1 5.56e7 31
2 1 5.56e7 31
```

3 Input files

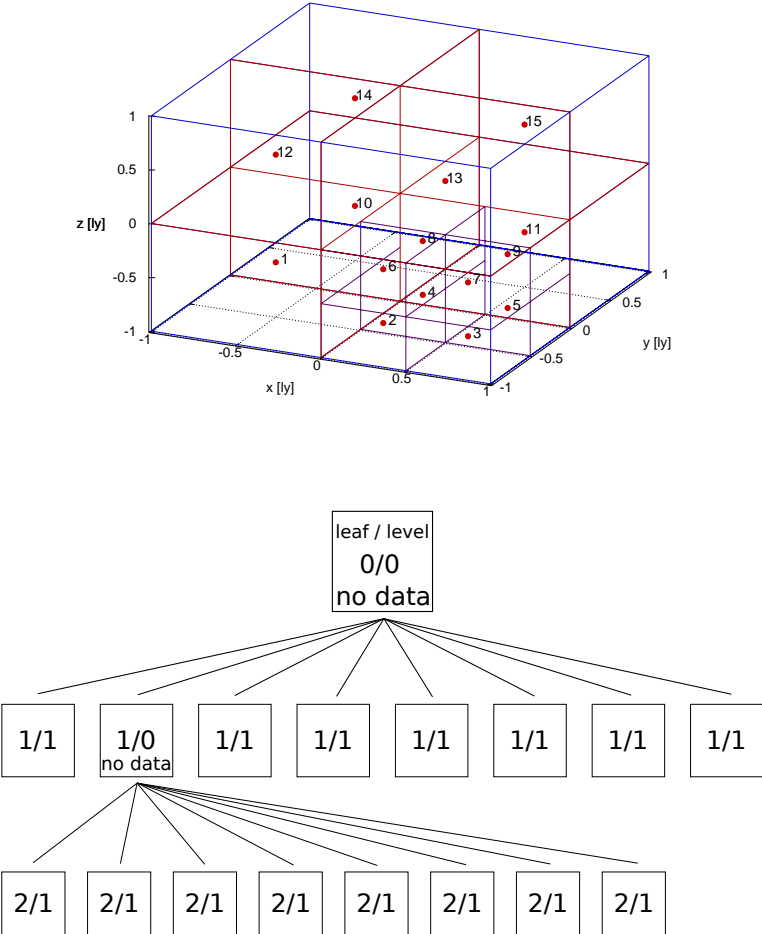


Figure 3.2: Exemplary octree grid (top) and its representation as graph (bottom) where level 0 represent the entire cube. The numbers represent the order of cells defined by their position within the octree graph.

```

2 1 5.56e7 31
2 1 5.56e7 31
2 1 5.56e7 31
2 1 5.56e7 31
1 1 1.43e5 25

```

This is an example octree grid with a maximal grid refinement of two and a side length of 2 ly. It contains mostly a constant gas number density and dust temperature of $n_g = 1.43 \times 10^5 \text{ m}^{-3}$ and $T_g =$

25 K, respectively, with a level one refinement. A smaller region has a level two refinement with $n_g = 5.56 \times 10^7 \text{ m}^{-3}$ and $T_g = 31 \text{ K}$.

3.3.5 Voronoi grid

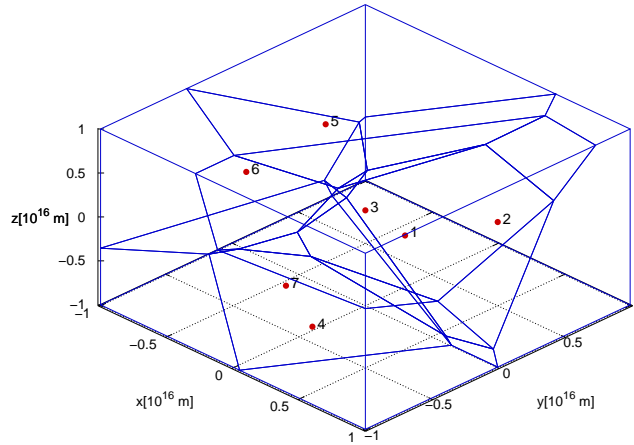


Figure 3.3: Exemplary voronoi grid. The numbers represent the order of cells defined by their appearance.

A Voronoi grid is unstructured and can easily imagined as a large number of connected soap bubbles. However, the order in which the cells are written to the grid files is not arbitrary. Each Voronoi cell knows the IDs of its neighboring cells. These IDs are identical with the order of appearance of the cells in the grid file. After the header follows an additional sequence of two numbers (double, 8 bytes), the number of cells N_c in the grid and the side length l_{\max} of the cube. The boundary of the grid is a cube with a side length of l_{\max} . Hence, the position of each cell within the grid is defined by the three numbers of its x -, y -, and z -coordinates. After the coordinates follows the volume of the cell and the list of physical parameters as defined in the header. The next number gives the number of neighbors N_{rmne} followed by the IDs of the neighboring cells. If the ID is negative then the ID stands for a wall of the surrounding cube ($1=x$, $2=-x$, $3=y$, $4=-y$, $5=z$, and $6=-z$ wall).

```
IDgrid (unsigned short, 2 bytes, 50 = voronoi)
Nphys (unsigned short, 2 bytes, maximal 21 possible physical quantities in each cell)
IDng ... IDp (unsigned short, 2 bytes, optionally and in arbitrary order)
Nc lmax (double, 8 bytes)
x y z (float, 4 bytes) volume (double, 8 bytes) ng ... p (float, 4 bytes) Nne 1 ... Nne (integer, 4 bytes, first cell)
x y z (float, 4 bytes) volume (double, 8 bytes) ng ... p (float, 4 bytes) Nne 1 ... Nne (integer, 4 bytes)
...
x y z (float, 4 bytes) volume (double, 8 bytes) ng ... p (float, 4 bytes) Nne 1 ... Nne (integer, 4 bytes, last cell)
```

The grid refinement as shown in Fig. 3.3 would result in the following sequence of values:

```
50 3 0 2 3
7 2.0e16
```

3 Input files

```

0.4e16 -0.8e16 -0.4e16 0.72e48    1.1e5 10 20 8 -5 -2 -3 2 0 1 5 6
-0.1e16 -0.5e16 -0.5e16 1.26e48    1.1e5 10 20 8 1 5 0 -5 -1 3 -3 2
0.4e16 0.6e16 -0.2e16 1.86e48    1.1e5 10 20 11 3 0 6 -5 -1 -4 -2 2-6 4 5
-0.6e16 -0.3e16 0.3e16 1.15e48    1.1e5 10 20 9 0 4 2 1 6 -1 -6 -3 3
0.3e16 0.0e16 0.0e16 0.70e48    1.1e5 10 20 7 3 -2 2 6 1 5 4
0.3e16 -0.3e16 0.5e16 1.17e48    1.1e5 10 20 9 3 5 6 4 -6 1 -2 0 -3
-0.4e16 0.1e16 0.7e16 1.13e48    1.1e5 10 20 7 -6 -4 -1 1 5 2 0

```

This is a example of an Voronoi grid with seven cells. The content is a constant gas number density of $n_g = 1.1 \times 10^5 \text{ m}^{-3}$, a dust temperature of $T_d = 10 \text{ K}$, and a gas temperature of $T_g = 20 \text{ K}$.

3.3.6 Unit conversion

POLARIS works internally strictly in SI units. In order to convert the physical parameters of the input grids, POLARIS provides a number of commands for the command file. The command `<conv_dens>` converts the densities of the input grid into number densities [m^{-3}]. Lengths and velocities can be converted in [m] and [m/s] by `<conv_len>` and `<conv_vel>`, respectively. The magnetic field can be converted into Tesla with the command `<conv_mag>`. Finally, the command `<mass_fraction>` defines the ratio of dust mass to gas mass ratio in order to calculate the dust density distribution, with the help of the average molecular wight defined by the command `<mu>`, if the dust density is not provided. The following example shows the conversion factors to convert cgs to SI:

```

# cgs into SI
<conv_dens> 1000 # cm^3 in m^3
<mu> 2.0
<conv_len> 0.01 # cm in m
<conv_mag> 1e-4 # G in T
<conv_vel> 0.01 # cm/s in m/s
<mass_fraction> 0.01 # dust mass is 1% of the total gas mass

```

HINTS:

- If a conversion of units was applied, the parameters of any newly written grid will be stored in SI. You have to consider this in the follow-up calculations accordingly.
- Instead of defining the conversion factors for cgs to SI, the command `<path_grid_cgs>` can be used to read a grid that uses strictly cgs units.

3.4 Dust properties

3.4.1 Dust cross sections

Some of the POLARIS RT simulations are dependent on the optical properties of dust grains. Such properties can individually be pre-calculated (e.g. MIEX [Wolf 2006](#) or DDSCAT [Draine & Flatau 2013](#)) and tabulated. The choice of grain size, dust materials, and size distribution is crucial in the simulation of synthetic observations. Hence, POLARIS can handle an arbitrary number of tabulated dust grain properties and creates a dust mixture dependent on user defined parameters. The input tables are plain text and follow the same commenting rules as the input command file (see Sect. 3.1). In contrast to the command files, here, the order of all values matters. Each dust parameters file starts with an arbitrary string describing the dust grain material. In the following line the number of dust grain sizes N_a , the number of wavelength N_λ , the number of inclination angles N_i , the aspect ratio s of the dust grains, the density ρ_{dust} [kg/m^3] of the dust grain material itself, the sublimation temperature T_{Sub} [K] of the dust grain material, a geometrical factor δ_{RAT} relevant for RAT alignment, and finally a number that defines the alignment behavior (0 = not aligned, 1 = aligned according to chosen alignment

mechanism) are listed. The next two lines are the exact dust grain sizes and wavelength, respectively, corresponding to the numbers of N_a and N_λ . Next, it follows a table running over wavelength and dust grain radii a . The dust grain radius a is defined to be the grain radius of a sphere of equivalent volume. This table contains the efficiencies of extinction ($Q_{ext,\perp}$, $Q_{ext,\parallel}$), scattering ($Q_{sca,\perp}$, $Q_{sca,\parallel}$), and absorption ($Q_{abs,\perp}$, $Q_{abs,\parallel}$) for light polarized perpendicular and parallel with respect to the grains minor symmetry axis. Furthermore, the table contains the efficiencies $Q_{trq,1}$ - Q_{trq,N_i} for RAT alignment (see Sect. 4.6.3) as well as the Henyey-Greenstein scattering parameters g_1 - g_{N_i} (see Sect. 4.6.1) one for each inclination angle. Later, the different cross sections can be calculated by POLARIS with $C = \pi a^2 Q$. In the general form the quantities in a dust parameters file have to be arranged as follows:

```

description string
#radii wavel. inclinations aspect_ratio density sub_temp delta align
Na Nλ N; s ρdust[kg/m3] Tsub[K] δRAT 0/1
#grain radii [m]
a1 ... aNa
#wavelength [m]
λ1 ... λNλ
#Qext,⊥ Qext,|| Qabs,⊥ Qabs,|| Qsca,⊥ Qsca,|| ΔQcirc Qtrq,1 ... Qtrq,Ni g1 ... gNi
Qext,⊥,1,1 Qext,||,1,1 Qabs,⊥,1,1 ...
...
Qext,⊥,Nλ,1 Qext,||,Nλ,1 Qabs,⊥,Nλ,1 ...
...
Qext,⊥,1,Na Qext,||,1,Na Qabs,⊥,1,Na ...
...
Qext,⊥,Nλ,Na Qext,||,Nλ,Na Qabs,⊥,Nλ,Na ...

```

For example, the POLARIS asto-silicate parameters file of oblate dust grains is created as follows:

```

#string ID
astronomical silicate (oblate shaped)
#nr_radii nr_wave. inc_angles aspect_ratio density sub_temp delta align
112 100 31 0.5 3800 1200 1.95675 1
#a_eff
5.00E-9 7.83E-9 1.08E-8 1.39E-8 1.72E-8 2.06E-8 ...
#wavelength
9.00E-8 2.63E-7 4.48E-7 6.46E-7 8.57E-7 1.00E-6 ...
#Qext1 Qext2 Qabs1 Qabs2 Qsca1 Qsca2 dQcirc Qtrq0 ...
8.84E-1 4.65E-1 8.66E-1 4.56E-1 1.80E-2 9.22E-3 2.71E-2 9.08E-9 ...
1.52E-2 1.76E-2 1.97E-2 2.17E-2 2.34E-2 2.48E-2 2.51E-2 2.67E-2 ...
...
1.95E-4 1.94E-4 1.94E-4 1.93E-4 1.93E-4 1.92E-4 1.92E-4 1.92E-4 ...

```

3.4.2 Scattering matrices

In the most general case the Müller matrix for scattering has also 4x4 entries that determine the polarization state of photons for each scattering event. Since such a matrix depends at least on the grain size a , dust material, wavelength λ , and the scattering angles δ and ϕ , the parameter space can be enormous (see Sect. 4.6.5 for details about the physics of scattering). This holds even more for the upcoming POLARIS mode for scattering on non-spherical dust grains. Hence, POLARIS does not read the files for the scattering matrices except for the simulation mode CMD_DUST_SCATTERING and Mie scattering (PH_MIE, see Sect. 4.6.1 for more information about phase functions). Considering the parameter space, the scattering matrices are stored in an extra directory with the same name as the dust parameters file. This directory contains several files with scattering matrices for each wavelength. Each matrix file in turn contains then the data over grain size, scattering angle ϕ and δ and a list of the actual entries of the matrix (in future we may split the files also for different grain sizes). Here, all data is stored in a

3 Input files

binary format as a two byte float for each parameter. Additionally, the directory needs also to contain the file '`scat.inf`'. This file contains only three lines specify the number of bins and matrix entries as plain text. In the general form the file '`scat.inf`' looks like this:

```
Na Nλ Nα Nφ Nθ
NM
N11 N12 N13 N14 N21 N22 N23 N24 N31 N32 N33 N34 N41 N42 N43 N44
```

Here, N_a is the number of dust grain sizes, N_λ is the number of wavelengths, N_α is implemented for future purposes and irrelevant at the moment, N_φ is the number of scattering angles in φ -direction, and N_θ is the number of scattering angles in θ -direction. Dependent on the dust grain model not all entries of the scattering matrix are necessary and some may be equal. Hence the total number of entries ($N_M \leq 16$) defined by the next line. The last line defines the scattering matrix itself. Here, the number is the position of entries in the binary file while its position defines the position within the scattering matrix. As an example:

```
#nr. of dust species #wav. #inc. angles #phi angle #theta angle
1      231      1      1      181

#data length
4

#position of matrix elements
#M11 M12 M13 M14 M21 M22 M23 M24 M31 M32 M33 M34 M41 M42 M43 M44
2    0    0    2    1    0    0    0    0    3    4    0    0   -4    3
```

This example shows a data set of scattering matrices for a single dust grains size $N_a = 1$, for $N_\lambda = 231$ wavelength, one scattering angle φ - direction $N_\varphi = 1$, and $N_\theta = 181$ in θ -direction. The total number of entries is $N_M = 4$. In this example, the scattering matrix itself is built up exactly as shown in Eq. 4.69.

3.4.3 Dust refractive index

As an alternative, the dust optical properties can also be calculated with the Wolf & Voshchinnikov approach and using a file containing the refractive index (Bohren & Huffman, 1983; Wolf & Voshchinnikov, 2004). The input tables are again plain text and similar to the dust cross section files. However, they need to have the ending '`.nk`'. Each dust refractive index file starts with an arbitrary string describing the dust grain material. In the following line the number of wavelengths N_λ , the number of inclination angles N_i , the aspect ratio s of the dust grains, the density ρ_{dust} [kg/m^3] of the dust grain material itself, the sublimation temperature T_{sub} [K] of the dust grain material, a geometrical factor δ_{RAT} relevant for RAT alignment, and finally a number that defines the alignment behavior (0 = not aligned, 1 = aligned according to chosen alignment mechanism) are listed. At the moment, only spherical dust grains can be calculated based on the refractive index. However, information about the non-spherical shape and alignment are already contained in the dust refractive index file for future use. The following lines have to contain the wavelength λ as well as the real and imaginary component of the refractive index n and k separated with at least a space character.

```
description string
# nr. of wavelengths inclinations aspect_ratio density sub_temp δ align
Nλ Ni s ρdust[kg/m3] Tsub[K] δRAT 0/1
λ1 n1 k1
λ2 n2 k2 ... λN nN kN
```

For example, the POLARIS astro-silicate parameters file of spherical dust grains is created as follows:

```
#string ID
astronomical silicate

#nr. of wavelength #inc. angles #aspect ratio #density [kg/m^3] #sub.temp #delta #align
100 1 1 3500 1200 0 0
```

```
#wavelength real refractive index imaginary refractive index
4.999999999999774e-08 8.27197764135000132e-01 2.685931626490000168e-01
5.564875580140000232e-08 7.621913301310000444e-01 3.246343812520000038e-01
6.19356804447999963e-08 6.38777991717000044e-01 5.901285004609999607e-01
6.893287112919999462e-08 8.504294128460000435e-01 8.380542302629999662e-01
...
2.00000000000000042e-03 3.432783175560000011e+00 2.465826813000000090e-02
```

3.4.4 Heat capacities / Enthalpies

The heat capacities (or enthalpies) are required to calculate the stochastic heating (i.e. quantum or single photon heating). The required '`calorimetry.dat`' file has to be in a sub-directory named after the dust parameters file at the location where the dust parameters files are. This file must contain the heat capacity (or enthalpy) for different temperatures (optional: grain sizes). An index is used to specify if heat capacities (0) or enthalpies (1) are used (type of calorimetry). The file has the following structure in case of heat capacities:

```
# nr. of temperatures
Ntemp
# temperature: T [K]
T0 T1 T1 ... TN-1
# type of calorimetry
0
# heat capacity C [J/K/m^3]
# C(T_0, a_0), C(T_0, a_1), C(T_0, a_2), ...
# C(T_1, a_0), C(T_1, a_1), C(T_1, a_2), ...
C(T0, a0), C(T0, a1), ... C(T0, aN-1)
C(T1, a0), C(T1, a1), ... C(T1, aN-1)
...
C(TN-1, a0), C(TN-1, a1), ... C(TN-1, aN-1)
```

For example, the POLARIS heat capacity file for the '`aPyM5.dat`' dust is as follows:

```
#nr. of temperatures
30
# temperature: T [K]
0.1 0.14522119293692692 0.2109016609370204 0.30626685580037694 ...
# heat capacity C [J/K/m^3]
# C(T_0, a_0), C(T_0, a_1), C(T_0, a_2), ...
# C(T_1, a_0), C(T_1, a_1), C(T_1, a_2), ...
0.8959215850801721 0.8959215850801721 0.8959215850801721 ...
2.412681532591634 2.412681532591634 2.412681532591634 ...
5.135704178483553 5.135704178483553 5.135704178483553 ...
10.972358781119063 10.972358781119063 10.972358781119063 ...
...
6801426.356038569 6801426.356038569 6801426.356038569 ...
```

3.5 The gas species parameters

3.5.1 LAMDA molecular database

POLARIS line radiative transfer (LRT) simulations need the pre-calculated quantum numbers, energy levels, Einstein coefficients, and collision rates characteristic for each species of gas species. These

3 Input files

molecular parameters files are publicly available at the LAMDA (Leiden Atomic and Molecular Database) website: <http://home.strw.LAMDAuniv.nl/~moldata/molecules.html>. The provided LAMDA file format is fully supported by POLARIS without any intermediate conversion step. Lines beginning with a ! are comments and will be ignored by the POLARIS command parser.

Since the LAMDA database is an external source, we just provide a short description of the file format in this manual as far as it is relevant for the POLARIS code. For additional information see <http://home.strw.LAMDAuniv.nl/~moldata/molformat.html>. The first parameter in a LAMDA file is a string with the name of the gas species. The next number is the molecular weight followed by the numbers of pre-calculated energy levels. In the following table the energy levels, the energy on each level itself, and the quantum number of each level are listed. The number of pre-calculated transitions is in the line followed by a second table. This table provides the an unique ID for each transition the number of energy levels between which the transition occurs, the Einstein A coefficient , as well as the characteristic frequency of the transition. The unique transition ID in this table is relevant for the POLARIS command files (see 3.1) and the Zeeman parameters file (see 3.5.2) in order to select the desired transitions. The next four lines define the number of considered collision partners to calculate the collisional excitation, a string identifying the collision partner and the reference of this data, the number of collision transitions, and finally the number of collision temperatures. The tables are at the end of the file and provide the physical parameters for all of permutations of collision partners, transitions and collision temperatures.

3.5.2 Zeeman parameters files

To consider the Zeeman splitting in LRT simulations, additional parameters complementing the LAMDA molecular parameters file are required. For further details about the underlying physical relevance of these parameters see Sect. 4.7.2. These additional parameters are listed in an extra file and shipped with the POLARIS package for different gas species. Please contact the developers, if this file is not existent for your desired gas species.

At the top is the name of the gas species corresponding to that of the LAMDA parameters file and in the second line is the radius of the gas species. The next number defines the amount of lines with Zeeman lines. In the following sections come the upper and lower level Landè g factors, the number of Zeeman upper and lower sub-levels, as well as the line strength between all Zeeman sub-levels.

In its general form the Zeeman file is ordered as follows (see Sect. 4.7 for details):

```
!Molecule name
!Molecule radius for collision calculations
!Number of transitions Ntr with Zeeman effect
!Corresponding transition index in LAMDA database of the first transition
!Lande factor of upper level of the first transition
!Lande factor of lower level of the first transition
!Number of Zeeman sub-levels in the upper level of the first transition
!Number of Zeeman sub-levels in the lower level of the first transition
!Line strength of  $\pi$  and  $\sigma_{\pm}$  transitions for all permutations quantum numbers M' and M'' ...
!Lande factor of upper level of the Ntr-th transition
!Lande factor of lower level of the Ntr-th transition
!Number of Zeeman sub-levels in the upper level of the Ntr-th transition
!Number of Zeeman sub-levels in the lower level of the Ntr-th transition
!Line strength of  $\pi$  and  $\sigma_{\pm}$  transitions for all permutations quantum numbers M' and M''
```

How the Zeeman parameters file of the gas species *OH* would look like, can be seen in Listing 3.2.

Listing 3.2: The Zeeman parameters file of the gas species *OH*.

```

!Molecule name
OH
!Molecule radius for collision calculations
0.958e-10
!Number of transitions with Zeeman effect
2
!Transition index in LAMDA database
2
!Lande factor of upper level
1.16828926744
!Lande factor of lower level
1.16828926744
!Number of Zeeman sub-levels in the upper level
3
!Number of Zeeman sub-levels in the lower level
3
!Line strength of  $\pi$  transition ( $M'=-1 \rightarrow M''=-1$ )
0.5
!Line strength of  $\pi$  transition ( $M'=0 \rightarrow M''=0$ )
0.0
!Line strength of  $\pi$  transition ( $M'=1 \rightarrow M''=1$ )
0.5
!Line strength of  $\sigma_+$  transition ( $M'=-1 \rightarrow M''=0$ )
0.25
!Line strength of  $\sigma_+$  transition ( $M'=0 \rightarrow M''=1$ )
0.25
!Line strength of  $\sigma_-$  transition ( $M'=1 \rightarrow M''=0$ )
0.25
!Line strength of  $\sigma_-$  transition ( $M'=0 \rightarrow M''=-1$ )
0.25
!Transition index in LAMDA database
3
!Lande factor of upper level
0.700973560462
!Lande factor of lower level
0.700973560462
!Number of Zeeman sub-levels in the upper level
5
!Number of Zeeman sub-levels in the lower level
5
!Line strength of  $\pi$  transition ( $M'=-2 \rightarrow M''=-2$ )
0.4
!Line strength of  $\pi$  transition ( $M'=-1 \rightarrow M''=-1$ )
0.1
!Line strength of  $\pi$  transition ( $M'=0 \rightarrow M''=0$ )
0.0
!Line strength of  $\pi$  transition ( $M'=1 \rightarrow M''=1$ )
0.1
!Line strength of  $\pi$  transition ( $M'=2 \rightarrow M''=2$ )
0.4
!Line strength of  $\sigma_+$  transition ( $M'=-2 \rightarrow M''=-1$ )
0.1
!Line strength of  $\sigma_+$  transition ( $M'=-1 \rightarrow M''=0$ )
0.15
!Line strength of  $\sigma_+$  transition ( $M'=0 \rightarrow M''=1$ )
0.15
!Line strength of  $\sigma_+$  transition ( $M'=1 \rightarrow M''=2$ )
0.1
!Line strength of  $\sigma_-$  transition ( $M'=2 \rightarrow M''=1$ )
0.1
!Line strength of  $\sigma_-$  transition ( $M'=1 \rightarrow M''=0$ )
0.15
!Line strength of  $\sigma_-$  transition ( $M'=0 \rightarrow M''=-1$ )
0.15
!Line strength of  $\sigma_-$  transition ( $M'=-1 \rightarrow M''=-2$ )
0.1

```

Table 3.4: Available commands and their default values for the POLARIS command files. The red names in brackets show for which simulation type (pipeline ID) the command can be used.

Command	Description
<i>Simulation types</i>	
<cmd> CMD_TEMP or CMD_TEMP_RAT or CMD_RAT or CMD_DUST_SCATTERING or CMD_DUST_EMISSION or CMD_LINE_EMISSION or CMD_SYNCHROTRON	Set the simulation type of the current task Default: No simulation will be performed without this command
<i>Detectors</i>	
<detector_dust ...> (DUST_EMISSION)	Detector for dust emission. See Sect. 4.5 Default: No dust detector
<detector_dust_healpix ...> (DUST_EMISSION)	Detector for dust emission (healpix background grid). See Sect. 4.5 Default: No dust detector
<detector_dust_polar ...> (DUST_EMISSION)	Detector for dust emission (polar background grid). See Sect. 4.5 Default: No dust detector
<detector_dust_slice ...> (DUST_EMISSION)	Detector for dust emission (slice background grid). See Sect. 4.5 Default: No dust detector
<detector_dust_mc ...> (DUST_SCATTERING)	Detector for emission scattered at the dust grains. See Sect. 4.5 Default: No dust scattering detector
<detector_line ...> (LINE_EMISSION)	Detector for line emission. See Sect. 4.5 Default: No line detector
<detector_line_healpix ...> (LINE_EMISSION)	Detector for line emission (healpix background grid). See Sect. 4.5 Default: No line detector
<detector_line_polar ...> (LINE_EMISSION)	Detector for line emission (polar background grid). See Sect. 4.5 Default: No line detector
<detector_line_slice ...> (LINE_EMISSION)	Detector for line emission (slice background grid). See Sect. 4.5 Default: No line detector
<gas_species> (LINE_EMISSION)	Gas species for line emission. See Sect. 4.7 Default: No gas species
<detector_sync ...> (SYNCHROTRON)	Detector for synchrotron emission. See Sect. 4.5 Default: No synchrotron detector
<detector_sync_healpix ...> (SYNCHROTRON)	Detector for synchrotron emission (healpix background grid). See Sect. 4.5 Default: No synchrotron detector
<max_subpixel_lvl> MAX_LEVEL (DUST_EMISSION, LINE_EMISSION)	Set the maximum level of subpixeling Default: One level

Table 3.5: Available commands and their default values for the POLARIS command files (continued). The red names in brackets show for which simulation type (pipeline ID) the command can be used.

Command	Description
<i>General</i>	
<path_grid> "/PATH/TO/GRID"	Path to the used grid (ALL) Default: No grid considered
<path_out> "/PATH/TO/RESULTS"	Path to the POLARIS results (ALL) Default: No grid considered
<start> START_INDEX (DUST_EMISSION, LINE_EMISSION, SYNCHROTRON)	Set the first considered detector (index as occurrence in command file) Default: Start with first detector
<stop> STOP_INDEX (DUST_EMISSION, LINE_EMISSION, SYNCHROTRON)	Set the last considered detector (index as occurrence in command file) Default: Stop after last detector
<conv_dens> FACTOR_DENS (ALL)	Set the conversion factor for the density Default: 1.0
<conv_len> FACTOR_LEN (ALL)	Set the conversion factor for the length Default: 1.0
<conv_mag> FACTOR_MAG (ALL)	Set the conversion factor for the magnetic field strength Default: 1.0
<conv_vel> FACTOR_VEL (ALL)	Set the conversion factor for the velocity Default: 1.0
<nr_threads> NR_THREADS (ALL)	Set the number of processor cores on which POLARIS can run Default: 1
<i>Radiation sources</i>	
<source_star nr_photons = > (TEMP, RAT, DUST_SCATTERING, DUST_EMISSION)	Stellar radiation source (see Sect. 4.2) Default: No stellar radiation source
<source_starfield nr_photons = > (TEMP, RAT, DUST_SCATTERING)	Starfield radiation source (see Sect. 4.2) Default: No starfield radiation source
<source_isrf nr_photons = > (TEMP, RAT)	Interstellar radiation field as radiation source (see Sect. 4.2) Default: No ISRF radiation source
<source_background nr_photons = > (DUST_EMISSION, LINE_EMISSION, SYNCHROTRON)	Background radiation source (see Sect. 4.2) Default: A basic background source will be initialized if required
<source_dust nr_photons = > (DUST_SCATTERING)	Use the dust grains as radiation source (activates self-scattering calculations, see Sect. 4.2) Default: The dust grains are not considered to calculate the radiation scattered at dust grains
<axis1> AXIS1_X AXIS1_Y AXIS1_Z (ALL)	Rotation axis for first rotation angle Default: (1, 0, 0)
<axis2> AXIS2_X AXIS2_Y AXIS2_Z (ALL)	Rotation axis for second rotation angle Default: (0, 1, 0)

3 Input files

Table 3.6: Available commands and their default values for the POLARIS command files (continued). The red names in brackets show for which simulation type (pipeline ID) the command can be used.

Command	Description
<i>Dust</i>	
<dust_component> or <dust_component id = >	Set the considered dust grain compositions (see Sect. 4.6.5) (ALL) Default: No dust grains used
<align> ALIG_PA or ALIG_RAT or ALIG_IDG or ALIG_GOLD or ALIG_INTERNAL	Considered alignment mechanism of non-spherical dust grains (DUST_EMISSION) Default: Random alignment
<sub_dust> 1 (yes) or 0 (no)	Enables/Disables sublimation of dust grains (sublimation temperature is set in the dust catalog) (TEMP, TEMP_RAT) Default: No sublimation
<f_highJ> F_HIGHJ	Set the f_{highJ} value for the radiative torque mechanism (DUST_EMISSION) Default: 0.25
<f_c> F_C	Set the f_{cor} value for the radiative torque mechanism (DUST_EMISSION) Default: 0.6
<adj_tgas> TEMP_FACTOR	Overwrite the gas temperature with the dust temperature times TEMP_FACTOR (TEMP, TEMP_RAT) Default: Keep gas temperature as it is in the grid
<mass_fraction> MASS_FRACTION	Set gas-to-dust mass ratio (ALL) Default: 0.01
<dust_offset> 1 (yes) or 0 (no)	Enables/Disables the use of the dust temperature of the input grid as an offset (see Sect. 4.6.2) (TEMP, TEMP_RAT) Default: Do not use the previous dust temperature
<radiation_field> 1 (yes) or 0 (no)	Enables/Disables the saving of the radiation field (required by <stochastic_heating>, see Sect. 4.6.2)
<rt_scattering> 0	Disables the usage of the radiation field to include scattering in the ray-tracing (DUST_EMISSION) Default: Use the radiation field to add scattered light to thermal emission
<full_dust_temp> 1 (yes) or 0 (no)	Enables/Disables the calculation of the dust temperature for each dust grain size (see Sect. 4.6.2) (TEMP, TEMP_RAT) Default: Calculate the dust temperature only for the effective dust grain size
<stochastic_heating> SIZE_LIMIT	Consider the emission of stochastically heated dust grains with a size < SIZE_LIMIT (see Sect. 4.6.2) (DUST_EMISSION) Default: Calculate the dust emission only from equilibrium temperature(s)
<phase_function> PH_HG, PH_MIE, or PH_ISO	Set the phase function used for the dust grains (Henyey-Greenstein, Mie or isotropic) (TEMP, RAT, DUST_SCATTERING) Default: PH_HG
<enfsca> 1 (yes) or 0 (no)	Enables/Disables the use of enforced first scattering (TEMP, RAT, DUST_SCATTERING) Default: Use enforced first scattering
<peel_off> 1 (yes) or 0 (no)	Enables/Disables the use of the peel-off technique (see Sect. 4.3.3) (DUST_SCATTERING) Default: Use the peel-off technique
<acceptance_angle> AC_ANGLE	Set the acceptance angle, if peel-off is not used (DUST_SCATTERING) Default: 1°

Table 3.7: Available commands and their default values for the POLARIS command files (continued). The red names in brackets show for which simulation type (pipeline ID) the command can be used.

Command	Description
	<i>Gas</i>
<mu> MU (ALL)	Average atomic mass unit per gas particle Default: 2.0
<vel_maps> 1 (yes) or 0 (no) (LINE_EMISSION)	Enables/Disables the creation of velocity channel maps Default: No velocity channel map will be created
<vel_is_speed_of_sound> 1 (yes) or 0 (no) (LINE_EMISSION)	Enables/Disables the interpretation of the velocity of the grid as multiple of the speed of sound Default: The velocity field of the grid is considered to have SI units
<kepler_star_mass> MASS_OF_CENTRAL_STAR (LINE_EMISSION)	Set the mass of the central star and enable the use of Keplerian rotation as the velocity field Default: Use the velocity field of the grid
<turbulent_velocity> V_TURBULENT (LINE_EMISSION)	Set the turbulent velocity of the gas phase to add extra Doppler broadening Default: 0 m s ⁻¹

Table 3.8: Available commands and their default values for the POLARIS command files (continued). The red names in brackets show for which simulation type (pipeline ID) the command can be used.

Command	Description
<i>Visualization</i>	
<write_inp_midplanes> INP_MIDPLANE_PIXEL	Enables the creation of midplane ‘.fits’ files (input grid, see Sect. 5.2) (ALL) Default: No midplane files
<write_out_midplanes> OUT_MIDPLANE_PIXEL	Enables the creation of midplane ‘.fits’ files (output grid, see Sect. 5.2) (ALL) Default: No midplane files
<write_3d_midplanes> PLANE or PLANE NR_SLICES or PLANE NR_SLICES Z_MIN, Z_MAX	Enables the creation of 3D midplane files (requires <write_xyz_midplanes> command) (ALL) Default: No 3D midplane files
<write_radiation_field> 1 (yes) or 0 (no)	Enables/Disables the inclusion of the radiation field into the midplane ‘.fits’ files (without direction, see Sect. 5.2) (ALL) Default: No radiation field included
<write_full_radiation_field> 1 (yes) or 0 (no)	Enables/Disables the inclusion of the radiation field into the midplane ‘.fits’ files (with direction, see Sect. 5.2) (ALL) Default: No radiation field included
<write_g_zero> 1 (yes) or 0 (no)	Enables/Disables the inclusion of the Habing field G_0 value into the midplane ‘.fits’ files (see Sect. 5.2; Habing, 1968; Mathis et al., 1983) (ALL) Default: No G_0 value included
<midplane_zoom> ZOOM_FACTOR	Set the zoom onto the midplane cut images (ALL) Default: No midplane zoom
<nr_gnu_points> GNU_POINTS	Enables/Disables the creation of Gnuplot files to visualize the grid (how many scalar points, see Sect. 5.3) (ALL) Default: No Gnuplot files
<nr_gnu_vectors> GNU_VECTORS	Enables/Disables the creation of Gnuplot files to visualize the grid (how many vectors, see Sect. 5.3) (ALL) Default: No Gnuplot files
<max_lines> GNU_LINES	Enables/Disables the creation of Gnuplot files to visualize the grid (how many lines points, see Sect. 5.3) (ALL) Default: No Gnuplot files
<amira_inp_points> INP_AMIRA_POINTS	Enables/Disables the creation of ANIRA files (input grid, see Sect. 5.4) (ALL) Default: No AMIRA files
<amira_out_points> OUT_AMIRA_POINTS	Enables/Disables the creation of ANIRA files (output grid, see Sect. 5.4) (ALL) Default: No AMIRA files

4 POLARIS pipeline

The POLARIS code works in independent distinct simulation modes. The choice of modes depends on the scientific interest of the user. All modes can be combined into a single command file. In this section we describe the different POLARIS modes and outline the underlying physical principles of dust and molecular line, and synchrotron RT, respectively, as well as the implemented numerical methods.

4.1 Photon propagation

4.1.1 The Stokes vector

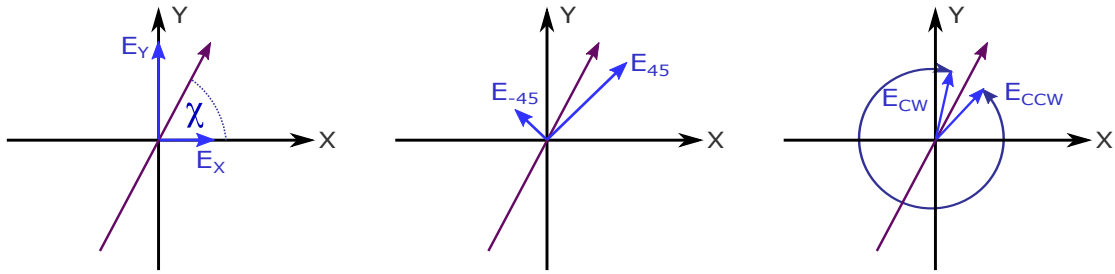


Figure 4.1: Representation of the same electric field vector in three different coordinate systems. Here, the quantity χ is the orientation angle as observed on the plane of the sky.

The polarization state of radiation along its path can be quantified by the four-component Stokes vector $\vec{S} = (I, Q, U, V)^T$ where the parameter I is the total intensity, Q and U describe the state of linear polarization, and V is for circular polarization. A bundle of polarized light can be projected on two different coordinate systems (see Fig. 4.1). Additionally, with the decomposition of polarized radiation in two clockwise and counterclockwise rotating waves gives the components the Stokes vector defined by

$$\vec{S} = \begin{pmatrix} I \\ Q \\ U \\ V \end{pmatrix} = \begin{pmatrix} |E_x|^2 + |E_y|^2 \\ |E_x|^2 - |E_y|^2 \\ |E_{45}|^2 - |E_{-45}|^2 \\ |E_{cw}|^2 - |E_{ccw}|^2 \end{pmatrix}. \quad (4.1)$$

According to the Stokes formalism, linear polarization is determined by

$$P_l = \frac{\sqrt{U^2 + Q^2}}{I} \in [0, 1] \quad (4.2)$$

and the position angle χ as observed on the plane of the sky is

$$\tan(2\chi) = \frac{U}{Q}. \quad (4.3)$$

The degree of circular polarization P_c is given by

$$P_c = \frac{V}{I} \in [-1, 1] \quad (4.4)$$

where $P_c = 1$ stands for circular polarization with the electric field vector rotating counter clockwise and $P_c = -1$ stands a rotation clockwise towards the observer. Additionally, each photon package in POLARIS keeps also track about the optical depth and column density along its path.

4.1.2 General radiative transfer equation

The POLARIS code solves the RT equation in all four Stokes parameters simultaneously. This problem can be expressed as

$$\frac{d}{d\ell} \vec{S} = -\hat{R}(\alpha) \hat{K} \hat{R}^{-1}(\alpha) \vec{S} + \vec{J} \quad (4.5)$$

Here, $\hat{R}(\alpha)$ is a rotation matrix, and \vec{J} is the contribution due to emission. The quantity \hat{K} is the Müller matrix describing the extinction, absorption, and scattering, respectively. Both \hat{K} as well as \vec{J} are defined by the characteristic physics of radiation interacting with gas species, free electrons, or dust, respectively. In the most general form the RT problem can be written as

$$\frac{d}{d\ell} \begin{pmatrix} I \\ Q \\ U \\ V \end{pmatrix} = - \begin{pmatrix} \alpha_I & \alpha_Q & \alpha_U & \alpha_V \\ \alpha_Q & \alpha_I & \kappa_V & \kappa_U \\ \alpha_U & -\kappa_V & \alpha_I & \kappa_Q \\ \alpha_V & -\kappa_U & -\kappa_Q & \alpha_I \end{pmatrix} \begin{pmatrix} I \\ Q \\ U \\ V \end{pmatrix} + \begin{pmatrix} j_I \\ j_Q \\ j_U \\ j_V \end{pmatrix} \quad (4.6)$$

Dependent on the physical problem some of the coefficients can be eliminated by rotating the polarized radiation from the lab frame into the target frame meaning the frame of the magnetic field or the symmetry axis of the dust grain, respectively. From the definition of the Stokes vector follows for the rotation:

$$\hat{R}(\alpha) = \begin{pmatrix} 1 & 0 & 0 & 0 \\ 0 & \cos(2\phi) & -\sin(2\phi) & 0 \\ 0 & \sin(2\phi) & \cos(2\phi) & 0 \\ 0 & 0 & 0 & 1 \end{pmatrix}. \quad (4.7)$$

Implemented in the POLARIS is the Runge-Kutta Fehlberg (RK45) solver in order to provide a high accuracy solution to the RT problem. This method uses an inbuilt step size ℓ correction to keep the error within below a threshold ϵ_{err} by comparing the forth order Runge Kutta approximation

$$y_{k+1} = y_k + \frac{25}{216} k_1 + \frac{1408}{2565} k_3 + \frac{2197}{4101} k_4 - \frac{1}{5} k_5 \quad (4.8)$$

with the fifth order solution

$$\hat{y}_{k+1} = y_k + \frac{25}{216} k_1 + \frac{1408}{2565} k_3 + \frac{2197}{4101} k_4 - \frac{1}{5} k_5 \quad (4.9)$$

Here, the factors are defined by

$$k_1 = If(t_k, y_k), \quad (4.10)$$

$$k_2 = If(t_k + \frac{1}{4}h, y_k + \frac{1}{4}k_1), \quad (4.11)$$

$$k_3 = If(t_k + \frac{3}{8}h, y_k + \frac{3}{32}k_1 + \frac{9}{32}k_2), \quad (4.12)$$

$$k_4 = If(t_k + \frac{12}{13}h, y_k + \frac{1932}{2197}k_1 - \frac{7200}{2197}k_2 + \frac{7296}{2197}k_3), \quad (4.13)$$

$$k_5 = If(t_k + h, y_k + \frac{439}{216}k_1 + 8k_2 - \frac{3680}{513}k_3 - \frac{854}{4104}k_4), \quad (4.14)$$

and

$$k_6 = If(t_k + \frac{1}{2}h, y_k + \frac{8}{27}k_1 + 2k_2 - \frac{3544}{2565}k_3 + \frac{1859}{4104}k_4 - \frac{11}{40}k_5) \quad (4.15)$$

where $f(t_k, y_k)$ represents the Stokes I component of Eq. 4.6. Finally, the total error is calculated with:

$$\epsilon = \frac{|\hat{y}_{k+1} - y_{k+1}|}{\epsilon_{\text{err}} |\hat{y}_{k+1} + \epsilon_{\text{abs}}|}. \quad (4.16)$$

If $\epsilon > 0$ a smaller step size ℓ_{new} for the next integration needs to be determined according to

$$\ell_{\text{new}} = \min(0.9 \cdot \ell_{\text{old}} \epsilon^{-0.2}; 0.25 \cdot \ell_{\text{old}}). \quad (4.17)$$

Otherwise, in the case of $\epsilon \leq 0$ the integration step is within the demanded error limit and the equation system of RT is considered to be solved. Dependent on the chosen POLARIS RT simulation mode this process stops when a photon package leaks from the grid or hits a detector. In POLARIS the errors $\epsilon_{\text{err}} = 10^{-8}$ and $\epsilon_{\text{abs}} = 10^{-30}$ by default and defined in the file '[typedefs.h](#)'.

4.1.3 Monte-Carlo (MC) photon transfer

This MC photon transfer scheme is applied in the grain alignment radius mode (CMD_RAT, see 4.6.4), the dust heating mode (CMD_TEMP, see 4.6.2), and in dust polarization runs with scattering (CMD_DUST_SCATTERING, see 4.6.5).

The MC photon transfer in POLARIS works with photon packages instead of single photon in order to make the propagation of light more efficient. Each photon package starts at a source (see Sect. 4.2) with a direction, energy per unit time, polarization state (Stokes vector) and one distinct wavelength. The probability of radiation-dust interaction is determined by the path length through the i -th cell ℓ_i , the cross section of extinction C_{ext} , and the dust number density n_d of the dust in each cell. A random number $z \in [0, 1]$ is chosen to sample an optical depth from the statistical function

$$\tau_{\text{st}} = -\ln(1 - z). \quad (4.18)$$

In general the path length ℓ_i is defined to be between the two cell walls where the photon package enters and leaves, respectively, the i -th cell. The total optical depth of the photon package accumulates along all the paths ℓ_i through each i -th cells is:

$$\tau_{\text{ext}} = \sum_{i=1}^N C_{\text{ext},i} n_{d,i} \ell_i. \quad (4.19)$$

where $C_{\text{ext},i}$ and $n_{d,i}$ are the local dust extinction cross section and the dust number density, respectively.

A photon package interacts with the dust when the condition

$$\tau_{\text{ext}} < \tau_{\text{st}} \quad (4.20)$$

is fulfilled in a particular cell. In this case the position of the photon package and, subsequently, the path length within that cell is adjusted to ensure $\tau_{\text{ext}} = \tau_{\text{st}}$.

The nature of the interaction itself can be either scattering, or absorption and re-emission. The wavelength-specific dust grain albedo determines the probability of scattering,

$$a(\lambda) = \frac{C_{\text{sca},\lambda}}{C_{\text{abs},\lambda} + C_{\text{sca},\lambda}} \in [0, 1]. \quad (4.21)$$

Here, $C_{\text{abs},\lambda}$ and $C_{\text{sca},\lambda}$ are the dust cross sections of absorption and scattering, respectively, and λ is the wavelength of the photon package. Note, that the cross sections are also dependent on the grain radius a . In the case of $z > a$ the photon package scatters on the dust grain. The scattering event changes the direction of the photon package by an angle of ψ , dependent on the characteristic phase function $\Psi(\psi)$ (see also 4.6.1). In the case of $z < a$ the photon package gets absorbed and instantaneously re-emitted by the dust grain in order to sustain LTE. Here, the direction of the thermal radiation is isotropic but the wavelength changes after re-emission. Assuming that the dust grain radiates like a black body, the new wavelength has to be sampled from a modified black body spectrum. The sampling function depends

on the simulation mode. In order ensure the correct remission for dust grains heated by radiation the sampling function is

$$p(\lambda, T_d) = \frac{\int_{\lambda}^{\lambda+d\lambda} C_{\text{abs},\lambda} \frac{dB_\lambda(T_{d,i})}{dT} d\lambda}{\int_{\lambda_{\min}}^{\lambda_{\max}} C_{\text{abs},\lambda} \frac{dB_\lambda(T_{d,i})}{dT} d\lambda} \quad (4.22)$$

with $B_\lambda(T_d)$ being the Planck function (see Bjorkman & Wood (2001)). In the mode for determining the alignment radius, the dust temperature remains constant and the new wavelength is sampled from

$$p(\lambda, T_d) = \frac{\int_{\lambda}^{\lambda+d\lambda} C_{\text{abs},\lambda} B_\lambda(T_d) d\lambda}{\int_0^{\infty} C_{\text{abs},\lambda} B_\lambda(T_d) d\lambda}, \quad (4.23)$$

The mode for polarized light due to dust scattering is monochromatic meaning without any absorption and re-emission at all.

4.1.4 MC noise estimation

The modes of dust grain heating (see Sect. 4.6.2), polarization by scattering (see Sect. 4.6.5), and the calculation of the radiation field (see Sect. 4.6.4) are based on the MC method, where photon packages propagate on probabilistic path was through the grid. The POLARIS modes making use of the MC method are based on quantities sampled by random numbers from physically motivated probability distribution functions. Consequently, the results are prone to noise that scales with the number N_{ph} of considered photon packages. The noise in MC simulations can be quantified by $\propto \frac{1}{\sqrt{N_{\text{ph}}}}$. Hence, the reduction of noise scales not linearly with the number of applied photon packages.

4.1.5 Ray-tracing

For the dust emission and LRT it is more sufficient to trace single rays through the grid towards the observer instead of performing a full MC RT simulation and is applied in the POLARIS modes of dust polarization by thermal re-emission (CMD_RAYTRACE) and LRT (CMD_LINETRANSFER). A way to quantify the range of wavelength where ray-tracing is applicable is by the albedo of the dust grain (see 4.21). As a rule of thumb scattering becomes irrelevant for $a < 0.1 - 0.01$ and ray-tracing can be applied. Using ray-tracing comes with the advantage of a reduced simulation run time and an excellent SNR.

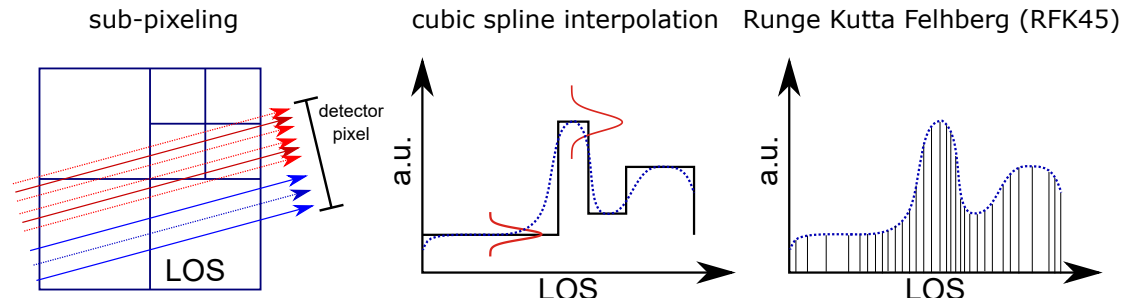


Figure 4.2: Solving the RT problem by ray-tracing follows the steps of sub-pixeling (see Sect 4.3.1), spline interpolation, and subsequent integration applying the RFK45 method.

Both, dust polarization and LRT require to solve the RT equations in the stokes vector formalism (see also Sect. 4.1.1). In order to reduce artifacts caused by grid geometry, we interpolate values with a cubic spline interpolation. This approach is especially advisable to avoid special problems concerning LRT (see Sect. 4.7).

4.2 Photon emitting sources

In a RT simulation a photon package starts its life cycle with a characteristic direction, energy per unit time, wavelength, and an initial degree of linear and circular polarization mimicking a certain type of photon emitting sources. In order to cover the broad variety of radiation emitting sources in astrophysics POLARIS provides several classes of sources.

- **Star:** This source takes no possible irregularities associated with the surface of the star such as sun spots or limb darkening into consideration. Hence, a star is considered to be a simple point source. The starting direction of each photon package is random. The distribution of wavelength is either sampled from

$$z = \frac{\int_{\lambda_i}^{\lambda_i + \Delta\lambda} L_\lambda d\lambda}{\int_0^\infty L_\lambda d\lambda} \quad (4.24)$$

where $z \in [0, 1]$ is a random number or the emission is calculated for WL_STEPS wavelengths between WL_MIN and WL_MAX as defined [src/typedefs.h](#) (Default: $\lambda \in [0.05 \times 10^{-6} \text{ m}, 2000.0 \times 10^{-6} \text{ m}]$). The second option is used when calculating RAT alignment radii or if the radiation field has to be calculated. In the first case, each newly created photon package carries an energy per unit time of

$$\dot{E} = \frac{L}{N_{\text{ph}}} \quad (4.25)$$

away, where N_{ph} is the total number of photon packages. In the second case, each newly created photon package carries an energy per unit time of

$$\dot{E} = \pi 4 \pi R_\odot^2 \frac{B_\lambda(T)}{N_{\text{ph}}} \quad (4.26)$$

away, where N_{ph} is the number of photon packages (emitted per per wavelength). A star can be defined by the following commands: <source_star nr_photons = "N_{ph}"> x [m] y [m] z [m] R_{*} [R_⊕] T_{*} [K]

Alternatively, the SED of the star can be defined by an external file with :
<source_star nr_photons = "N_{ph}"> x [m] y [m] z [m] "path"

Examples:

```
<source_star nr_photons = "5e6"> 1.15e2 4.16e2 1.8e1 12 17000
<source_star nr_photons = "8e9"> 2.32e9 19.9e7 1.3e8 "/PATH/T0/THE/STELLAR/sed.dat
    ↪ "
```

- **Starfield:** This diffuse source is intended to mimic a spacial extended source such as a star field located in a region small in comparison to the entire model space. This source is similar to the star source. However, the photon packages start not from a single point. The starting point of the emitted photon packages follow a 3D Gaussian distribution meaning that the probability to start at a position toward the center of the sphere is higher. A star can be defined by the commands
<source_starfield nr_photons = "N_{ph}"> x [m] y [m] z [m] R_{*} [R_⊕] T_{*} [K] μ_f [m]
or <source_starfield nr_photons = "N_{ph}"> x [m] y [m] z [m] μ_f [m] "path"
where μ_f is the variance of the 3D Gaussian distribution.

Examples:

```
<source_starfield nr_photons = "5e6"> 1.15e2 4.16e2 1.8e1 12 23e4 1e18
<source_starfield nr_photons = "8e9"> 2.32e9 19.9e7 1.3e8 1e18 "/PATH/T0/THE/
    ↪ STELLAR/spec.dat"
```

- **ISRF:** The ISRF contributes also to the overall radiation field inside the model space and is therefore of relevance for the calculation of the RAT alignment efficiency and the dust temperature. As for the point source the ISRF source sends photon packages in random direction. However, the starting point is from the surface of the smallest sphere enclosing the grid. The ISRF emission spectrum can be defined by an external SED file or by providing the G_0 value for the Mathis ISRF (for the Mathis ISRF, see [Mathis et al., 1983](#); [Camps et al., 2015](#)). This type of source can only be defined once per simulation.

The ISRF source can be defined by the commands:

```
<source_isrf nr_photons = "Nph"> "path"
or <source_isrf nr_photons = "Nph"> G0
```

Example:

```
<source_isrf nr_photons = "1e7">
    ↪ "/PATH/T0/POLARIS/input/interstellar_radiation_field.dat"
<source_isrf nr_photons = "1e7"> 1
```

- **Background:** The background source is designed to simulate a collection of objects outside of the grid. The background source is defined by a pixel matrix where each pixel has its characteristic SED, intensity, and state of linear and circular polarization. This type of source defines also the starting values of the stokes vector for ray-tracing and LRT simulations. All POLARIS simulations can contain an arbitrary number of distinct background sources.

The background source is defined by an set of parameters or an external file containing a pixel matrix: `<source_background nr_photons = "Nph"> f [a.u.] Teff [K] q u v α1 [°] α2 [°]`
`<source_background nr_photons = "Nph"> "path" α1 [°] α2 [°]`

In the case of an constant background source the intensity follows $I_\lambda = f \times B_\lambda(T_{\text{eff}})$ with a scaling factor f and an effective temperature T_{eff} , where as the quantities $q = Q/I$, $u = U/I$, and $v = V/I$ are the Stokes parameters normalized by intensity. The angles $α_1$ [°] and $α_2$ [°] are the rotation angles around the user defined axis (see Sect. [4.4](#)).

Examples:

```
<source_background nr_photons = "1e5"> 1e18 30000 1 0 0 90 45
<source_background nr_photons = "1e5"> "/PATH/T0/THE/background_source.dat" 90 45
```

- **Dust:** Since the dust grains have a certain temperature, they contribute also to the radiation field in the model space (available for `CMD_DUST_SCATTERING` simulations to consider self-scattering and `CMD_DUST_EMISSION` simulations to calculate the radiation field). The dust containing cells are considered as separate photon package emitting sources and the individual cell i is chosen for the emission at a certain wavelength λ according to the following equation:

$$z = \frac{L_{i,\lambda}}{\sum_{i=0}^{N_{\text{cells}}} L_{i,\lambda}} \quad (4.27)$$

where $z \in [0, 1]$ is a random number and L_i is defined as follows:

$$L_{i,\lambda} = 4\pi N_{i,d} C_{\text{abs},\lambda} B_\lambda(T_{i,d}) \quad (4.28)$$

The photon package starts from a random position evenly distributed in the entire cell volume. Since the photons packages are sampled over all cells via the total dust emission, the energy per unit time and wavelength of an individual photon package is determined by the dust properties with a modified black body spectrum as follows:

$$\dot{E}_\lambda = \frac{4\pi}{N_{\text{ph}}} \sum_{i=0}^{N_{\text{cells}}} N_{i,d} C_{\text{abs},\lambda} B_\lambda(T_{i,d}) \quad (4.29)$$

where $N_{i,d}$ is the number of dust grains in the cell i . The dust as a source of radiation can simply switched on and off by writing the tag

```
<source_dust nr_photons = "Nph">
```

In the command file where N_{ph} defines the number of photon packages to be emitted from each cell.

Example:

```
<source_dust nr_photons = "1e6">
```

HINTS:

- The external file for the SED is a simple table in the form

```
#λ [m] Lλ [W/m]
```

```
... ...  
... ...  
... ...
```

- The external file for the matrix of the background source is a simple table in the form

```
#λ [m] Lλ [W/m] q u v
```

```
... ...  
... ...  
... ...
```

- A background source is required for any RT simulation based on ray-tracing. If no background source was defined in the command file a default source will automatically be created with all parameters set to zero.

- The star source can also be used to add the direct attenuated emission of a star to a ray-tracing simulation (e.g. if the scattered light is considered in ray-tracing simulations via the radiation field).

- The range of wavelengths has to be equal or larger than the wavelength range defined in the `src/typedefs.h` (Default: $\lambda \in [0.05 \times 10^{-6} \text{ m}, 2000.0 \times 10^{-6} \text{ m}]$). This range can be adjusted by changing `WL_MIN`, `WL_MAX`, and `WL_STEPS` in the `src/typedefs.h` file (use `./install_polaris.sh -u` afterwards). Intermediate values are calculated by means of cubic spline interpolation.

4.3 Optimization techniques

A 3D MC RT simulation is challenging concerning run time and the capabilities of available computational equipment. For this reason POLARIS is equipped with several optimization algorithms to perform RT calculations on a reasonable time and a high SNR.

4.3.1 Sub-pixeling

Using only one ray per detector pixel one may lose information of sub-structures in the model smaller than the size of the bin (see Fig. 4.2). In POLARIS each detector pixel starts with four rays as a first step. Here, POLARIS keeps track of the exact cells the ray passes. If two neighboring rays pass exactly the same cells the rays are combined to a single ray. In the opposite case, when neighboring rays pass different cells each ray is again split into four sub-rays. Since no RT equations are solved in this step, the splitting of rays comes with almost no additional time. Once, the optimal number of rays per pixel is known POLARIS starts with the ray-tracing along each ray. However, allowing POLARIS to split rays down to the smallest sizes can result in an enormous slow down for the actual ray-tracing since the RT problem needs to be solved for all the rays separately. Hence, it is recommended to limit the maximal

level of splitting. The command is:

```
<max_subpixel_lvl> Nsplit
```

Hence, each detector pixel gets hit by a maximal number of $4^{N_{\text{split}}}$ rays. When the sub-pixel level is not set the level is 3 by default.

Example:

```
<max_subpixel_lvl> 3
```

HINTS:

- For spherical or cylindrical grids, the usage of the polar ray-tracing detector is recommended. The amount of rays is arranged to fit to the spherical or cylindrical distribution of cells. Subsequently, the Stokes vector in each map pixel is calculated by 2D interpolation. To use the polar ray-tracing grid, simply use `detector_dust_polar` instead of `detector_dust`. For more details, see Sect. 4.5.

4.3.2 Enforced first scattering

In optically thin regions an interaction between dust and radiation is highly unlikely and a significantly high amount of photon packages can escape the grid without any interaction at all. In POLARIS the photon package can be forced to interact at least once with the dust according to the method presented in [Cashwell \(1957\)](#) in order to increase the SNR. For each newly created photon package, an optical depth τ_{esc} is calculated from the starting point to the boundaries of the grid along the current direction. A new optical depth τ_{forced} to the first interaction point is then randomly selected from

$$\tau_{\text{forced}} = -\log(1 - z(1 - f_e)) \quad (4.30)$$

with a random number z and the factor $f_e = \exp(-\tau_{\text{esc}})$. In order to compensate for the forced interaction the photon package p_0 has to be split in two packages p_1 and p_2 with their energy adjusted by $E_1 = (1 - f_e)E_0$ and $E_2 = f_eE_0$ at the forced interaction point. From this point on each photon package follows independently the usual propagation scheme (see Sect. 4.1.3 and also Fig. 4.3) until it reaches to the boundaries of the grid or a detector. The command that enables the forced first scattering technique is `<enfsca> 1`. It can only be used for simulations with `CMD_DUST_SCATTERING`.

Example:

```
<enfsca> 1 # forced first scattering will be applied
```

4.3.3 Peel-off technique

Most of the photon packages do not leak from the grid with directions towards a detector and a huge amount of information is lost. This results also in a bad signal-to noise ratio. In order to overcome this weakness POLARIS makes use of the peel-off technique (see [Yusef-Zadeh et al., 1984](#)). Here, at each scattering point a fraction of light is also scattered in direction of the detector. The energy of the peel-off photon package E_{po} has to be adjusted by

$$E_{\text{po}} = E_{\text{pp}}\Phi(\psi)\exp(-\tau_{\text{det}}) \quad (4.31)$$

where the probability of scattering in direction of the detector is determined by the phase function $\Phi(\psi)$ (see Sect. 4.6.1 and Fig. 4.3) and the angle ψ is between original direction and detector direction. The optical depth τ_{det} is integrated along the line of sight between the position of the scattering event and the detector position. Although, the optical depth towards the observer has to be calculated for each scattering event, the peel-off technique results in synthetic images with an excellent signal-to-noise ratio even with a reduced number of photon packages. The command that enables the peel-off technique is `<peel_off> 1`. It can only be used for simulations with `CMD_DUST_SCATTERING`.

Example:

```
<peel_off> 1 # forced first scattering will be applied
```

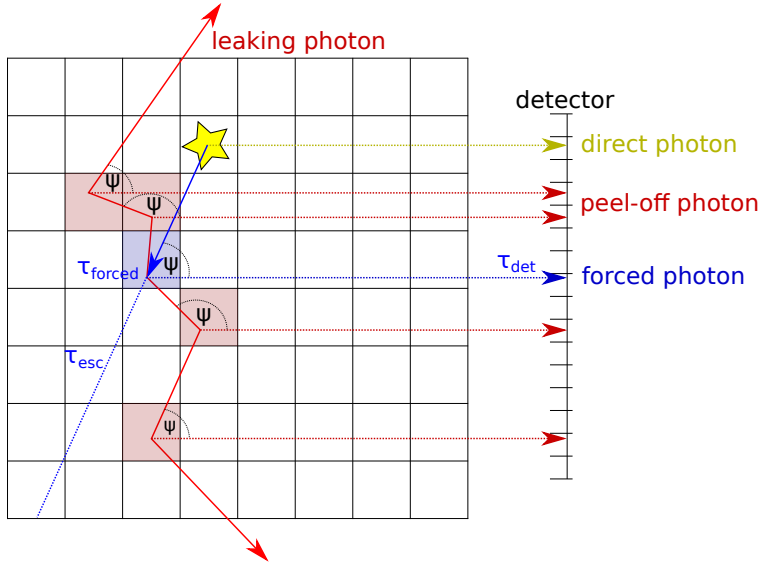


Figure 4.3: Sketch of the implemented forced first scattering scheme and the peel-off technique.

4.3.4 Wavelength range selection

Stars and star fields emit photons in the full wavelength range of its black body SED which depends on its characteristic temperature. However, wavelengths at both ends of the SED can be neglected since they do not contribute significantly to the total emitted energy of the source. This reduces the number of wavelength to be considered and subsequently the computational efforts. POLARIS adjusts the SED of any source automatically so that maximal $10^{-6}\%$ of the total luminosity gets lost. This technique is standard in POLARIS and can not be switched off. However, if the radiation field has to be saved in the grid by using `<radiation_field> 1`, each wavelength will be used and no wavelength will be neglected.

4.4 Grid rotation

The grid is by default orientated in an external coordinate system with the xy-plane towards the observer and the z-axis along the LOS. In order to re-orientate the grid for dust scattering, dust ray-tracing, or line RT two arbitrary rotation axis can be defined.

```
<axis1> x [a.u.] y [a.u.] z [a.u.]
<axis2> x [a.u.] y [a.u.] z [a.u.]
```

By default the first rotation axis the x-axis (100) and the second rotation axis is along the y-axis (001).

Examples:

```
<axis1> 1 0 0 # defining the x axis as first rotation axis
<axis2> 1 1 1 # defining a diagonal direction as second rotation axis
```

Later, these rotation axis define the orientation of the grid with respect to the detector (see [4.5](#)).

HINTS:

- The vectors defining the two axis will automatically be normalized.
- Both rotation axes are independent from each other and do not rotate itself around the rotation angle.

4.5 Detector parameters

The POLARIS code provides two main classes of detectors. The plane detector and the spherical (healpix) detector. The plane detector should be used when the observer is far away from the grid and the rays can be considered to be parallel from each other. This kind of detector is available for MC dust scattering (CMD_DUST_SCATTERING), ray-tracing for thermal emission of dust grains (CMD_DUST_EMISSION), LRT (CMD_LINETRANSFER), and synchrotron RT (CMD_SYNCHROTRON). A plane detector is characterized by its distance, viewing angles, wavelength, and the number of pixel. The exact command for a detector depends on the kind of POLARIS simulation mode.

For observations considering dust scattering (CMD_DUST_SCATTERING) a plane detector is defined by:

```
<detector_dust_mc nr_pixel = "Npixel"> λmin λmax Nλ α1 [deg] α2 [deg] D [m]
```

where N_{pixel} is the number of pixel, λ_{min} is the shortest wavelength, λ_{max} is the longest wavelength, N_{λ} is the amount of wavelengths used for simulation (if 1, only λ_{min} is used), α_1 and α_2 are the rotation angles around the first and second rotation axis (see Sect. 4.4), and D is the distance to the observer.

An optional feature is the zoom of the detector. This can be done by adding the desired side-lengths to the command line (available for each plane detector).

```
<detector_dust_mc nr_pixel = "Npixel"> ... dx [m] dy [m]
```

Another optional feature is the definition of individual numbers of pixel for each direction (available for each plane detector).

```
<detector_dust_mc nr_pixel = "Npixel,x*Npixel,y"> ...
```

Examples:

```
<detector_dust_mc nr_pixel = "256"> 1e-6 2e-6 2 15.1 0 4.31998E+18
<detector_dust_mc nr_pixel = "256*128"> 1e-6 1e-5 2 35.1 0 4.31998E+18 149597870700.0
    ↪ 149597870700.0
```

For observations considering ray-tracing of the dust thermal emission (CMD_DUST_EMISSION) a plane detector is defined by:

```
<detector_dust nr_pixel = "Npixel"> λmin λmax Nλ IDsource α1 [deg] α2 [deg] D [m]
```

The only difference to the scattering detector is the definition of ID_{source} . This ID is related to the index of the defined background sources (has to be 1, if no background source is defined). In contrast to the scattering detector, the ray-tracing detectors can make use of a background grid that is not the same as the used 2D Cartesian pixel map. Other options are '**polar**' or '**slice**'. They are chosen by writing `<detector_dust_polar` or `<detector_dust_slice`. The '**polar**' grid can only be used if the underlying 3D grid is spherical or cylindrical and it should be used if the 3D grid contains a lot of cell close to the center ($f_r > 1.0$). The '**slice**' background grid has only a analyzing purpose. Here, the 2D Cartesian background grid is put inside of the grid as a horizontal slice. Each ray-tracing pixel starts at different positions in the grid. For instance, this can be used to create contour height plots of the optical depth.

In addition to the zoom feature, the ray-tracing detector can also be shifted in both directions. This can be done by adding the desired shift of the detector to the command line.

```
<detector_dust nr_pixel = "Npixel"> ... dx [m] dy [m] Δx [m] Δy [m]
```

Examples:

```
<detector_dust nr_pixel = "256"> 1e-6 2e-6 2 1 15.1 0 4.31998E+18
<detector_dust nr_pixel = "256*128"> 1e-6 2e-6 2 1 35.1 0 4.31998E+18 149597870700.0
    ↪ 149597870700.0 14959787070.0 -14959787070.0
<detector_dust_polar nr_pixel = "256"> 1e-6 2e-6 2 1 35.1 0 4.31998E+18
<detector_dust_slice nr_pixel = "256"> 1e-6 2e-6 2 1 35.1 0 4.31998E+18
```

For observations considering ray-tracing of the spectral line emission (CMD_LINE_EMISSION) a plane detector is defined by:

```
<detector_line nr_pixel = "Npixel" vel_channels = "Nvel"> ID_gas species ID_transition ID_source
    ↪ v_min,max [m/s] α1 [deg] α2 [deg] D [m]
```

where N_{vel} is the number of the applied velocity bins, $ID_{\text{gas species}}$ is the ID of a gas species (atom-/molecules) previously defined in the command file, $ID_{\text{transition}}$ is the ID of the line transition corresponding to the ID in the Leiden molecular database file (see Sect. 3.5), and $v_{\text{min,max}}$ defines the upper and lower limits of the velocity range.

Examples:

```
<detector_line nr_pixel = "256" vel_channels = "35"> 1 2 1 1e5 15.1 0 4.31998E+18
<detector_line nr_pixel = "256*128" vel_channels = "101"> 1 5 1 1e5 35.1 0 4.31998E+18
    ↪ 149597870700.0 149597870700.0 14959787070.0 -14959787070.0
<detector_line_polar nr_pixel = "256" vel_channels = "35"> 1 5 1 1e5 35.1 0 4.31998E+18
<detector_line_slice nr_pixel = "256" vel_channels = "101"> 1 5 1 1e5 35.1 0 4.31998E+18
```

HINTS:

- Use an odd number of velocity bins N_{vel} to ensure to observe at the exact transition frequency ν_{ij}

Defining a detector for a POLARIS synchrotron run is similar to the definition of a dust detector for ray-tracing. For observations considering synchrotron emission and Faraday rotation (CMD_SYNCHROTRON) a plane detector is defined by:

```
<detector_sync nr_pixel = "Npixel"> λ_min λ_max Nλ ID_source α1 [deg] α2 [deg] D [m]
```

The zoom feature of the synchrotron detector as well as the shifting in both directions can be defined by:

```
<detector_sync nr_pixel = "Npixel"> ... dx [m] dy [m] Δx [m] Δy [m]
```

Examples:

```
<detector_sync nr_pixel = "256"> 0.71 0.81 2 1 15.1 0 4.31998E+18
<detector_sync nr_pixel = "256*128"> 0.71 0.81 2 35.1 0 4.31998E+18 149597870700.0
    ↪ 149597870700.0 14959787070.0 -14959787070.0
```

A spherical detector should be used when the observer has a position within the grid and the rays are coming from the outside (a surrounding sphere). This kind of detector is not yet available for the dust scattering mode and is purely based on ray-tracing.

For spherical detectors the ray-tracing starts from of a sphere with a diameter that is larger than the side length of the grid and ends at the exact position of the observer. The starting points are equally distributed on the surface of the sphere according to the HEALPIX pixelation¹. This makes the POLARIS spherical detector directly comparable to Planck data and comes with the advantage that each point on the sphere is surrounded the same surface area.

In order to perform ray-tracing with aligned dust grains, the spherical detector can be defined by:

```
<detector_dust_healpix nr_sides = "Nsides"> λ_min λ_max Nλ ID_source rx [m] ry [m] rz [m]
    ↪ l_min [deg] l_max [deg] b_min [deg] b_max [deg]
```

¹<https://healpix.jpl.nasa.gov>

Here, r_x , r_y , and r_z is the position of the observer within the grid and N_{sides} defines the number of sides according to the HEALPIX algorithm. The HEALPIX algorithm requires for the number of sides N_{sides} to be to the base of 2 e.g. 1, 2, 4, 8 The total number of detector pixel is then defined by $N_{\text{pixel}} = 12 N_{\text{sides}}^2$. By default the spherical detector covers the full sky and points in direction of the center of the grid. The quantities l_{\min} , l_{\max} , b_{\min} , and b_{\max} are optional and define the minimum and maximum of the longitude and latitude, respectively, of the area on the sphere to be observed. However, in contrast to the galactic coordinate system the angles are defined to be $l \in [-180, 180]$ and $b \in [-90, 90]$.

Example:

```
<detector_dust_healpix nr_sides = "32"> 1e-6 1e-5 2 1 1.65e+20 0 0 -80 80 -45 45
```

A LRT detector is defined by:

```
<detector_line_healpix nr_sides = "N_sides" vel_channels = "N_vel"> ID_gas species ID_transition
ID_source v_min,max [m/s] r_x [m] r_y [m] r_z [m] l_min [deg] l_max [deg] b_min [deg] b_max [
→ deg] v_x [m/s] v_y [m/s] v_z [m/s]
```

Here, the quantities v_x v_y , and v_z are also optional and define the velocity of the observer relative to the grid.

Example:

```
<detector_line_healpix nr_sides = "32" vel_channels = "35"> 1 2 1 1e5 1.96e+20 0 0 -180
→ 180 -3.5 3.5 1.5e3 -1e3 0
```

Following our previous scheme, the HEALPIX synchrotron detector is defined by:

```
<detector_sync_healpix nr_sides = "N_sides"> λ_min λ_max Nλ ID_source r_x [m] r_y [m] r_z [m]
→ l_min [deg] l_max [deg] b_min [deg] b_max [deg]
```

Example:

```
<detector_sync_healpix nr_sides = "512"> 0.03 0.7 11 1.65e+20 0 0 -80 80 -45 45
```

4.6 Dust continuum radiative transfer

4.6.1 Phase functions

Light propagating through a dusty medium will change its direction by scattering on a single dust grains. The angular distribution of scattering on a grain at a given wavelength is given by the phase function ϕ . Many phase functions have been proposed to account for dust with different shapes, sizes, and properties of grain materials. POLARIS allows to choose the kind of phase function used in the different MC based modes.

- Isotropic scattering:

In the case of isotropic scattering each direction has the same probability after the scattering event. The same sampling process is also applied by the thermal remission. The new photon package direction \vec{r}' is sampled from a uniform distribution of points on the surface of a unit sphere and depends on the three parameters $u = 1 - 2z_1$, $t = 2\pi z_2$, and $r = \sqrt{1 - u^2}$ and can be calculated by

$$\vec{r}' = (r \cos(t), r \sin(t), u)^T. \quad (4.32)$$

Here, the quantities z_1 and z_2 are random numbers. This phase function is available for all MC based POLARIS modes. In order to activate isotropic scattering the line

```
<phase_function> PH_ISO
```

needs to be in the command file.

- Anisotropic scattering:

In contrast to isotropic scattering, anisotropic scattering is characterized by a preferential scattering directions. The Henyey-Greenstein (HG) phase function is the most widely used parametrization of the phase function and provides a good single-parameter approximation with

$$\phi(\psi) = \frac{1}{4\pi} \frac{1 - g^2}{[1 + g^2 - 2 * \cos(\psi)]^{\frac{3}{2}}}. \quad (4.33)$$

This phase function depends on scattering angle ψ and the asymmetry parameter $g \in [-1, 1]$ where $g = 0$ means isotropic scattering, $g = 1$ backward scattering, and $g = -1$ forward scattering, respectively. The anisotropy parameter g is pre-calculated dependent on material, grain size, and wavelength, and provided by the dust parameters file (Sect. 3.4). The HG phase function can be selected with:

```
<phase_function> PH_HG
```

The HG phase function is the standard phase function.

In the case of homogeneous and spherical dust grains a solution to the scattering problem can be found with Mie scattering theory. Here, the phase function of scattering can be expanded in terms of an infinite series of associated Legendre polynomials. The coefficients of the series can be calculated with the refractive index of the dust grain material. This allows to calculate the new scattering direction by utilizing the pre-calculated values of the scattering matrix. The S_{11} element of the scattering matrix can be used by POLARIS to calculate the phase function (see 4.6.5 for details). The Mie scattering phase function is only available for the MC dust polarization mode and can be activated by

```
<phase_function> PH_MIE
```

A MC mode with scattering on non-spherical dust grains is currently in development.

4.6.2 Dust heating

The command that identifies the dust heating mode is CMD_TEMP. This mode is a combination of the methods of continuous absorption Lucy (1999) and immediate re-emission Bjorkman & Wood (2001). As a minimal requirement the input grid needs the 3D gas density distribution. Additionally, a dust model and at least one photon emitting source is required. However, if the grid contains no further physical parameters, no follow-up RT calculations (e.g. dust polarization) are possible. The dust shape and the possible alignment of non-spherical dust grains has no influence on the resulting dust temperature distribution. For this POLARIS mode the dust grains are considered to be spherical in the dust heating mode. This reduces the required computational efforts dramatically.

In the beginning of the dust heating mode the emissivity

$$j_l(T_d) = n_d \int C_{\text{abs},\lambda} B_\lambda(T_d) d\lambda \quad (4.34)$$

is pre-calculated for a range of dust temperatures $T_d \in [1 \text{ K}, 4000 \text{ K}]$ and tabulated. Each photon package starts with an energy per unit time $\epsilon/\Delta t$ and a wavelength λ . In each cell with volume V_{cell} , we store the energy per unit time

$$\dot{E} = n_d \frac{\epsilon}{V_{\text{cell}} \Delta t} \sum_i C_{\text{abs},\lambda_i} \times I_i + \Delta \dot{E} \quad (4.35)$$

that all passing photon packages deposit along their paths / during the MC dust heating simulation. The quantity $\Delta \dot{E}$ describes the offset in the dust heating simulation in the case of an already exiting dust

temperature.

If the photon package interacts by means of absorption and re-emission (see also 4.1.3) a new wavelength is sampled from

$$z = \frac{\int_{\lambda_{\min}}^{\lambda_i} C_{\text{abs},\lambda} \frac{dB_{\lambda}(T_{d,i})}{dT} d\lambda}{\int_{\lambda_{\min}}^{\lambda_{\max}} C_{\text{abs},\lambda} \frac{dB_{\lambda}(T_{d,i})}{dT} d\lambda} \quad (4.36)$$

to LTE . Since the temperature changes by each absorption event the new wavelength cannot be sampled from the Planck function but by its temperature derivative in order to ensure a correct spectrum of the emitted photons (compare Eq. 4.23). Finally, we compare \dot{E} with the tabulated and cubic spline interpolated values of $j(T_d)$ in the end of the MC simulation in order to determine the dust temperature T_d . The newly calculated grid ('grid_temp.dat') will be stored in the defined output directory. If the grid contains no dust temperature at all the grid will be extended by one additional physical parameter.

We provide a minimal example command file for the dust heating mode in Listing 4.1. As a radiation source a single solar like star at the center of the grid is defined sending 10^6 photon packages into the grid. The dust model consists only of silicate grains. Besides the path to the dust parameters file, no further parameters are defined. This means we consider the full size range with an size distribution exponent of $q = -3.5$ for the dust model. Again, we define the path of the input grid and the path for the resulting grid and additional output files (e.g. plots). In this simulation we use the maximal possible number of threads of the machine (<nr_threads> -1). For the dust-to-gas mass ratio we use the usual value of 1%. POLARIS can not directly calculate a gas temperature. However, a fixed ratio of gas temperature T_d to dust temperature T_d can be assumed with the command <adj_tgas>. Any possible input gas temperature is lost if this command is defined. If stochastic heating should be considered for the thermal emission of the dust grains, either the radiation field or the effective temperature due to stochastic heating has to be saved in the grid with the command <radiation_field> 1 or <stochastic_heating> SIZE_LIMIT. Saving the radiation field offers more flexibility and precision, since the probability distribution of temperatures will be used in the dust emission and the maximum size can be varied between each dust emission simulation. However, saving the radiation field significantly increases the grid memory size (by around 400 doubles per cell) and the calculation of the dust emission takes more time if the stochastic heating is considered by using the probability distribution of temperatures that is calculated out of the radiation field.

Additionally, a dust temperature can also already be contained in the input grid e.g. as a result of a MHD simulation. This temperature may emerge from different physical processes (e.g. gas-dust collisions or compression) other than radiation-dust interaction. Hence, it may be of interest to combine both dust temperatures by defining the command <dust_offset> (0=off and 1=on). Here, POLARIS performs the reverse calculation by comparing the input dust temperature with the pre-calculated values of $j(T_d)$ in order to determine the offset of $\Delta\dot{E}$ in each cell (see Eq. 4.35). The resulting final dust temperature is higher as the sum of both separate temperatures.

Instead of only calculating the dust temperature distribution for an average dust grain size, a dust temperature can be calculated for each dust grain size individually by adding the following command to the CMD_TEMP simulation:

```
<full_dust_temp> 1
```

The resulting temperature containing grid will be adjusted accordingly (see 5.1) and any follow-up simulation of the thermal emission with this grid will use the temperatures of each grain size. As a consequence, the considered dust composition cannot not be changed after the temperature calculation (which in general should not be done).

4.6.3 Grain alignment theories

Besides Zeeman splitting the extensive treatment of imperfectly aligned dust grains in the RT simulations is one of the unique features of the POLARIS code. A unifying theory of dust grain alignment is still missing. For this reason POLARIS allows to choose from the major classes of dust grain alignment theories developed so far. In this section we intent to provide a short summary about this theories and their physical implications.

Listing 4.1: Example command file to calculate the dust temperature distribution.

```

<task> 1
#pipeline ID for dust heating
<cmd> CMD_TEMP

#A star in the center as radiation source
<source_star nr_photons = "1e6"> 0 0 0 1 6000

#Silicate as only dust components
<dust_component> "PATH/T0/POLARIS/input/dust/silicate_oblate.dat"

#path of the input grid file
<path_grid> "PATH/T0/YOUR/grid.dat"

#path for all output data
<path_out> "PATH/WHERE/THE/RESULTS/SHOULD/BE/SAVED/temp/"

#Maximal nr. of available threads for parallel computing
<nr_threads> -1

#dust to gas mass ratio
<mass_fraction> 0.01 # optional

#dust to gas temperature ratio
<adj_tgas> 10 # optional

#dust to gas temperature ratio
<dust_offset> 1 # optional

#calculate the dust temperature for each dust grain size individually
<full_dust_temp> 0 # optional

#save the 3D radiation field in the grid to use it for e.g. stochastic heating
<radiation_field> 0 # optional

#Save the effective temperature from stochastic heating for
#dust grains with a size up to 10 nm
<stochastic_heating> 1e-8
</task>

```

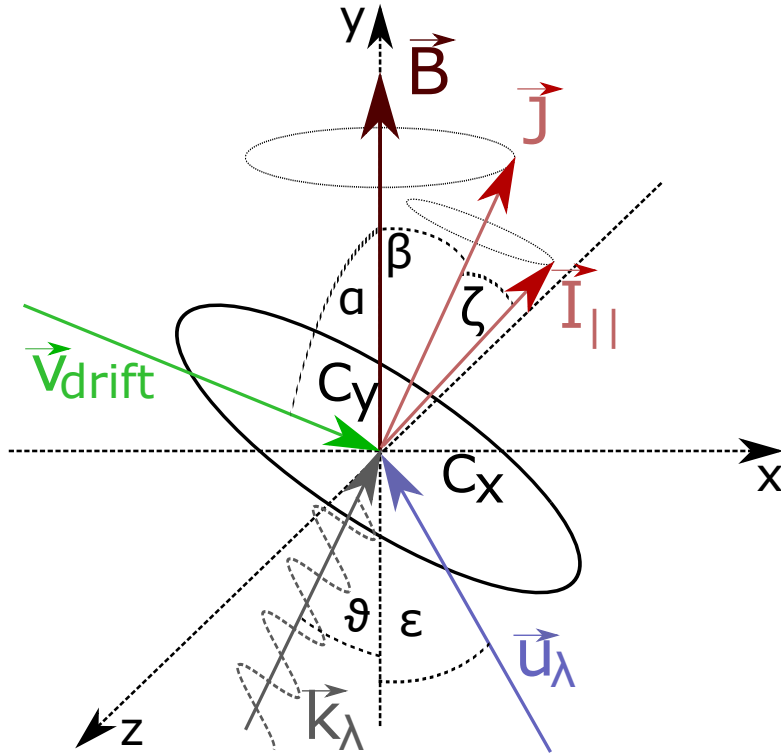


Figure 4.4: Geometrical configuration of a dust grain partially aligned with its angular momentum \vec{J} to the magnetic field direction \vec{B} . The precession of \vec{J} around \vec{B} defines the cone angle β and the precession of maximum moment of inertia \vec{I} around \vec{J} defines the angle of internal alignment ζ . Here, the angle θ is defined to be between direction of incident light \vec{k} and \vec{B} . The angles α and ϵ are between the direction of the supersonic velocity stream \vec{v}_g and \vec{B} and between the anisotropy \vec{u}_λ in the radiation field and \vec{B} , respectively. The vector \vec{v}_{rel} is the projection of \vec{v}_g on the direction of the magnetic field direction \vec{B} .

Considering the violent environment in most astrophysical processes the perfect alignment of non-spherical dust grains with respect to the magnetic field direction is permanently disturbed (see Fig. 4.4). This leads to the precession angles of β and ζ . The angle β is defined to be between the angular momentum of the dust grain \vec{J} and the magnetic field \vec{B} and ζ is between the maximum moment of inertia \vec{I} and \vec{J} . The larger the precession angles are the more the non-spherical dust grains appear to be spherical. Consequently, the resulting polarization becomes reduced. A measurement to quantify this is the so called Rayleigh reduction factor

$$R = \left\langle G(\cos^2(\beta)) G(\cos^2(\zeta)) \right\rangle \in [0, 1] \quad (4.37)$$

where $R = 1$ stands for the maximal possible polarization of a dust grain and $R = 0$ when polarization is completely suppressed. The Rayleigh reduction factor is defined by the precession angles averaged over distribution functions where $G(x) = 1.5x - 0.5$. In order to reduce the computational time we assume the precession angles to be mostly independent with

$$\langle G(X) G(Y) \rangle \approx \langle G(X) \rangle \times \langle G(Y) \rangle (1 + f_c). \quad (4.38)$$

where f_c is a correlation factor and $f_c = 0.6$ stands for no correlation at all. For most cases $f_c \approx 0.6$ and of minor relevance. However, if required it can be changed by the user with the command `<f_c> 0.6`. The distribution functions in turn depend heavily on the considered dust grain alignment theory.

Imperfect internal (II) alignment:

In order to consider the effects of internal alignment in your RT calculations include `<align> ALIG_INTERNAL` in your command file.

Even without an external disturbance a non-spherical dust grain can not be expected to align perfectly with the magnetic field. Due to internal thermal fluctuations the dust grain performs an precession of $\vec{I}_{||}$ around \vec{J} with an opening angle of ζ between both quantities (see [Lazarian & Roberge, 1997](#), for details). This effect is related to the internal temperature of the dust. Hence, the distribution function of II alignment follows a Boltzmann distribution

$$f(\zeta) \approx \exp\left(-\alpha \left[1 + \delta \sin^2(\zeta)\right]\right) \quad (4.39)$$

where $\alpha = J_{eff}^2 / 2I_{||}k_B T_d$ and $\delta = h - 1$, $h = I_{||}/I_{\perp}$ is the ratio of the minimal and maximal momenta of inertia and J_{eff} is the rms value of the angular momentum. The calculation of J_{eff} in turn depends on the additionally considered alignment mechanisms (see the following Sects.). This substitutions allow to calculate the Rayleigh reduction factor with $x = \alpha \times \delta$

$$\langle G(\cos^2(\zeta)) \rangle = \frac{e^x}{\sqrt{\pi x} \times \text{erfi}(\sqrt{x})} - \frac{1}{2x} \quad (4.40)$$

Imperfect Davis – Greenstein (IDG) alignment

The IDG can be switched on by adding `<align> ALIG_IDG` to the command file.

This theory provides a steady state solution for dust grain alignment by balancing the disturbances on the grain by random gas collisions with the alignment effects of paramagnetic relaxation (Davis-Greenstein effect) in the dust grain material ([Davis & Greenstein, 1951](#); [Spitzer & McGlynn, 1979](#)). Solving the equations of state the Rayleigh reduction factor can be calculated with

$$\langle \cos^2(\beta) \rangle = \left(1 - \sqrt{\frac{\xi^2(a)}{1 - \xi^2(a)}}\right) \arcsin \frac{\sqrt{1 - \xi^2(a)}}{1 - \xi^2(a)}. \quad (4.41)$$

where

$$\xi^2(a) = \frac{a + \delta_0 \times \frac{T_d}{T_g}}{a + \delta_0}. \quad (4.42)$$

Here, the critical parameter is

$$\delta_0 = 2.07 \times 10^{20} \frac{B^2}{n_g T_d \sqrt{T_g}}, \quad (4.43)$$

which provides an upper threshold of dust grain alignment. Dust grains with sizes $a > \delta_0$ do not contribute significantly to polarization. The constant 2.07×10^{20} is adequate for most paramagnetic materials. However, it can be changed by the user with the command `<delta0>`.

As for the angular momentum of internal alignment we use the approximation:

$$J_{eff}^2 \approx \sqrt{(1 + 0.5s^{-2})(1 + T_d/T_g)} \times (2I_{||}k_B T_g)^2. \quad (4.44)$$

GOLD (magneto mechanical) alignment

The original Gold alignment described only the alignment of dust grains in the presence of a velocity field ([Gold, 1952](#)). Later, this theory was extended to model also the influence of the magnetic field (magneto mechanical alignment, see [Lazarian, 1995](#); [Lazarian et al., 1996](#); [Lazarian & Efroimsky, 1996](#)). For considering GOLD alignment write `<align> ALIG_GOLD` in your command file.

In GOLD alignment two forces act on the dust grain simultaneous caused by an directed gas stream and the alignment by the magnetic field. This leads to a dependency of dust grain alignment on the angle α

between the predominate direction of the velocity stream and the magnetic field direction. As a solution for the Rayleigh reduction factor the GOLD alignment theory provides

$$\langle \cos^2(\beta) \rangle = \begin{cases} \frac{\sqrt{-g} \arcsin(\sqrt{-s/(1+g)})}{s \arctan(\sqrt{sg/(1+s+g)})} - 1/s & \text{if } s < 0 \\ \frac{\sqrt{-g} \sinh^{-1}(\sqrt{s/(1+g)})}{s \tanh^{-1}(\sqrt{-sg/(1+s+g)})} - 1/s & \text{if } s > 0 \end{cases} \quad (4.45)$$

with the anisotropy factor of the gas stream

$$s = -\frac{1}{2} \frac{\langle v_{\text{rel}}^{\vec{r}} \rangle - 3 \langle v_{\text{rel}}^{\vec{r}} \rangle}{\langle v_{\text{rel}}^{\vec{r}} \rangle - \langle v_{\text{rel}}^{\vec{r}} \rangle} \quad (4.46)$$

Here, $v_{\text{rel}}^{\vec{r}}$ is the projection of the relative drift velocity v_{rel} between the gas and dust component on the magnetic field direction and g is a geometrical factor.

In order to calculate the II alignment the angular momentum of GOLD alignment can be approximated by

$$J_{\text{eff}}^2 \approx k_B I_{||}(2/h + 1) \left(\frac{T_g + T_d}{2} + \frac{\mu m_H v_{\text{rel}}^2}{6k_B} \right) \quad (4.47)$$

with the molecular mass μm_H of the gas. The GOLD alignment requires an supersonic velocity stream with a Mach - number $M > 1$. Dust grains with smaller number are assumed to be not aligned. Therefore, POLARIS calculates

$$M = \frac{v_{\text{rel}}}{\sqrt{k_B T_g / \mu m_H}} \quad (4.48)$$

, for each cell of the grid. The average mass of a gas particle in these calculations can be controlled with the command `<mu>`. As for the coupling efficiency between magnetic field and dust grain alignment we demand:

$$|\vec{B}| > 4.1 \times 10^{-18} a \frac{n_g \sqrt{T_g T_d}}{s^2} \quad (4.49)$$

The same limitation of the magnetic field applies also to RAT alignment. In the case of other dust grain materials you can use the command `<larm_f>` to alter the pref actor of Eq. 4.49.

It needs to be emphasized that this model of mechanical alignment turned out to be unreliable and might be updated on a short term to keep up with current research on that field.

Radiative torque (RAT) alignment

This alignment theory can be switches on with the command `<align> ALIG_RAT`.

The implementation in POLARIS is based on the work presented in [Draine & Weingartner \(1996\)](#), [Draine & Weingartner \(1997\)](#), [Weingartner & Draine \(2003\)](#), [Lazarian & Hoang \(2007\)](#), and [Hoang et al. \(2018\)](#). RAT alignment balances the influences of random gas bombardment, paramagnetic dissipation in the dust grain material, and the radiative pressure due to an isotropic radiation field. In order for this alignment theory to work efficiently the angular velocity ω_{gas} caused by gas collisions has to be smaller as the angular velocity ω_{rad} because of radiative pressure by a factor of ≈ 3 . This ratio can be calculated by

$$\left(\frac{\omega_{\text{rad}}}{\omega_{\text{gas}}} \right)^2 = \frac{a_{\text{alg}} \rho_d}{\delta m_H} \left(\frac{t_{\text{gas}}}{(t_{\text{gas}} + t_{\text{rad}}) n_g k_B T_g} \int Q_{\Gamma}(\epsilon) \lambda \gamma_{\lambda} \bar{u}_{\lambda} d\lambda \right)^2. \quad (4.50)$$

where, ρ_d is the grain material density, δ is a geometry factor, $Q_{\Gamma}(\epsilon)$ is the radiative torque efficiency (see Sect. 3.4), ϵ is the angle between the predominant direction of radiation and the magnetic field, and the characteristic time scales t_{gas} and t_{rad} are the drag times corresponding to gas drag and thermal emission drag, respectively.

The critical quantities here are the local mean energy density \bar{u}_{λ} is the wavelength specific anisotropy factor γ_{λ} varies between $\gamma_{\lambda} = 1$ for an unidirectional radiation field and $\gamma_{\lambda} = 0$ for completely isotropic radiation. Both, mean energy density \bar{u}_{λ} and anisotropy factor γ_{λ} can be calculated by POLARIS in

an extra RT mode (see 4.6.4). Given that \bar{u}_λ and γ_λ are known, POLARIS is able to determine the characteristic dust grain size a_{alg} at which dust grains start to align ($\omega_{\text{rad}} > \omega_{\text{gas}}$).

An analytically distribution function for the precession angle β and, subsequently, the Rayleigh reduction factor is unknown so far. However, the Rayleigh reduction factor can be estimated. Solving the equations of state reveals two attractor points in the parameters space of RAT theory with different angular momenta. Dust grains at the attractor point with a high angular momentum (high-J) can be assumed to aligned perfectly where as the second attractor point is internally not perfectly aligned or rather $\langle G(\cos^2(\zeta)) \rangle < 1$. Defining $f_{\text{high-J}}$ to be the fraction of dust grains that settle at the high-J attractor point the Rayleigh reduction factor can be approximated with

$$R \approx \begin{cases} f_{\text{high-J}} + (1 - f_{\text{high-J}}) \langle G(\cos^2(\zeta)) \rangle & \text{if } a \geq a_{\text{alg}} \\ 0 & \text{if } a < a_{\text{alg}} \end{cases} \quad (4.51)$$

The angular momentum for II alignment is assumed to be $J_{\text{eff}}^2 \approx 2I_{\parallel}/k_B T_g$. The POLARIS code assumes a value of $f_{\text{high-J}} = 0.25$ however this values can be changed with the command `<f_highJ>`.

Combined of Rayleigh reduction factors

Since all these alignment theories have their place and are most likely simultaneously at work POLARIS allows to calculate a combined Rayleigh reduction factor with

$$R_{\circ} \approx \frac{R_{\text{IDG}} + R_{\text{RAT}} + R_{\text{GOLD}} + R_{\text{IDG}}R_{\text{RAT}} + R_{\text{RAT}}R_{\text{GOLD}} + 3R_{\text{IDG}}R_{\text{RAT}}R_{\text{GOLD}}}{1 + 2R_{\text{IDG}}R_{\text{RAT}} + 2R_{\text{IDG}}R_{\text{GOLD}} + 2R_{\text{RAT}}R_{\text{GOLD}} + 2R_{\text{IDG}}R_{\text{RAT}}R_{\text{GOLD}}} \quad (4.52)$$

However, this is a first approximation and has to be taken with care. In order to combine the alignment theories you can list any number of combination of alignment commands in your command file e.g.

```
<align> ALIG_INTERNAL
<align> ALIG_RAT
<align> ALIG_GOLD
<align> ALIG_IDG
```

4.6.4 The grain alignment radius a_{alg}

The command that identifies the RAT alignment radius mode is `CMD_RAT`. In order to solve Eq. 4.50 the local mean energy density \bar{u}_λ and the wavelength specific anisotropy factor γ_λ need to be determined. Here, POLARIS uses a MC mode where we store the direction and magnitude of the energy density \vec{u}_λ in each cell. For the mean energy density per path length and wavelength we derive

$$\vec{u}_{\lambda,i} = \frac{\epsilon}{c\Delta t V_{\text{cell}}} \frac{\vec{k} \times \vec{l}_i}{|\vec{k}|} \quad (4.53)$$

where \vec{k} is the wave vector of each photon package. This allows to calculate the mean energy density

$$\bar{u}_\lambda = \sum_{i=1}^{N_{\text{ph}}} |\vec{u}_{\lambda,i}| \quad (4.54)$$

and the anisotropy parameter

$$\gamma_\lambda = \frac{1}{\bar{u}_\lambda} \left| \sum_{i=1}^{N_{\text{ph}}} \vec{u}_{\lambda,i} \right| \in [0; 1] \quad (4.55)$$

The RAT alignment radius mode is the most memory demanding one since four values (8 bytes, double, $(u_x, u_y, u_z)_{\lambda, Z}$, and \bar{u}_λ) per wavelength and cell need to be stored and updated when a new photon package passes the cell. Finally, POLARIS solves Eq. 4.50 in order to calculate the minimal dust grain

Listing 4.2: Example command file to calculate the dust temperature distribution.

```

<task> 1
#pipeline ID for RAT alignment radius simulation
<cmd> CMD_RAT

#A star in the center as radiation source
<source_star nr_photons = "1e6"> 0 0 0 1 6000

# Silicate as only dust components
<dust_component> "PATH/T0/POLARIS/input/dust/silicate_oblate.dat"

#path of the input grid file
<path_grid> "PATH/WHERE/THE/RESULTS/SHOULD/BE/SAVED/temp/grid_temp.dat"

#path for all output data
<path_out> "PATH/WHERE/THE/RESULTS/SHOULD/BE/SAVED/rat/"

#Maximal nr. of threads for parallel computing
<nr_threads> -1

#dust to gas mass ratio
<mass_fraction> 0.01 # optional
</task>

```

alignment radius a_{alg} in each cell. A new grid will be created that contains all the physical input quantities extended by the alignment radius a_{alg} and stored as '`grid_rat.dat`' in the output path. We provide a minimal example command file for the RAT alignment mode in Listing 4.2.

POLARIS also allows the calculation of both, the dust temperature and RAT alignment radius at once by using `CMD_TEMP_RAT` instead of `CMD_TEMP` or `CMD_RAT`. The output grid will be named '`grid_temp.dat`', and includes both quantities.

4.6.5 Dust Intensity and polarization maps

Polarization by non-spherical dust grains

Describing the RT problem without scattering for aligned dust grains in the Stokes vector formalism leads to the following system of equations: Here, n_d is the dust number density $d l$ is the infinitesimal path length element, and $B_\lambda(T_d)$ is the Planck function for a give dust temperature T_d . Focusing on extinction the entries of the cross sections matrix can be calculated with:

$$C_{\text{ext},x} = \langle C_{\text{ext}} \rangle + \frac{1}{3} R \times (C_{\text{ext},||} - C_{\text{ext},\perp}) \quad (4.56)$$

$$C_{\text{ext},y} = \langle C_{\text{ext}} \rangle + \frac{1}{3} R \times (C_{\text{ext},||} - C_{\text{ext},\perp}) (1 - 3 \sin^2(\theta)) \quad (4.57)$$

where $C_{\text{ext},x}$ is the extinction cross section along the grains major axis and $C_{\text{ext},y}$ is the cross section long the minor axis while the angle θ is between incident light and magnetic field direction (see Fig. 4.4). Note that cross sections and the Rayleigh reduction factor are also dependent on wavelength and grain radius. For oblate dust grains the cross section of extinction is

$$C_{\text{ext}} = 0.5(C_{\text{ext},x} + C_{\text{ext},y}), \quad (4.58)$$

the cross section of linear polarization is defined as

$$C_{\text{pol}} = 0.5(C_{\text{ext},x} - C_{\text{ext},y}), \quad (4.59)$$

while

$$\langle C_{\text{ext,pol}} \rangle = (2C_{\text{ext,||}} + C_{\text{ext,\perp}}) / 3, \quad (4.60)$$

is the average cross section of a spherical dust grain of equivalent volume. The Rayleigh reduction factor depends on the selected dust grain alignment theories as introduced in Sect. 4.6.3 and is calculated by POLARIS for each radiation-dust interaction separately. The are the same for the cross sections of scattering C_{sca} , absorption C_{abs} and $C_{\text{abs,pol}}$, and circular polarization $C_{\text{circ,pol}}$.

Finally, the cross sections are weighted over the grain size distribution $n_d(a) \propto a^{-q}$ between a minimal a_{\min} and maximal a_{\max} grain size and the different materials are mixed. Here, we define N_{mat} as the amount of dust grain materials and Ξ_i are the corresponding material fractions with $\sum_{i=1}^{N_{\text{mat}}} \Xi_i = 1$.

In this case the reference frame of the dust grain is defined by the alignment direction. For a Stokes vector rotated into the reference frame of the dust the dust RT the extinction coefficients are $\alpha_U = \alpha_V = \kappa_U = \kappa_V = 0$, The same hold for the emissivity coefficients $j_U = j_V = 0$. Hence, Eq. 4.6 is completely defined by the remaining extinction coefficients

$$\alpha_I = n_d \sum_{i=1}^{N_{\text{mat}}} \Xi_i, \int_{a_{\min}}^{a_{\max}} C_{\text{ext}} n_d(a) da \quad (4.61)$$

$$\alpha_Q = n_d \sum_{i=1}^{N_{\text{mat}}} \Xi_i, \int_{a_{\min}}^{a_{\max}} C_{\text{ext,pol}} n_d(a) da \quad (4.62)$$

and

$$\kappa_Q = -n_d \sum_{i=1}^{N_{\text{mat}}} \Xi_i, \int_{a_{\min}}^{a_{\max}} C_{\text{circ,pol}} n_d(a) da \quad (4.63)$$

as well as the emission coefficients

$$j_I = n_d \sum_{i=1}^{N_{\text{mat}}} \Xi_i, \int_{a_{\min}}^{a_{\max}} C_{\text{abs}} n_d(a) da \quad (4.64)$$

and

$$j_Q = n_d \sum_{i=1}^{N_{\text{mat}}} \Xi_i, \int_{a_{\min}}^{a_{\max}} C_{\text{abs,pol}} n_d(a) da \quad (4.65)$$

The dust grain model can be defined by:

`<dust_component> "path" Ξ_i q a_{\min} a_{\max}`

where "path" is the path to a single dust parameters file, Ξ_i is the mass fraction of the material, q is the exponent of the grain size power-law distribution, and a_{\min} and a_{\max} are the dust grain radii which have to be in the range as defined in the dust parameters file (see Sect. 3.4). POLARIS can handle an arbitrary number of materials.

In addition, more options to define the dust model can be applied by using the following definition:

`<dust_component> "path" "size_keyword" Ξ_i ρ_{material} [kg/m3] a_{\min} a_{\max} p_0 ...`

Here, ρ_{material} is the material density of the dust composition (a value of 0 uses the material density of the dust parameters file). As the "size_keyword", several size distributions can be used:

- 'plaw' (power-law distribution)

$$n_d(a) = a^{p_0} \quad (4.66)$$

- 'plaw-ed' (power-law distribution + exponential decay)

$$n_d(a) = a^{p_0} \cdot \exp\left(-\left(\frac{a - p_1}{p_2}\right)^{p_3}\right) \quad (4.67)$$

- 'logn' (log-normal distribution)

$$n_d(a) = \exp\left(-0.5 \left(\frac{\log(a) - \log(p_0)}{p_1}\right)^2\right) \quad (4.68)$$

Another optional feature is the usage of different dust compositions in the grid (see 3.3.1). To enable this feature, the dust components need an additional index, which can be defined as follows (not dependent on following parameters):

```
<dust_component id = "IDdust"> ...
```

If no ID_{dust} is given, a value of zero is assumed and multiple dust components with the same ID_{dust} will be mixed together as long as their total mass fraction equals to one.

Examples:

```
<dust_component> "PATH/T0/POLARIS/input/dust/silicate Oblate.dat" 0.625 -3.5 5e-9 0.25e
    ↪ -6
<dust_component id = "1"> "PATH/T0/POLARIS/input/dust/silicate Oblate.dat" 0.625 -3.5 5e
    ↪ -9 0.25e-6
<dust_component> "PATH/T0/POLARIS/input/dust/silicate Oblate.dat" "plaw" 1.0 3500 5e-9
    ↪ 1.13e-6 -3.5
```

A POLARIS simulation run considering ray-tracing and different alignment mechanisms and detector types may look like Listing 4.3.

The emission from radiation scattered at dust grains can be considered in the ray-tracing technique if the radiation field was saved in PcodeCMD_TEMP simulations (see Sect. 4.6.2). If this was not the case, the radiation field can be calculated right before the CMD_DUST_EMISSION simulation, by defining a combination of stellar and/or dust sources in the cmd file. However, this approach to consider scattered light is only physically sufficient if the radiation field is dominated by radiation coming from a single direction and the regions dominating the scattered light have to be optically thin (usually working for circumstellar disks). Use the command <rt_scattering> 0, if the scattered light should not be considered, but the radiation field is stored in the grid.

The emission of stochastically heated dust grains can be calculated in CMD_DUST_EMISSION simulations. This is done for the smallest dust grains whose heat capacity is so small that the assumption of thermal equilibrium is not valid anymore. In POLARIS the stochastic heating algorithm is implemented according to the work of Camps et al. (2015). The required heat capacities will be taken from the file '**heat_capacity.dat**' in the sub-directory **dust_catalog_name/** where the chosen dust catalog file is saved (see Sect. 3.4.4). In the command file, this calculation can be enabled with the following command:

```
<stochastic_heating> as,max
```

The probability distribution of temperatures due to stochastic heating will be calculated from the radiation field for all dust grain sizes up to a_{s,max} to calculate the thermal emission of the dust grains in CMD_DUST_EMISSION simulations. Therefore, the CMD_TEMP simulation had to be executed with the command <radiation_field> 1. An alternative way is to calculate an effective temperature out of the probability distribution of temperatures in CMD_TEMP simulations by using ,max<stochastic_heating> \$a_s\$ there. If this happened and the grid contains not the radiation field or <stochastic_heating> is not defined in the CMD_DUST_EMISSION simulation, these effective temperatures are used. To avoid unwanted behavior, please use only one of the approaches (<stochastic_heating> at CMD_TEMP or CMD_DUST_EMISSION).

Polarization by scattering on spherical dust grains

(this POLARIS feature is currently re-designed and this section may change in the future)

The probability for a scattering event is quantified by the optical depth (see Sect. 4.1.3). Rather than converting the radiation to internal energy, it emits the same amount of energy in a different direction

Listing 4.3: Example command file to calculate the polarized dust emission.

```

<task> 1
#polarization by aligned dust
<cmd> CMD_DUST_EMISSION

#a star in the center as radiation source
#used for radiation field calculation if not done with CMD_TEMP
<source_star nr_photons = "1e6"> 0 0 0 1 6000

#the thermal emission of the dust grains only used
#for radiation field calculation if not done with CMD_TEMP
<source_dust nr_photons = "1e4">

#silicate as only dust components
<dust_component> "PATH/TO/POLARIS/input/dust/silicate_oblate.dat" 0.7 -3.5 24.2e-9 1.13e
    ↳ -6
<dust_component> "PATH/TO/POLARIS/input/dust/graphite_oblate.dat" 0.3 -3.5 24.2e-9 1.13e
    ↳ -6

#path of the input grid file
<path_grid> "PATH/WHERE/THE/RESULTS/SHOULD/BE/SAVED/rat/grid_rat.dat"

#oath for all output data
<path_out> "PATH/WHERE/THE/RESULTS/SHOULD/BE/SAVED/dust_polarization/"

#considered alignment mechanisms
<align> ALIG_IDG
<align> ALIG_RAT
<align> ALIG_INTERNAL

#additional alignment parameters
<f_c> 0.6 #correlation
<f_highJ> 0.5 #ration of grains at highJ attractor point

#definition of the 1st rotation axis (e.g. x-axis)
<axis1> 1 0 0

#definition of plane detectors (e.g. rotation arround x-axis)
<detector_dust nr_pixel = "320"> 93 96 1 1 0 0 3.1e18 1
<detector_dust nr_pixel = "320"> 93 96 1 1 45 0 3.1e18 1
<detector_dust nr_pixel = "320"> 93 96 1 1 90 0 3.1e18 1

#definition of spherical detectors (e.g. different pos.)
<detector_dust_healpix nr_sides = "256"> 96 96 1 1 1.65e+16 0 0 -80 80 -45 45
<detector_dust_healpix nr_sides = "256"> 96 96 1 1 1.65e+16 0 0 -80 80 -45 45

#uses 32 cores
<nr_threads> 32

#dust to gas mass ratio
<mass_fraction> 0.01 # optional

#stochastic heating for grains with a radius of up to 50nm
<stochastic_heating> 5e-8
</task>

```

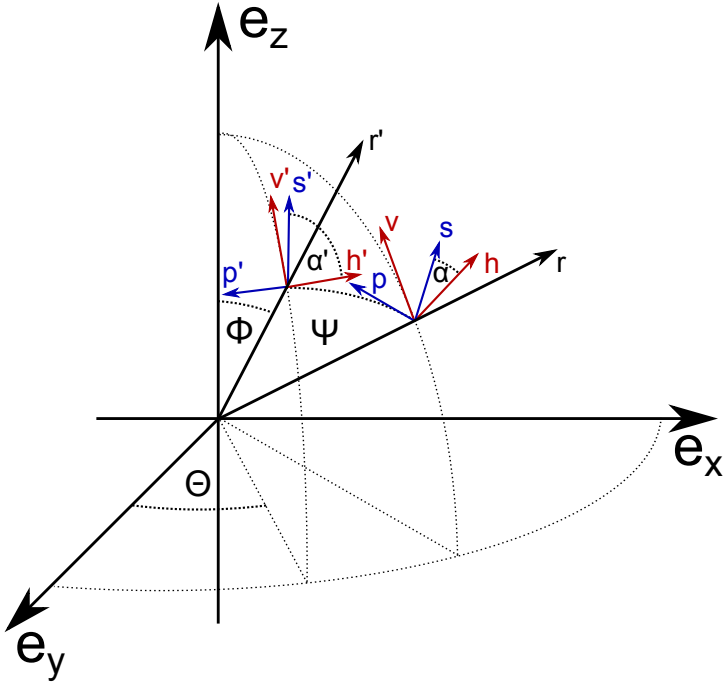


Figure 4.5: Geometrical configuration of scattering on spherical dust grains. The scattered light is redirected along the scattering plane by an angle of ψ . In order to apply the Müller matrix $\hat{S}(\psi)$, the target coordinate system $(\vec{p}, \vec{s}, \vec{r})$ has to be transformed in the lab coordinate system $(\vec{v}, \vec{h}, \vec{r})$ along the angle α .

and the polarization state of light becomes altered where as the wavelength remains the same. When describing polarized light at the physical level of radiative transfer theory, the change in the Stokes vector can be calculated with the help of the Müller matrix or scattering matrix $\hat{S}(\psi)$. The elements of the Müller matrix are dependent and for spherical dust grains we get

$$\hat{S}(\psi) = \begin{pmatrix} S_{11} & S_{12} & 0 & 0 \\ S_{12} & S_{11} & 0 & 0 \\ 0 & 0 & S_{33} & S_{34} \\ 0 & 0 & -S_{34} & S_{33} \end{pmatrix}. \quad (4.69)$$

Note that the scattering matrix elements are also a function of material, grain size, wavelength and scattering angle. The parameters of the Stokes vector before \vec{I} and after \vec{I}' each scattering event is determined by the Müller matrix with $\vec{I}' \propto \hat{S}(\psi)\vec{I}$. The direction of propagation \vec{r}' after the scattering defines the so called scattering plane with the original direction of radiation \vec{r} . The coordinate system of the Stokes vector $(\vec{r}, \vec{h}, \vec{v})$ is usually defined with respect to an external coordinate system. Here, \vec{v} is parallel to the z-axis of the external coordinate system and perpendicular to the direction of propagation \vec{r} with $\vec{h} = \vec{v} \times \vec{r}$. In order to apply the Müller matrix the Stokes vector has to be transformed into the same coordinate system as the scattering plane $(\vec{p}, \vec{s}, \vec{v})$ where \vec{p} is in the scattering plane and $\vec{s} = \vec{p} \times \vec{r}$. The rotation angle α is defined to be between the vectors \vec{s} and \vec{h} and the scattering angle ψ between \vec{r}' and \vec{r} is defined by

$$\cos(\psi) = \vec{r}' \cdot \vec{r}. \quad (4.70)$$

Since the Stokes parameters I and V are invariant under transformation, the rotation matrix that transforms the Stokes vector into the coordinate system of the scattering plane is:

After the scattering event, the stokes vector is in the new coordinate system ($\vec{r}', \vec{h}', \vec{v}'$). In order to align the new coordinate system again with the external coordinate system, the Stokes vector has to be rotated by an angle of α' . Finally, the change in the Stokes vector because of scattering can be calculated with

$$\vec{S}' = \hat{R}(-\alpha) \hat{S}(\psi) \hat{R}(\alpha') \vec{S}. \quad (4.71)$$

After each scattering event a new direction of the photon package has to be determined. For scattering on spherical dust grains the phase function is $\Phi(\theta) \propto S_{11}(\theta)$.

An example file for dust scattering may be written as Listing 4.4

4.7 Line radiative transfer (LRT)

In contrast to dust RT the in LRT a transition between two characteristic energy level $E_i \leftrightarrow E_j$ of a certain gas species occurs at a distinct frequency ν_{ij} . Here, the sub-indices i and j refer to the upper and lower energy level, respectively. The probability for the different kinds of possible transition are characterized by the Einstein coefficients A_{ij} for spontaneous emission, B_{ij} for stimulated emission, and B_{ji} for absorption. Additionally, we consider the collisional (de-)excitation with the collision rate $C_{ij} = n_c \gamma_{ij}$ where n_c is the number density of the collision partners and γ_{ij} is the collision rate. The number density n_c can be taken from the input grid while the transitions coefficients are provided by a LAMDA molecular parameters file (see Sect. 3.5).

Focusing on a single line transition between the upper level j to the lower level i the RT equation can be written as

$$\frac{dI_{ij}}{d\ell} = -\kappa_{ij} I_{ij} + j_{ij} \quad (4.72)$$

where emission coefficient $j_{i,j}$ and absorption coefficient $\kappa_{i,j}$. Here, polarization does not play a role and the RT problem is fully described by the propagation of the intensity I .

In POLARIS the thermal movement of gas species is considered to be the dominant cause of line broadening. The cubic spline interpolation of the velocity (see Sect. 4.3.1 and Sect. 4.1.5) and the RKF45 solver ensures that the broadened transition lines smoothly overlap. Hence, the characteristic transition frequency ν_{ij} is no longer a single peak but follow a Gaussian distribution function

$$\Phi_{i,j}(\nu) = \frac{c}{\sqrt{\pi} v_{\text{tot}} \nu} \exp\left(-\left[\frac{c(\nu - \nu_{i,j})}{v_{\text{tot}} \nu}\right]^2\right) \quad (4.73)$$

Here, c is the speed of light and the total thermal velocity is

$$v_{\text{tot}} = \sqrt{\left(\frac{2k_B T_g}{m_{\text{mol}}}\right)^2 + v_{\text{turb}}^2} \quad (4.74)$$

where v_{turb} is the micro-turbulent component and $\frac{2k_B T_g}{m_{\text{mol}}}$ is the kinetic velocity of the gas species. Hence, the coefficients of absorption and emission can be written as

$$j_{i,j} = \frac{\hbar\nu}{4\pi} N n_i A_{i,j} \Phi_{i,j}(\nu) \quad (4.75)$$

and

$$\alpha_{i,j} = \frac{\hbar\nu}{4\pi} N (n_j B_{j,i} - n_i B_{i,j}) \Phi_{i,j}(\nu) \quad (4.76)$$

respectively, where n_i is the number of electrons on the i -th level. Balancing the full RT equation with the contributions of collisional excitation and de-excitation and the mean intensity

$$J_{i,j} = \frac{1}{4\pi} \int \int I_\nu \Phi_{i,j}(\nu) d\Omega d\nu \quad (4.77)$$

gives

Listing 4.4: Example command file to calculate the stellar emission scattered at dust grains.

```

<task> 1
# polarization by dust scattering
<cmd> CMD_DUST_SCATTERING

#A star in the center as radiation source
<source_star nr_photons = "1e6"> 0 0 0 1 6000

# Silicate as only dust components
<dust_component> "PATH/T0/POLARIS/input/dust/silicate_oblate.dat" 0.7 -3.5 24.2e-9 1.13e
    ↪ -6
<dust_component> "PATH/T0/POLARIS/input/dust/graphite_oblate.dat" 0.3 -3.5 24.2e-9 1.13e
    ↪ -6

#path of the input grid file
<path_grid> "PATH/WHERE/THE/RESULTS/SHOULD/BE/SAVED/temp/grid_temp.dat"

#path for all output data
<path_out> "PATH/WHERE/THE/RESULTS/SHOULD/BE/SAVED/mc_dust/"

# phase function has is Mie scattering
<phase_function> PH_MIE

# enforced first scattering is switched on
<enfsca> 1

# definition of the first detector
<detector_dust_mc nr_pixel = "290"> 1e-6 2e-6 2 0 0 4.31998E+18
# definition of a second detector
<detector_dust_mc nr_pixel = "290"> 1e-6 2e-6 2 0 0 4.31998E+18

# star as radiation source
<source_star nr_photons = "1000000"> 0.0001 0.0001 0.0001 2 4000

uses 32 cores
<nr_threads> 32

#dust to gas mass ratio
<mass_fraction> 0.01 # optional
</task>

```

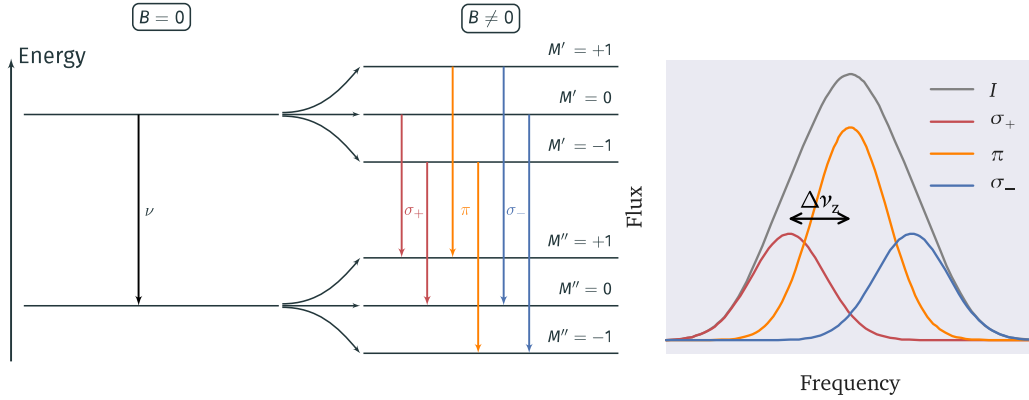


Figure 4.6: Left panel: Splitting of molecular lines transitions in the absence and presence of a magnetic field. Right panel: Line profile of the π and σ_{\pm} transitions with thermal, natural, as well as pressure broadening.

$$\sum_{i>j} [n_i A_{ij} + (n_i B_{ij} - n_j B_{ji}) J_{i,j}] - \sum_{i<j} [n_j A_{ji} + (n_j B_{ji} - n_i B_{ij})] + \sum_i (n_i C_{ij} + n_j C_{ji}) \quad (4.78)$$

This system of equations is solved with the help of Gaussian elimination.

The command to define all the parameters for a gas species to be observed is

```
<gas_species> "path" POP a
```

Here, the path gives the LAMDA gas species parameters file, a is the abundance with respect to the total gas density, and POP stands for the index for the different implemented methods for calculating the level populations (1: LTE, 2: FEP, 3: LVG; see Sect. 4.7.1).

Example:

```
<gas_species> "/PATH/TO/POLARIS/input/gas/co.dat" 2 1e-7
```

The defined gas species can then selected by a line detector with an ID coinciding with the order of appearance in the command file (see Sect. 4.5 for defining the line detector).

4.7.1 Level population approximations

In order to perform LRT simulations one needs to calculate the level populations. Several numerical methods are known to calculate level populations considering different local conditions.

Local thermodynamic equilibrium (LTE)

For this approximation it is assumed that the different level populations are thermalized meaning that excitation temperature T_{exc} and kinetic gas temperature T_g are equal:

$$T_g = T_{\text{exc}} = \frac{\hbar v_{i,j}}{k_B} \left[\ln \left(\frac{g_i n_j}{g_j n_i} \right) \right]^{-1} \quad (4.79)$$

Here, n_i is the number of electrons in the i -th level of the gas species, g_i is the corresponding statistical weight and $v_{i,j}$ is the frequency characteristic for that transition. Hence, the level populations follow the Boltzmann distribution with

$$\frac{n_i}{n_j} = \frac{g_i}{g_j} \exp \left(\frac{\hbar v_{i,j}}{k_B T_g} \right) \quad (4.80)$$

This approximation can be adequate when the optical depth of a transition is so high that the collisional and radiative excitations and de-excitation, respectively, are approximately in equilibrium. In order to apply LTE in LRT simulations the flag `POP_LTE` need to be added in the command line defining the gas species.

Full escape probability (FEP)

FEP assumes that any newly created photon can escape the grid without any further interactions. The level populations can then be calculated by simply applying an external radiation field $J_{i,j} = J_{\text{ext}}$ to Eq. 4.78.

Hence, the FEP method applies for low molecular abundances. Considering FEP in a POLARIS run the flag `POP_LTE` needs to be added.

Large velocity gradient (LVG)

This approximation assumes that a photon can easily escape from the grid because of a large gradient in the velocities of neighboring regions. For the LVG the mean intensity is due to the local transition and an external radiation field

$$J_{i,j} = (1 - \beta)S_{i,j} + \beta J_{\text{ext}} \quad (4.81)$$

Here, β is the probability for the photons to escape from the grid and is given by

$$\beta = \frac{1 - \exp(-\tau_{i,j})}{\tau_{i,j}} \quad (4.82)$$

where as

$$S_{i,j} = \frac{j_{i,j}}{\alpha_{i,j}} = \frac{n_i A_{i,j}}{n_j B_{ji} - n_i B_{ij}} \quad (4.83)$$

is the source function of the transition. For this approximation the required optical depth $\tau_{i,j}$ can be calculated as

$$\tau_{ij} = \frac{c^3 n_g A_{ij}}{8\pi v_{ij}^3 |dv/dI|} \left(\frac{g_i}{g_j} n_j - n_i \right) \quad (4.84)$$

given a large enough velocity gradient $|dv/dI|$. This approximation can be applied when the variations in velocity are larger than the local thermal and micro-turbulent velocities. Using LVG requires the tag `POP_LVG`. At the beginning of each LRT run POLARIS pre-calculates the level population for each cell of the grid. The methods of LTE and FEP require little computational efforts. In contrast, LVG is more time consuming for a large number of cells since its need to solve Eq. 4.78 iteratively. However, the calculation of level populations is parallelized in POLARIS.

HINTS:

- If the abundance a is negative, this number means the abundance is taken from the input grid.

An exemplary LRT command file in POLARIS may look like as shown in Listing 4.5.

4.7.2 LRT with Zeeman effect

In POLARIS, the implementation of LRT including Zeeman splitting is based on the work of Larsson et al. (2014). The energy levels of a gas species can split into separate distinct sub-level when a gas species is exposed by an external magnetic field (see Sect. 4.6). This splitting of spectral lines is referred as to Zeeman effect. Here, the degeneracy of the sub-level is given by $2J + 1$ and the magnetic quantum number can get the values of

$$m_j = [-J, -J + 1, \dots, J - 1, J]. \quad (4.85)$$

Listing 4.5: Example command file to calculate the spectral line emission of a gas species.

```

<task> 1
# command that defines the line radiative transfer
<cmd> CMD_LINE_EMISSION

# no subpixeling
<max_subpixel_lvl> 0

# a star in the center as radiation source
<source_star nr_photons = "1e6"> 0 0 0 1 6000

# graphite as a single dust component
<dust_component> "PATH/TO/POLARIS/input/dust/graphite_oblate.dat"

#path of the input grid file
<path_grid> "PATH/WHERE/THE/RESULTS/SHOULD/BE/SAVED/temp/grid_temp.dat"

#path for all output data
<path_out> "PATH/WHERE/THE/RESULTS/SHOULD/BE/SAVED/mc_dust/"

# definition of the rotation axes
<axis1> 1 0 0
<axis2> 0 1 1

# 1st gas species is SO
<gas_species> "/home/data/so.dat" 1 1e-7
# 2nd gas species is CO
<gas_species> "/home/data/co.dat" 1 1e-5

#detector for 1st gas species with transition nr. 4 in LAMDA file)
<detector_line nr_pixel = "380" vel_channels = "35"> 1 4 1 1e5 0 0 4.73E+016
#detector for 2nd gas species with transition nr. 3 in LAMDA file)
<detector_line nr_pixel = "380" vel_channels = "35"> 2 3 1 1e5 0 0 4.73E+016

uses 32 cores
<nr_threads> 32

#dust to gas mass ratio
<mass_fraction> 0.01 # optional
</task>

```

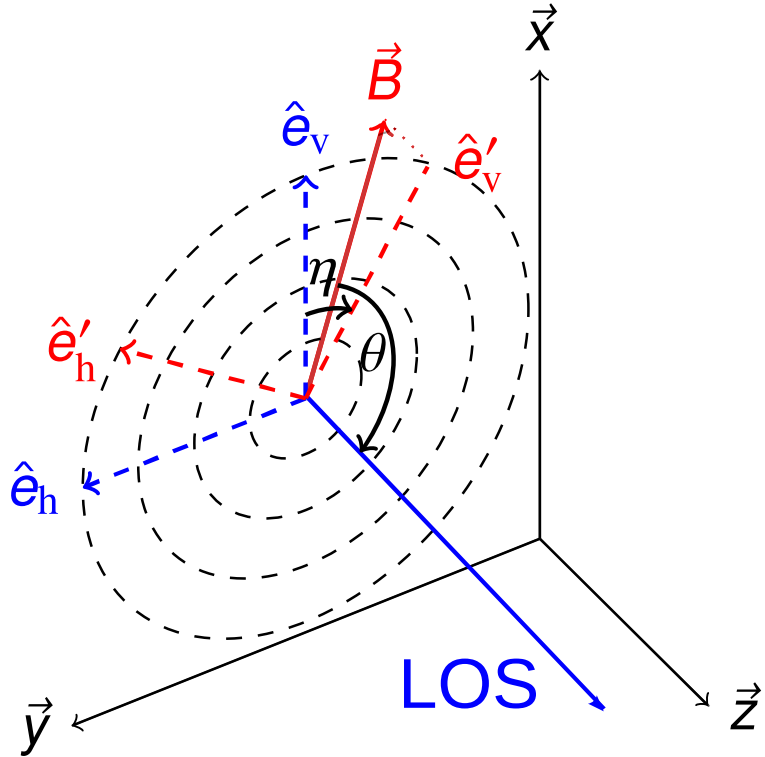


Figure 4.7: Definition of the coordinate systems and rotation angle for the LRT with Zeeman effect. The external coordinate system given by the unit vectors \hat{e}_v and \hat{e}_h and the coordinate system of the Stokes vector is defined by \hat{e}'_v and \hat{e}'_h . The angle η is between the two vectors \hat{e}_v and \hat{e}'_v while the angle θ is between the magnetic field \vec{B} and the LOS.

The energy of any transition is given by:

$$\Delta E = -(\bar{\mu} \vec{B}) = g_J \mu_0 \Delta m_J B. \quad (4.86)$$

Here, B is the magnetic field strength, μ_0 is the Bohr magneton. The Landè factor g_J is defined as a fraction of quantum numbers and a gas species specific constant g_s by

$$g_J = g_s \frac{J(J+1) + S(S+1) + N(N+1)}{2J(J+1)}. \quad (4.87)$$

The difference in energy between different sub-level allows to calculate the characteristic frequency of each transition

$$\nu_0 = \frac{B \mu_0}{h} (g_{J'} m_{J'} - g_{J''} m_{J''}) \quad (4.88)$$

where ' and '' indicate the upper and lower sub-level, respectively.

However, not all permutations of transitions are possible. The rules for allowed transitions are $\Delta m_J = \pm 1$ (called σ_{\pm} transition), $\Delta m_J = 0$ (π transition) if $\Delta J = 0, \pm 1$.

As with dust polarization the LRT problem needs to be solved in the Stokes vector formalism, since the Zeeman effect leads to light polarization. The equation of LRT including the Zeeman effect is similar to Eq. 4.6 and can be written as:

$$\frac{d\vec{I}_v}{d\ell} = -(\hat{K}_{v,A} + \hat{K}_{v,B})(\vec{I}_v - \vec{S}_v). \quad (4.89)$$

The matrices $\hat{K}_{v,A}$ and $\hat{K}_{v,B}$ are for extinction and magneto-optical effects. For extinction the matrix can be calculated as

$$\hat{K}_{v,A} = \frac{n_i}{2} s_{N',N'',J',J''} \sum_{m',m''} (s_{m',m''} F_A(v', a) \hat{A}_{m',m''}) \quad (4.90)$$

and the magneto mechanical matrix is defined to be:

$$\hat{K}_{v,B} = n_i s_{N',N'',J',J''} \sum_{m',m''} (s_{m',m''} F_B(v', a) \hat{B}_{m',m''}) . \quad (4.91)$$

Here, $s_{N',N'',J',J''}$ is the line strength for the $N' \rightarrow N''$ and $J' \rightarrow J''$ transition and $s_{m',m''}$ is the relative line strength between the Zeeman $m_J \rightarrow m_J'$ sub-level.

The angles θ and η are defined to be between magnetic field and line of sight and the coordinate system of the Stokes vector and the coordinate system of the model space (see Fig. 4.7 for details) in order to take care of an arbitrary orientations. This allow to calculate the polarization rotation matrices

$$\hat{A}_{\sigma\pm} = \begin{pmatrix} 1 + \cos^2(\theta) & \cos(2\eta) \sin^2(\theta) & \sin(2\eta) \sin^2(\theta) & \mp \cos(\theta) \\ \cos(2\eta) \sin^2(\theta) & 1 + \cos^2(\theta) & 0 & 0 \\ \sin(2\eta) \sin^2(\theta) & 0 & 1 + \cos^2(\theta) & 0 \\ \mp \cos(\theta) & 0 & 0 & 1 + \cos^2(\theta) \end{pmatrix} \quad (4.92)$$

and

$$\hat{A}_\pi = \begin{pmatrix} \sin^2(\theta) & -\cos(2\eta) \sin^2(\theta) & -\sin(2\eta) \sin^2(\theta) & 0 \\ -\cos(2\eta) \sin^2(\theta) & \sin^2(\theta) & 0 & 0 \\ \sin(2\eta) \sin^2(\theta) & 0 & \sin^2(\theta) & 0 \\ \mp \cos(\theta) & 0 & 0 & 1 + \cos^2(\theta) \end{pmatrix} \quad (4.93)$$

for the σ_\pm and π transitions, respectively. For the magneto-optical effects the rotation matrices are defined as

$$\hat{B}_{\sigma\pm} = \begin{pmatrix} 0 & 0 & 0 & 0 \\ 0 & 0 & \mp 2 \cos(\theta) & \sin(2\eta) \sin^2(\theta) \\ 0 & \mp 2 \cos(\theta) & 0 & -\cos(2\eta) \sin^2(\theta) \\ 0 & \sin(2\eta) \sin^2(\theta) & -\cos(2\eta) \sin^2(\theta) & 0 \end{pmatrix} \quad (4.94)$$

and

$$\hat{B}_\pi = \begin{pmatrix} 0 & 0 & 0 & 0 \\ 0 & 0 & 0 & -\sin(2\eta) \sin^2(\theta) \\ 0 & 0 & 0 & -\cos(2\eta) \sin^2(\theta) \\ 0 & \sin(2\eta) \sin^2(\theta) & -\cos(2\eta) \sin^2(\theta) & 0 \end{pmatrix} . \quad (4.95)$$

Subsequently, for the polarization exist two extreme cases. In the first case the magnetic field is parallel along the line of sight. Here, the Zeeman effect is governed by the σ_\pm transitions and radiation becomes only circularly polarized. In the second case B is perpendicular along the line of sight coming with the σ_\pm transitions polarized vertically to the magnetic field and the π transition polarized horizontally to the magnetic field. The relative line strength $s_{m',m''}$ is defined for each transition as a characteristic fraction of quantum numbers (see Tab. 4.1).

ΔJ	π	σ_\pm
+1	$\frac{3(J+1)^2 - 3m_J^2}{2(J+1)(2J+1)(2J+3)}$	$\frac{3(J+1 \pm m_J)(J+2 \pm m_J)}{4(J+1)(2J+1)(2J+3)}$
0	$\frac{3m_J^2}{J(J+1)(2J+1)}$	$\frac{3(J \mp m_J)(J+1 \pm m_J)}{2J(J+1)(2J+1)}$
-1	$\frac{3J^2 - 3m_J^2}{2J(2J-1)(2J+1)}$	$\frac{3(J \mp m_J)(J-1 \mp m_J)}{4J(2J-1)(2J+1)}$

Table 4.1: Relative line strength $s_{m',m''}$ for different ΔJ , π , and σ_\pm transitions.

As with simple LRT without Zeeman effects the characteristic Zeeman transitions are thermally broadened caused by different relative velocities of the gas species with respect to the observer. Additionally,

Zeeman transitions are naturally broader as a consequence of quantum mechanics. Energy states with a shorter decay rate is associated with a larger uncertainty in energy and vice versa because of Heisenberg's uncertainty principle. Consequently, the transition frequency is broader dependent on the decay rate of each level. Occasional collisions with other gas species can cause collisional de-excitations. This depends on the pressure of the gas and each line shape broadens even more.

In Eq. 4.90 and Eq. 4.91, the functions $F_A(v', a)$ and $F_B(v', a)$ are the line shape function that models the thermal, natural, as well as pressure broadening of line transition. The parameters are defined to be as $v' = \frac{v_0 + \Delta v_0 - v}{v_D}$, $a = \frac{\gamma}{4\pi\Delta v_D}$ where Δv_D is the Doppler broadening width and γ is the pressure broadening width. Both $F_A(v', a)$ and $F_B(v', a)$ can be combined resulting in the Faddeeva function defined as

$$w(z) = F_A(v', a) + iF_B(v', a) = \frac{1}{2\pi} \int_{-\infty}^{\infty} \frac{e^{-y^2}}{z - y} dy \quad (4.96)$$

with $z = v' + ia$. In the POLARIS code the solution to this problem is solved with the help of the C++ Faddeeva package ¹. The Faddeeva function may in principle also be applied for simple LRT. However, the LAMDA files do not provide the necessary parameters to do so. This may be solved in a future version of POLARIS. For Zeeman splitting there is a correlation between the Stokes V parameter and the first velocity derivative dI/dv

$$V = \frac{dI}{dv} \Delta v \cos(\theta) \quad (4.97)$$

where

$$\Delta v = \frac{\mu_0}{h} (g_J' m_J' - g_J'' m_J'') . \quad (4.98)$$

Bohr magneton μ_0 and the Planck constant h are known and the quantities g_J' and m_J' can be pre-calculated for each gas species. Hence, the line of sight magnetic field strength $B \cos(\theta)$ can be calculated with POLARIS by simulating the Stokes I and V parameters and the subsequent fitting of $\frac{dI}{dv}$ onto V .

In POLARIS a LRT run including the Zeeman effect is almost identical to a simple RT as presented in the previous section. However, simulating the Zeeman effect requires the quantities of the Landè factor (see Eq. 4.87) and the relative line strength (see Tab. 4.1). The values for these quantities need to be delivered in an extra file (see Sect. 3.5.2) corresponding to the Leiden molecular file. Instead of a single path for the LAMDA file one needs to add a second path to the corresponding Zeeman file:

```
<gas_species> "path" POP a "path Zeeman"
```

Example:

```
<gas_species> "/PATH/T0/POLARIS/input/gas/oh.dat" 1 1e-5 "/PATH/T0/POLARIS/input/gas/
    ↪ oh_zeeman.dat"
```

An exemplary LRT command file in POLARIS with Zeeman splitting may look like as shown in Listing 4.6.

4.8 Synchrotron RT

When a moving electron is forced on a curved path or an orbit it emits radiation. In particular free electrons in the ISM gyrate around the magnetic field lines. This leads to polarized radiation as well as rotation of the polarization plane of background radiation (Faraday effect).

For a complete synchrotron RT, one needs to consider two different species of electrons: cosmic ray (CR) electrons and thermalized relativistic electrons. Synchrotron intensity as well as linear and circular polarization emerges mostly from CR electrons whereas thermal electrons dominate Faraday rotation (FR) and Faraday conversion (FC). The synchrotron RT problem can be solved with integrals over modified Bessel functions. However, due to performance reasons the implementation in POLARIS follows

¹ http://ab-initio.mit.edu/wiki/index.php/Faddeeva_Package, Copyright © 2012 Massachusetts Institute of Technology

Listing 4.6: Example command file to calculate the spectral line emission with Zeeman splitting of a gas species.

```

<task> 1
# command that defines the line radiative transfer
<cmd> CMD_LINE_EMISSION

# no subpixeling
<max_subpixel_lvl> 0

# a star in the center as radiation source
<source_star nr_photons = "1e6"> 0 0 0 1 6000

# graphite as a single dust component
<dust_component> "PATH/TO/POLARIS/input/dust/graphite_oblade.dat"

#path of the input grid file
<path_grid> "PATH/WHERE/THE/RESULTS/SHOULD/BE/SAVED/temp/grid_temp.dat"

#path for all output data
<path_out> "PATH/WHERE/THE/RESULTS/SHOULD/BE/SAVED/mc_dust/"

# definition of the rotation axes
<axis1> 1 0 0
<axis2> 0 1 1

# 1st gas_species is S0
# this gas_species is WITHOUT Zeeman effect
<gas_species> "PATH/TO/POLARIS/input/gas/s0.dat" 1 1e-7

# 2nd gas_species is OH
# the abundance is taken from the 3rd position (hence -3) of the grid ratios
# this gas_species is WITH Zeeman effect
<gas_species> "PATH/TO/POLARIS/input/gas/oh.dat" 1 -3 "PATH/TO/POLARIS/input/gas/
    ↪ so_zeeman.dat"

# detector for 1st gas species with transition nr. 4 in LAMDA file)
<detector_line nr_pixel = "380" vel_channels = "35"> 1 4 1 1e5 0 0 4.73E+016
# detector for 2nd gas_species with transition nr. 2 in LAMDA file AND Zeeman file)
<detector_line nr_pixel = "380" vel_channels = "35"> 2 2 1 1e5 0 0 4.73E+016
# detector for 2nd gas_species with transition nr. 3 in LAMDA file AND Zeeman file)
<detector_line nr_pixel = "380" vel_channels = "35"> 2 3 1 1e5 0 0 4.73E+016

#uses 32 cores
<nr_threads> 32

#dust to gas mass ratio
<mass_fraction> 0.01 # optional
</task>

```

the approach of applying fitting functions approximating the integral solutions. These fitting functions provide high accuracy solutions for typical ISM-like conditions. The implementation in POLARIS is based on the equations and fitting functions presented in Pandya et al. (2016) and Dexter (2016).

4.8.1 CR electrons

The energy of CR electrons follow a power-law distribution

$$N_{\text{CR}}(\gamma) = \begin{cases} n_{\text{CR}} \gamma^p (p-1) (\gamma_{\min}^{p-1} - \gamma_{\max}^{p-1}) & \text{if } \gamma_{\min} < \gamma < \gamma_{\max} \\ 0 & \text{otherwise} \end{cases} \quad (4.99)$$

where $\gamma = (1 - \beta^2)^{1/2}$ is the Lorentz factor, $\beta = v/c$, n_{CR} is the CR electron density, p is a power-law index. The distribution has sharp lower and upper at cut-offs γ_{\min} and γ_{\max} , respectively.

By rotating the Stokes vector in the direction of the magnetic field, some of the coefficients can be eliminated. For extinction this leads to $\alpha_U = \kappa_U = 0$ and for the emissivity coefficient $j_U = 0$.

The remaining coefficients of emissivity can be approximately be calculated by

$$j_I(\lambda) = \gamma_{\min}^{1-p} \frac{1}{\lambda_c} \frac{n_{\text{CR}} e^2 3^{\frac{p}{2}} (p-1) \sin(\theta)}{2(p+1) (\gamma_{\min}^{1-p} - \gamma_{\max}^{1-p})} \times \Gamma\left(\frac{3p-1}{12}\right) \Gamma\left(\frac{3p+19}{12}\right) \left(\frac{\lambda_c}{\lambda \sin(\theta)}\right)^{-\frac{p-1}{2}}, \quad (4.100)$$

$$j_Q(\lambda) = j_I(\lambda) \left(-\frac{p+1}{p+7/3}\right), \quad (4.101)$$

and

$$j_V(\lambda) = j_I(\lambda) \left(-\frac{171}{250} \frac{\lambda_c p^{\frac{1}{2}}}{3\lambda \tan(\theta)}\right) \quad (4.102)$$

where $\Gamma(x)$ is the gamma function, the angle θ is between the direction of light propagation and the magnetic field, and the quantity

$$\lambda_c = \frac{2\pi m_e c^2}{eB} \quad (4.103)$$

is defined to be the characteristic cyclotron wavelength. It follows that the maximal possible degree of linear polarization is directly connected to the power-law index p since:

$$\max(P_l) = \frac{|j_Q|}{j_I} = \frac{p+1}{p+7/3}. \quad (4.104)$$

The approximate solutions of CR electron emission coefficients are

$$\alpha_I(\lambda) = \gamma_{\min}^{1-p} \frac{n_{\text{CR}} e^2}{v m_e c} \frac{3^{\frac{p+1}{2}} (p-1)}{4 (\gamma_{\min}^{1-p} - \gamma_{\max}^{1-p})} \times \Gamma\left(\frac{3p+12}{12}\right) \Gamma\left(\frac{3p+22}{12}\right) \left(\frac{\lambda_c}{\lambda \sin(\theta)}\right)^{-\frac{p+2}{2}}, \quad (4.105)$$

$$\alpha_Q(\lambda) = \frac{996 \alpha_I(\lambda)}{1000} \left(-\frac{3(p-1)^{\frac{43}{500}}}{4}\right), \quad (4.106)$$

and

$$\alpha_V(\lambda) = \alpha_I(\lambda) k_V(\theta) \left[-\frac{7}{4} \left(\frac{71p}{100} + \frac{22}{625}\right)^{\frac{197}{500}}\right] \times \left[\left(\sin^{-\frac{48}{25}}(\theta) - 1\right)^{\frac{64}{125}} \left(\frac{\lambda_c}{\lambda}\right)^{-\frac{1}{2}}\right]. \quad (4.107)$$

In contrast to polarized RT with dust, for synchrotron there is also a conversion between the Stokes components I and V as well as Q and U . However, for CR electrons the Faraday coefficients have just an minor effect on linear polarization compared to those of thermal electrons and we consider them approximately to be $\kappa_Q = \kappa_V = 0$.

4.8.2 Thermal electrons

Thermal electrons follow a Maxwell Jüttner distribution (a relativistic Maxwellian energy distribution):

$$N_{\text{th}}(\gamma) = \frac{n_{\text{th}} \gamma^2 \beta \exp(-\gamma/\Theta)}{\Theta K_2(1/\Theta)} \quad (4.108)$$

where n_{th} is the thermal electron density and the dimensionless temperature is defined as

$$\Theta = \frac{k_B T_e}{m_e c^2} \quad (4.109)$$

Here, k_B is the Boltzmann constant, T_e is the electron temperature and m_e is the electron mass. For typical ISM and molecular cloud conditions $\Theta \ll 1$. Hence, thermal electrons do not contribute to emission and absorption and we assume $j_{l,Q,V} = \alpha_{l,Q,V} = 0$. In the case of thermal electrons the coefficients of FR and FC can be written as

$$\kappa_Q(\lambda, \delta) = -\frac{1}{4\pi^2} \frac{n_{\text{th}} e^4 B^2}{m_e^3 c^6} \lambda^3 \quad (4.110)$$

and

$$\kappa_V(\lambda, \delta) = -\frac{1}{\pi} \frac{n_{\text{th}} e^2 B}{m_e^2 c^4} \lambda^2 \cos(\delta). \quad (4.111)$$

4.8.3 Synchrotron run with both electrons species

A synchrotron run in POLARIS requires at least the parameters for the CR electron component meaning the quantities of number density of CR electrons n_{CR} , the minimal Lorentz-factor γ_{\min} , the maximal Lorentz-factor γ_{\max} , and the power-law index p need to be provided by the grid (see Tab. 3.3 for details). The distribution of thermal electrons n_{th} is optional.

When CR electron as well thermal electrons are defined in the grid POLARIS solves the RT equation considering both species simultaneously with as well as the isolated components meaning. Consequently, the resulting POLARIS synchrotron detector file contains two times the information compared to a POLARIS dust detector file.

An exemplary synchrotron command file is shown in Listing 4.7.

Listing 4.7: Example command file to calculate the synchrotron polarization and emission.

```

<task> 1
<cmd> CMD_SYNCHROTRON #command that defines the synchrotron ray-tracing

#plane synchrotron detector
<detector_sync nr_pixel = "800"> 7.35E-01 7.35E-01 1 1 45.0 45.0 1.543e+19

#maximal sub-pixel level
<max_subpixel_lvl> 0

#input grid incuding gas and electron densities
<path_grid> "/home/User/synchrotron/grid.dat"

#path for the results
<path_out> "/home/User/synchrotron/results/pol_syn/"

#number of threads
<nr_threads> 64

#plotting of the input midplanes
<write_inp_midplanes> 128

#define of the rotation axis
<axis1> 1 1 0 #optional
<axis2> 0 1 1 #optional

</task>

```

5 Output data

POLARIS creates automatically all the directorys it needs to store the resulting simulation data and plots if they do not already exist. Hence, there's no need for the user to create any extra directory in advance. The output path is completely defined by the command:

```
<path_out> "output_path"
```

were the path needs to follow the rules of the applied operating system (e.g. Windows or Linux).

Example:

```
# Linux path  
<path_out> "/home/user/polaris_projects/results/important_project01/"
```

```
# Windows path  
<path_out> "C:\user\polaris_projects\results\important_project01\"
```

If a directory is missing along the hierarchy of the path it will be created by POLARIS from there. It is also recommended to use absolute paths instead of paths relative to the directory containing the POLARIS executable. Additionally, POLARIS creates two the two directory for **data/** and **plots/** in the **output_path/**.

After each POLARIS simulation, the results are stored in the **data** directory. The only exception is the resulting grid file. Here, POLARIS saves each newly created grid directly into the **output_path/**.

5.1 Output grids

The POLARIS simulations to calculate the dust temperature distribution (CMD_TEMP) and the calculation of the maximal dust grain alignment radius a_{alg} (CMD_RAT) create a new grid including these information. These grids have exactly the same file format as the input grid. If there is no data position reserved in the input grid, then the data length of the grid will be extended. In this case the total size of the resulting grid will be larger than the input grid. However, if the input grid already contains the values of dust temperature or alignment radius, these parameters will be overwritten. For the dust temperature distribution, the amount of additional data positions varies depending on the chosen command. If **<full_dust_temp>** is enabled, a data position of the dust temperature for each dust grain size will be created and filled in the grid. If **<stochastic_heating>** **max_size** is set, the dust grains with a size less than the **max_size** get, in addition to **<full_dust_temp>**, a data position for each temperature defined in the **'heat_capacity.dat'** file.

The new grids have the file names **'grid_temp.dat'** in the case of dust heating and **'grid_rat.dat'** in the case of the maximal dust grain alignment radius a_{alg} , respectively. These grids are the only files that are directly written into the output path instead of the **data/** directory.

HINT: Each newly created grid is in SI and no further unit conversion is require for any followup simulation.

5.2 Detector files

Most results from POLARIS simulations are saved as **'.fits'** files¹. To realize this, POLARIS takes advantage of the CCfits² and cfitsio³ packages. The POLARIS package is shipped with both libraries

¹General information about **'.fits'** files can be found at https://fits.gsfc.nasa.gov/fits_documentation.html

²See <https://heasarc.gsfc.nasa.gov/fitsio/ccfits/>

³See <https://heasarc.gsfc.nasa.gov/fitsio/fitsio.html>

5 Output data

and the installer takes care of their installation. In the following, the structure of the `'.fits'` files for each simulation will be described.

Midplane cuts

With every run of POLARIS cuts through the midplanes of the grid can be created. Up to two different midplane `'.fits'` files will be created with each task that included the `<write_inp_midplanes>` and/or `<write_out_midplanes>` commands. The `'input_midplane.fits'` file can be created by each run of POLARIS and includes cuts of the quantities contained in the input grid. Each simulation with POLARIS that is creating an output grid (see above) can also create an `'output_midplane.fits'` file that contains the cuts for each quantity that changed or was created due to the simulation (for additional quantities see Tables 3.8). A description of the structure of these midplane `'.fits'` files can be found in Fig. 5.1, which shows the header and additional comments. The header of the midplane files contains three to four different representations (units) of the spatial axes. With a viewing program like `ds9`, switching between these representations can be done by changing the WCS. Example images made with `ds9` can be found in Sect. 6.

If the command `<write_3d_midplanes>` is used, the midplanes are created slightly different. Instead of having slices through each plane (`'xy'`, `'xz'`, `'yz'`), only one plane is used and multiple slices at different positions of the third axis are created to obtain a 3-dimensional impression of the grid quantities.

Emission maps

Simulations of the thermal dust grain emission `CMD_DUST_EMISSION`, the radiation scattered at dust grains `CMD_DUST_SCATTERING` and synchrotron emission `CMD_SYNCHROTRON` will create an emission map with the filename `'polaris_detector_nrXXXX.fits'`. The `'X'` stand for the detector index with four digits (e.g. 0001 for first detector defined in the `'cmd_file'`). In addition to the spatial axes, one axis is provided for the different wavelength IDs and one for the quantities like intensity and optical depth. A description of the structure of these emission map `'.fits'` files can be found in Fig. 5.2, which shows the header and additional comments.

Emission SEDs

Simulations of the thermal dust grain emission `CMD_DUST_EMISSION` and the radiation scattered at dust grains `CMD_DUST_SCATTERING` will create a spectral energy distribution from the emission maps with the filename `'polaris_detector_nrXXXX_sed.fits'`. The `'X'` stand for the detector index with four digits (e.g. 0001 for first detector defined in the `'cmd_file'`). These file are essentially a sum over the spatial axes of the emission maps to provide a fast access to the SED of large simulations. A description of the structure of these emission SED `'.fits'` files can be found in Fig. 5.2, which shows the header and additional comments.

Velocity channel maps

Simulations of the line radiative transfer `CMD_LINE_EMISSION` will create velocity channel maps for each velocity channel with the filenames `'vel_channel_maps_species_XXXX_line_YYYY_vel_ZZZZ.fits'`. The `'X'` stand for the gas species index with four digits, the `'Y'` stand for the transition index with four digits and the `'Z'` stand for the current velocity channel (e.g. 0001_line_0001_vel_0001 for first gas species, the first transition defined in the `'cmd_file'` and the first velocity channel, which is located at `-MAXVEL`). In addition, the column density and the magnetic field analysis (for Zeeman simulations) will be written in an extra file (`'vel_channel_maps_species_XXXX_line_YYYY_extra.fits'`). A description of the structure of these velocity channel maps `'.fits'` files can be found in Fig. 5.4, which shows the header and additional comments.

Figure 5.1: Header of an '`input_midplane.fits`' file including comments to explain the file structure.

```

SIMPLE = T / file does conform to FITS standard
BITPIX = -64 / number of bits per data pixel
NAXIS = 4 / number of data axes
NAXIS1 = 256 / length of data axis 1
NAXIS2 = 256 / length of data axis 2
NAXIS3 = 3 / different planes (xy, xz, yz)
NAXIS4 = 13 / different quantities (see MIDPLANEX)
EXTEND = T / FITS dataset may contain extensions
COMMENT FITS (Flexible Image Transport System) format is defined in 'Astronomy
COMMENT and Astrophysics', volume 376, page 359; bibcode: 2001A&A...376..359H
CTYPE1 = 'PARAM' / type of unit 1
CRVAL1 = -44704051205273.4 / value of axis 1
CRPIX1 = 1 / pixel where CRVAL1 is defined
CDELT1 = 350620009453.125 / delta of axis 1
CUNIT1 = 'm' / unit of axis 1
CTYPE1B = 'PARAM' / type of unit 1
CRVAL1B = -298.828125 / value of axis 1
CRPIX1B = 1 / pixel where CRVAL1 is defined
CDELT1B = 2.34375 / delta of axis 1
CUNIT1B = 'AU' / unit of axis 1
CTYPE1C = 'PARAM' / type of unit 1
CRVAL1C = -0.00144875963301446 / value of axis 1
CRPIX1C = 1 / pixel where CRVAL1 is defined
CDELT1C = 1.13628206510938E-05 / delta of axis 1
CUNIT1C = 'pc' / unit of axis 1
CTYPE2 = 'PARAM' / type of unit 2
CRVAL2 = -44704051205273.4 / value of axis 2
CRPIX2 = 1 / pixel where CRVAL2 is defined
CDELT2 = 350620009453.125 / delta of axis 2
CUNIT2 = 'm' / unit of axis 2
CTYPE2B = 'PARAM' / type of unit 2
CRVAL2B = -298.828125 / value of axis 2
CRPIX2B = 1 / pixel where CRVAL2 is defined
CDELT2B = 2.34375 / delta of axis 2
CUNIT2B = 'AU' / unit of axis 2
CTYPE2C = 'PARAM' / type of unit 2
CRVAL2C = -0.00144875963301446 / value of axis 2
CRPIX2C = 1 / pixel where CRVAL2 is defined
CDELT2C = 1.13628206510938E-05 / delta of axis 2
CUNIT2C = 'pc' / unit of axis 2
HIERARCH MIDPLANE1 = 'gas_density' / quantity of 1. image
HIERARCH MIDPLANE2 = 'gas_temperature' / quantity of 2. image
HIERARCH MIDPLANE3 = 'delta' / quantity of 3. image
HIERARCH MIDPLANE4 = 'mag_total' / quantity of 4. image
HIERARCH MIDPLANE5 = 'mag_x' / quantity of 5. image
HIERARCH MIDPLANE6 = 'mag_y' / quantity of 6. image
HIERARCH MIDPLANE7 = 'mag_z' / quantity of 7. image
HIERARCH MIDPLANE8 = 'vel_total' / quantity of 8. image
HIERARCH MIDPLANE9 = 'vel_x' / quantity of 9. image
HIERARCH MIDPLANE10 = 'vel_y' / quantity of 10. image
HIERARCH MIDPLANE11 = 'vel_z' / quantity of 11. image
HIERARCH MIDPLANE12 = 'mach' / quantity of 12. image
HIERARCH MIDPLANE13 = 'larm' / quantity of 13. image

```

5 Output data

Figure 5.2: Header of an '`polaris_detector_nrXXXX.fits`' file including comments to explain the file structure.

```

SIMPLE = T / file does conform to FITS standard
BITPIX = -64 / number of bits per data pixel
NAXIS = 4 / number of data axes
NAXIS1 = 256 / length of data axis 1
NAXIS2 = 256 / length of data axis 2
NAXIS3 = 1 / the wavelength axis
NAXIS4 = 6 / different quantities (see CUNIT4)
EXTEND = T / FITS dataset may contain extensions
COMMENT FITS (Flexible Image Transport System) format is defined in 'Astronomy
COMMENT and Astrophysics', volume 376, page 359; bibcode: 2001A&A...376..359H
CTYPE1 = 'PARAM' / type of unit 1
CRVAL1 = -44704051205273.4 / value of axis 1
CRPIX1 = 1 / pixel where CRVAL1 is defined
CDELT1 = 350620009453.125 / delta of axis 1
CUNIT1 = 'm' / unit of axis 1
CTYPE1A = ... See midplane header ...
CTYPE2 = 'PARAM' / type of unit 2
CRVAL2 = -44704051205273.4 / value of axis 2
CRPIX2 = 1 / pixel where CRVAL2 is defined
CDELT2 = 350620009453.125 / delta of axis 2
CUNIT2 = 'm' / unit of axis 2
CTYPE2A = ... See midplane header ...
CTYPE3 = 'PARAM' / type of unit 3
CRVAL3 = 1 / value of axis 3
CRPIX3 = 1 / pixel where CRVAL3 is defined
CDELT3 = 1 / delta of axis 3
CUNIT3 = 'Wavelength index' / unit of axis 3
CTYPE4 = 'PARAM' / type of unit 4
CRVAL4 = 1 / value of axis 4
CRPIX4 = 1 / pixel where CRVAL4 is defined
CDELT4 = 1 / delta of axis 4

CUNIT4 = 'I, Q, U, V [Jy/px], optical depth, column density [m^-2]' / unit of axis 4
ETYPE = 'thermal emission' / type of emission
... or ...
CUNIT4 = 'I, Q, U, V, I_direct, I_scat [Jy/px]' / unit of axis 4
ETYPE = 'scattered emission / direct stellar emission' / type of emission
... or ...
CUNIT4 = 'I, Q, U, V, [Jy/px], ...' / unit of axis 4
ETYPE = 'synchotron emission' / type of emission

ID = 1 / detector id
HIERARCH WAVELENGTH1 = 0.000849466675 / value of 1. wavelength
DISTANCE= 4.31994861405407E+18 / distance to object
RAXIS1X = 1. / rotation axes 1 (x component)
RAXIS1Y = 0. / rotation axes 1 (y component)
RAXIS1Z = 0. / rotation axes 1 (z component)
RANGLE1 = 0. / rotation angle 1 [\si{\degree}]
RAXIS2X = 0. / rotation axes 2 (x component)
RAXIS2Y = 1. / rotation axes 2 (y component)
RAXIS2Z = 0. / rotation axes 2 (z component)
RANGLE2 = 0. / rotation angle 2 [\si{\degree}]
DETGRID = 'Plane / Cartesian background grid' / description of the detector grid

```

Figure 5.3: Header of an '`polaris_detector_nrXXXX_sed.fits`' file including comments to explain the file structure.

```

SIMPLE = T / file does conform to FITS standard
BITPIX = -64 / number of bits per data pixel
NAXIS = 3 / number of data axes
NAXIS1 = 1 / the wavelength axis
NAXIS2 = 1 / dummy to have one line, if opened as image
NAXIS3 = 6 / different quantities (see CUNIT4)
EXTEND = T / FITS dataset may contain extensions
COMMENT FITS (Flexible Image Transport System) format is defined in 'Astronomy
COMMENT and Astrophysics', volume 376, page 359; bibcode: 2001A&A...376..359H
CTYPE1 = 'PARAM' / type of unit 1
CRVAL1 = 1 / value of axis 1
CRPIX1 = 1 / pixel where CRVAL1 is defined
CDELT1 = 1 / delta of axis 1
CUNIT1 = 'Wavelength index' / unit of axis 1
CTYPE2 = 'PARAM' / type of unit 2
CRVAL2 = 1 / value of axis 2
CRPIX2 = 1 / pixel where CRVAL2 is defined
CDELT2 = 1 / delta of axis 2
CUNIT2 = 'None' / unit of axis 2

CUNIT3 = 'I, Q, U, V [Jy/px], optical depth' / unit of axis 3
ETYPE = 'thermal emission' / type of emission
... or ...
CUNIT3 = 'I, Q, U, V, I_scat [Jy/px]' / unit of axis 3
ETYPE = 'scattered emission / direct stellar emission' / type of emission

ID = 1 / detector id
HIERARCH WAVELENGTH1 = 0.000849466675 / value of 1. wavelength
DISTANCE= 4.31994861405407E+18 / distance to object
RAXIS1X = 1. / rotation axes 1 (x component)
RAXIS1Y = 0. / rotation axes 1 (y component)
RAXIS1Z = 0. / rotation axes 1 (z component)
RANGLE1 = 0. / rotation angle 1 [ $\text{\si{\degree}}$ ]
RAXIS2X = 0. / rotation axes 2 (x component)
RAXIS2Y = 1. / rotation axes 2 (y component)
RAXIS2Z = 0. / rotation axes 2 (z component)
RANGLE2 = 0. / rotation angle 2 [ $\text{\si{\degree}}$ ]
DETGRID = 'Plane / Cartesian background grid' / description of the detector grid

```

5 Output data

Figure 5.4: Header of a `'vel_channel_maps_species_XXXX_line_YYYY_vel_ZZZZ.fits'` file including comments to explain the file structure.

```

SIMPLE = T / file does conform to FITS standard
BITPIX = -64 / number of bits per data pixel
NAXIS = 3 / number of data axes
NAXIS1 = 256 / length of data axis 1
NAXIS2 = 256 / length of data axis 2
NAXIS3 = 6 / length of data axis 3
EXTEND = T / FITS dataset may contain extensions
COMMENT FITS (Flexible Image Transport System) format is defined in 'Astronomy
COMMENT and Astrophysics', volume 376, page 359; bibcode: 2001A&A...376..359H
CTYPE1 = 'PARAM' / type of unit 1
CRVAL1 = -44704051205273.4 / value of axis 1
CRPIX1 = 1 / pixel where CRVAL1 is defined
CDELT1 = 350620009453.125 / delta of axis 1
CUNIT1 = 'm' / unit of axis 1
CTYPE1A = ... See midplane header ...
CTYPE2 = 'PARAM' / type of unit 2
CRVAL2 = -44704051205273.4 / value of axis 2
CRPIX2 = 1 / pixel where CRVAL2 is defined
CDELT2 = 350620009453.125 / delta of axis 2
CUNIT2 = 'm' / unit of axis 2
CTYPE1A = ... See midplane header ...
CTYPE3 = 'PARAM' / type of unit 3
CRVAL3 = 1 / value of axis 3
CRPIX3 = 1 / pixel where CRVAL3 is defined
CDELT3 = 1 / delta of axis 3
CUNIT3 = 'I, Q, U, V [Jy/px], optical depth, column density [m^-2]' / unit of a
HIERARCH GAS_SPECIES = 'C180' / name of the observed gas_species
TRANS = 1 / transition index number (see leiden database)
HIERARCH LEVEL_UPPER = 2 / upper energy level index number (see leiden dat
HIERARCH LEVEL_LOWER = 1 / lower energy level index number (see leiden dat
FREQ = 109782173400. / frequency of the simulated transition
VCH = 1 / current velocity channel
CHANNELS= 35 / number of velocity channels
MAXVEL = 3000. / maximum velocity of the velocity channels (-max
ZEEMAN = F / is zeeman splitting in the simulations consider
DISTANCE= 4.31994861405407E+18 / distance to object
RAXIS1X = 1. / rotation axes 1 (x component)
RAXIS1Y = 0. / rotation axes 1 (y component)
RAXIS1Z = 0. / rotation axes 1 (z component)
RANGLE1 = 90. / rotation angle 1 [\si{\degree}]
RAXIS2X = 0. / rotation axes 2 (x component)
RAXIS2Y = 1. / rotation axes 2 (y component)
RAXIS2Z = 0. / rotation axes 2 (z component)
RANGLE2 = 0. / rotation angle 2 [\si{\degree}]

```

Integrated velocity channel map

Simulations of the line radiative transfer `CMD_LINE_EMISSION` will create an integrated velocity channel map with the filename '`int_channel_map_species_XXXX_line_YYYY.fits`'. The '`X`' stand for the gas species index with four digits and the '`Y`' stand for the transition index with four digits (e.g. `0001_line_0001` for first gas species and first transition defined in the '`cmd_file`'). A description of the structure of these integrated velocity channel map `.fits` files can be found in Fig. 5.5, which shows the header and additional comments.

Line spectrum

Simulations of the line radiative transfer `CMD_LINE_EMISSION` will create a line spectrum with the file-name '`line_spectrum_species_XXXX_line_YYYY.fits`'. The '`X`' stand for the gas species index with four digits and the '`Y`' stand for the transition index with four digits (e.g. `0001_line_0001` for first gas species and first transition defined in the '`cmd_file`'). A description of the structure of these line spectrum `.fits` files can be found in Fig. 5.6, which shows the header and additional comments.

Healpix map (all-sky-map)

If the healpix background grid is chosen for ray-tracing simulations (`CMD_DUST_EMISSION`, `CMD_SYNCHROTRON`, `CMD_LINE_EMISSION`), the resulting `.fits` files will have a different structure. Due to the standardized structure of these files, they can easily be post-processed by programs like `healpy`. A description of the structure of these healpix `.fits` files can be found in Fig. 5.7, which shows the header and additional comments.

5.3 Gnuplot

Several results of POLARIS can be plotted as a Gnuplot⁴ script. The Gnuplot software allows to create plots as well as the 3D representation of scientific data. POLARIS can create Gnuplot scripts for the 3D data of the physical parameters of the input grids and output grids. The data representation is either point-like (e.g. density, temperatures) or vector-like (e.g. magnetic field, velocities). Writing such files is optional and can be switched on by adding the lines

```
<nr_gnu_points> Np
<nr_gnu_vectors> Nv
<max_lines> Nl
```

to the command file. A Gnuplot script is in plain text. Hence, it is not recommended to plot the maximal amount of grid points, vectors, and lines. Here, they can be limited by the numbers N_p , N_v , and N_l , respectively.

Example:

```
<nr_gnu_points> 4000
<nr_gnu_vectors> 4000
<max_lines> 300
```

The POLARIS code plots automatically also the cross sections of the defined dust model (see Sect. 4.6.5). This is for the single dust materials as well as the dust mixtures. Dependent on the selected POLARIS simulation mode a source file will be created. This files contains 3D representation of the position and parameters of the defined stars and starfields, respectively (see Sect. 4.2). All the Gnuplot files require no further editing by the user and can directly be used for interpretation, representation, and analysis of the resulting simulation data.

⁴See https://en.wikipedia.org/wiki/Scalable_Vector_Graphics

Figure 5.5: Header of an '`int_channel_map_species_XXXX_line_YYYY.fits`' file including comments to explain the file structure.

```

SIMPLE = T / file does conform to FITS standard
BITPIX = -64 / number of bits per data pixel
NAXIS = 3 / number of data axes
NAXIS1 = 128 / length of data axis 1
NAXIS2 = 128 / length of data axis 2
NAXIS3 = 6 / different quantities (see CUNIT3)
EXTEND = T / FITS dataset may contain extensions
COMMENT FITS (Flexible Image Transport System) format is defined in 'Astronomy
COMMENT and Astrophysics', volume 376, page 359; bibcode: 2001A&A...376..359H
CTYPE1 = 'PARAM' / type of unit 1
CRVAL1 = -44528741200546.9 / value of axis 1
CRPIX1 = 1 / pixel where CRVAL1 is defined
CDELT1 = 701240018906.25 / delta of axis 1
CUNIT1 = 'm' / unit of axis 1
CTYPE1A = ... See midplane header ...
CTYPE2 = 'PARAM' / type of unit 2
CRVAL2 = -44528741200546.9 / value of axis 2
CRPIX2 = 1 / pixel where CRVAL2 is defined
CDELT2 = 701240018906.25 / delta of axis 2
CUNIT2 = 'm' / unit of axis 2
CTYPE2A = ... See midplane header ...
CTYPE3 = 'PARAM' / type of unit 3
CRVAL3 = 1 / value of axis 3
CRPIX3 = 1 / pixel where CRVAL3 is defined
CDELT3 = 1 / delta of axis 3
CUNIT3 = 'I, Q, U, V [Jy/px], optical depth, column density [m^-2]' / unit of axis 3
HIERARCH GAS_SPECIES = 'C180' / name of the observed gas_species
TRANS = 1 / transition index number (see leiden database)
HIERARCH LEVEL_UPPER = 2 / upper energy level index number (see leiden database)
HIERARCH LEVEL_LOWER = 1 / lower energy level index number (see leiden database)
FREQ = 109782173400. / frequency of the simulated transition
CHANNELS= 201 / number of velocity channels
MAXVEL = 3000. / maximum velocity of the velocity channels (-max
ZEEMAN = F / is zeeman splitting in the simulations consider
DISTANCE= 4.31994861405407E+18 / distance to object
RAXIS1X = 1. / rotation axes 1 (x component)
RAXIS1Y = 0. / rotation axes 1 (y component)
RAXIS1Z = 0. / rotation axes 1 (z component)
RANGLE1 = 90. / rotation angle 1 [\si{\degree}]
RAXIS2X = 0. / rotation axes 2 (x component)
RAXIS2Y = 1. / rotation axes 2 (y component)
RAXIS2Z = 0. / rotation axes 2 (z component)
RANGLE2 = 0. / rotation angle 2 [\si{\degree}]

```

Figure 5.6: Header of an '`line_spectrum_species_XXXX_line_YYYY.fits`' file including comments to explain the file structure.

```

SIMPLE = T / file does conform to FITS standard
BITPIX = -64 / number of bits per data pixel
NAXIS = 3 / number of data axes
NAXIS1 = 201 / different velocity channels
NAXIS2 = 1 / dummy to have one line, if opened as image
NAXIS3 = 4 / different quantities (see CUNIT3)
EXTEND = T / FITS dataset may contain extensions
COMMENT FITS (Flexible Image Transport System) format is defined in 'Astronomy
COMMENT and Astrophysics', volume 376, page 359; bibcode: 2001A&A...376..359H
CTYPE1 = 'VELO' / type of unit 1
CRVAL1 = -3000. / value of axis 1
CRPIX1 = 1 / pixel where CRVAL1 is defined
CDELT1 = 30. / delta of axis 1
CUNIT1 = 'm/s' / unit of axis 1
CTYPE2 = 'PARAM' / type of unit 2
CRVAL2 = 1 / value of axis 2
CRPIX2 = 1 / pixel where CRVAL2 is defined
CDELT2 = 1 / delta of axis 2
CUNIT2 = 'I, Q, U, V [Jy/px], optical depth, column density [m^-2]' / unit of a
HIERARCH GAS_SPECIES = 'C180' / name of the observed gas_species
TRANS = 1 / transition index number (see leiden database)
HIERARCH LEVEL_UPPER = 2 / upper energy level index number (see leiden database)
HIERARCH LEVEL_LOWER = 1 / lower energy level index number (see leiden database)
FREQ = 109782173400. / frequency of the simulated transition
CHANNELS= 201 / number of velocity channels
MAXVEL = 3000. / velocity of the velocity channels (-maxvel to maxvel)
ZEEMAN = F / is zeeman splitting in the simulations consider
DISTANCE= 4.31994861405407E+18 / distance to object
RAXIS1X = 1. / rotation axes 1 (x component)
RAXIS1Y = 0. / rotation axes 1 (y component)
RAXIS1Z = 0. / rotation axes 1 (z component)
RANGLE1 = 90. / rotation angle 1 [\si{\degree}]
RAXIS2X = 0. / rotation axes 2 (x component)
RAXIS2Y = 1. / rotation axes 2 (y component)
RAXIS2Z = 0. / rotation axes 2 (z component)
RANGLE2 = 0. / rotation angle 2 [\si{\degree}]

```

5 Output data

Figure 5.7: Header of the first extension of a healpix `'.fits'` file including comments to explain the file structure.

```

XTENSION= 'BINTABLE' / binary table extension
BITPIX = 8 / 8-bit bytes
NAXIS = 2 / 2-dimensional binary table
NAXIS1 = 48 / width of table in bytes
NAXIS2 = 12288 / number of rows in table
PCOUNT = 0 / size of special data area
GCOUNT = 1 / one data group (required keyword)
TFIELDS = 6 / different quantities/wavelengths/frequencies
TTYPE1 = 'I_STOKES (WAVELENGTH = 8.500000e-04 [m])' / label for field 1
TFORM1 = 'D' / data format of field: 8-byte DOUBLE
TUNIT1 = 'Jy/px' / physical unit of field
TTYPE2 = 'Q_STOKES (WAVELENGTH = 8.500000e-04 [m])' / label for field 2
TFORM2 = 'D' / data format of field: 8-byte DOUBLE
TUNIT2 = 'Jy/px' / physical unit of field
TTYPE3 = 'U_STOKES (WAVELENGTH = 8.500000e-04 [m])' / label for field 3
TFORM3 = 'D' / data format of field: 8-byte DOUBLE
TUNIT3 = 'Jy/px' / physical unit of field
TTYPE4 = 'V_STOKES (WAVELENGTH = 8.500000e-04 [m])' / label for field 4
TFORM4 = 'D' / data format of field: 8-byte DOUBLE
TUNIT4 = 'Jy/px' / physical unit of field
TTYPE5 = 'OPTICAL_DEPTH (WAVELENGTH = 8.500000e-04 [m])' / label for field 5
TFORM5 = 'D' / data format of field: 8-byte DOUBLE
TTYPE6 = 'COLUMN_DENSITY' / label for field 6
TFORM6 = 'D' / data format of field: 8-byte DOUBLE
TUNIT6 = 'm^-2' / physical unit of field
EXTNAME = 'HEALPIX_EXTENSION' / name of this binary table extension
PIXTYPE = 'HEALPIX' / Pixel algorithm
ORDERING= 'RING' / Ordering scheme
INDXSCHM= 'IMPLICIT' / Indexing scheme
NSIDE = 32 / Resolution Parameter
FIRSTPIX= 0 / First pixel (0 based)
LASTPIX = 12287 / Last pixel (0 based)
CROTA2 = 0 / Rotation Angle (Degrees)

ETYPE = 'thermal emission' / type of emission
... or ...
ETYPE = 'synchotron emission' / type of emission
... or ...
HIERARCH GAS_SPECIES = 'C180' / name of the observed gas_species
TRANS = 1 / transition index number (see leiden database)
HIERARCH LEVEL_UPPER = 2 / upper energy level index number (see leiden dat
...
ID = 1 / detector id
HIERARCH OBS_POSITION_X = 0. / x-axis position of observer
HIERARCH OBS_POSITION_Y = 0. / y-axis position of observer
HIERARCH OBS_POSITION_Z = 0. / z-axis position of observer
HIERARCH OBS_VELOCITY_X = 0. / velocity of observer in x direction
HIERARCH OBS_VELOCITY_Y = 0. / velocity of observer in y direction
HIERARCH OBS_VELOCITY_Z = 0. / velocity of observer in z direction
HIERARCH LONGITUDE_MIN = 0. / minimum considered galactic longitude
HIERARCH LONGITUDE_MAX = 6.28318530717959 / maximum considered galactic longitud
HIERARCH LATITUDE_MIN = 0. / minimum considered galactic latitude
HIERARCH LATITUDE_MAX = 3.14159265358979 / maximum considered galactic latitude

```

5.4 AMIRA

AMIRA⁵ is a software for the visualization of large scientific data but is not for free. POLARIS supports the AMIRA format for 3D data. An AMIRA file can be created for the physical parameters of the input grid (e.g. gas temperature or density) as well as the output grid (e.g. dust temperature, RAT alignment radius) . Adding the following commands to the command file results in an AMIRA file for each of the physical parameters sampled over N_{bins} bins in each direction:

```
<amira_inp_points> Nbins
<amira_out_points> Nbins
```

Example:

```
<amira_inp_points> 100
<amira_out_points> 500
```

The AMIRA file is in plane text with a short header and a data section running over the z, y, and x-direction. Writing an AMIRA file is a problem that cannot be parallelized and can take up to one hour. Hence, the number of bins N_{bins} has to be chosen carefully.

⁵See <https://www.fei.com/software/amira-3d-for-life-sciences/>

6 Quickstart guide

To try out the main capabilities of POLARIS, use the following step-by-step instruction. The example simulations are based on a model of a circumstellar disk with characteristics shown in Table 6.1. In this model, we assumes compact, homogeneous, and spherical dust grains with a composition of 62.5% silicate and 37.5% graphite (MRN-dust, Mathis et al. 1977; optical properties from Weingartner & Draine 2001).

We consider furthermore a density distribution with a radial decrease based on the work of Hayashi (1981) for the minimum mass solar nebular. Combined with a vertical distribution due to hydrostatic equilibrium similar to the work of Shakura & Sunyaev (1973), we obtain the following equation:

$$\rho_{\text{disk}} = \rho_0 \left(\frac{R_{\text{ref}}}{\bar{\omega}} \right)^a \exp \left(-\frac{1}{2} \left[\frac{z}{H(\bar{\omega})} \right]^2 \right). \quad (6.1)$$

Here, $\bar{\omega}$ is the radial distance from the central star in the disk midplane, z is the distance from the midplane of the disk, R_{ref} is a reference radius, and $H(\bar{\omega})$ is the scale height. The density ρ_0 is derived from the disk (gas) mass. The scale height is a function of $\bar{\omega}$ as follows:

$$H(\bar{\omega}) = h_0 \left(\frac{\bar{\omega}}{R_{\text{ref}}} \right)^b. \quad (6.2)$$

The parameters a and b set the radial density profile and the disk flaring, respectively.

6.0.1 Unpack the examples

The first step is to unpack the example package. This package is shipped with POLARIS and includes grids and command files to perform the following example simulations. To extract the example package, go into your POLARIS directory and enter the following command:

```
tar -xf examples.tar.xz -C projects/
```

Now, you have everything you need for the following examples in your `projects/disk/` directory. However, to use any of the example command files, the paths to the POLARIS directory has to be adjusted. To do this, change any occurrence of `/YOUR/POLARIS/PATH/` in the command files to your path of the POLARIS installation.

6.0.2 Dust temperature distribution

The dust temperature distribution can be simulated by assuming that the dust grains are in equilibrium with the radiation field. To do this, enter the following command ($t \sim 3 \text{ min}$):

```
polaris /YOUR/POLARIS/PATH/projects/disk/example/temp/POLARIS.cmd
```

The temperature distribution can be visualized with the `'.fits'` file viewer `ds9`. You find the `'.fits'` files in the `projects/disk/example/temp/data/` directory. The temperature distributions should look like those in Fig. 7.1. The creation of proper plots can be realized by e.g. Python scripts using `matplotlib` and `astropy`. However, especially if you do not have similar scripts, we suggest to use our toolkit `PolarisTools` for visualization (see 7).

Table 6.1: Characteristics and default parameters of the considered circumstellar disk model ('disk').

<i>Central star</i>		
Radiation source	't_tauri'	
Effective temperature	T_{star}	4000 K
Stellar radius	R_{star}	$0.9 R_{\odot}$
Stellar mass	M_{star}	$0.7 M_{\odot}$
<i>Disk model</i>		
Distance to star/disk	d	140 pc
Inner radius	R_{in}	0.1 au
Outer radius	R_{ou}	300 au
Scale height	h_0	10 au
Characteristic radius	R_{ref}	100 au
Radial density decrease	a	1.625
Disk flaring	b	1.125
Grid geometry	'spherical'	
Cells in r -direction	n_r	100
Step width factor in r	sf_r	1.03
Cells in θ -direction	n_{θ}	91
Step width factor in θ	sf_{θ}	1.0 (sinus distribution)
Cells in ϕ -direction	n_{ϕ}	1
Inclination	i	0° (face-on), 90° (edge-on)
<i>Gas species</i>		
Gas species	'co'	
Transitions frequency	ν_0	230.538 GHz
Abundance	CO/H	10^{-4}
Spectral resolution	$\Delta\nu_{\text{res}}$	132 MHz (171 m s^{-1})
Gas mass	M_{gas}	$10^{-4} M_{\odot}$
Gas-to-dust mass ratio	$M_{\text{gas}} : M_{\text{dust}}$	100 : 1
Turbulent velocity	v_{turb}	100 m s^{-1}
Velocity field	Keplerian	
<i>Dust grains</i>		
Dust grain composition	'mrn' (silicate, graphite)	
Minimum dust grain size	a_{\min}	5 nm
Maximum dust grain size	a_{\max}	250 nm
Size exponent	α_{size}	-3.5
<i>Magnetic field</i>		
Magnetic field strength	B_z	1 mG

6.0.3 Dust thermal emission

Based on the dust temperature distribution, the thermal emission of the dust grains at $\lambda \sim 850 \mu\text{m}$ can be simulated. To do this, enter the following command ($t \sim 30 \text{s}$):

```
polaris /YOUR/POLARIS/PATH/projects/disk/example/dust/POLARIS.cmd
```

You find the `.fits` files in the `projects/disk/example/dust/data/` directory. The intensity map should look like Fig. 7.2 (left).

6.0.4 Dust thermal emission (with grain alignment)

Based on the dust temperature distribution, the thermal emission of aligned non-spherical dust grains at $\lambda \sim 850 \mu\text{m}$ can be simulated. To do this, enter the following command ($t \sim 30 \text{s}$):

```
polaris /YOUR/POLARIS/PATH/projects/disk/example/dust_pa/POLARIS.cmd
```

In this simulation, the disk is observed edge-on and the spherical dust grains will be replaced by oblate dust grains which are perfectly perpendicular aligned with their longest axis to the magnetic field. Since this guide only shows the capabilities of POLARIS, it is sufficient to use the dust temperature distribution which was simulated with spherical dust grains. Otherwise, the temperature distribution needs to be calculated again with oblate dust grains. You find the `.fits` files in the `projects/disk/example/dust_pa/data/` directory. The intensity map should look like Fig. 7.3 (left).

6.0.5 Scattered stellar emission

Based on the dust density distribution, the stellar radiation at $\lambda = 1 \mu\text{m}$ scattered at the spherical dust grains can be simulated. To do this, enter the following command ($t \sim 5 \text{ min}$):

```
polaris /YOUR/POLARIS/PATH/projects/disk/example/dust_mc/POLARIS.cmd
```

The disk is inclined by 60° to achieve a better visual impression of the scattered light. You find the `.fits` files in the `projects/disk/example/dust_mc/data/` directory. Polarization maps can be calculated from these `.fits` files that should look like Fig. 7.4 (top).

6.0.6 Thermal emission and scattered stellar emission

The stellar emission scattered at spherical dust grains can also be included in the thermal emission calculation. To do this, the temperature calculation needs to be repeated with the `<radiation_field> 1` option by entering the following command ($t \sim 2 \text{ min}$):

```
polaris /YOUR/POLARIS/PATH/projects/disk/example2/temp/POLARIS.cmd
```

Then, the thermal emission and scattered stellar emission of the dust grains at $\lambda = 1 \mu\text{m}$ can be simulated. To do this, enter the following command ($t \sim 5 \text{ min}$):

```
polaris /YOUR/POLARIS/PATH/projects/disk/example2/dust/POLARIS.cmd
```

The disk is inclined by 60° to achieve a better visual impression of the scattered light. You find the `.fits` files in the `projects/disk/example2/dust/data/` directory. Polarization maps can be calculated from these `.fits` files that should look like Fig. 7.4 (bottom).

6.0.7 Spectral line emission

Based on the gas temperature distribution, the spectral line emission of the $\text{C}^{18}\text{O } J = 1 \rightarrow 0$ transition ($\nu \sim 109 \text{ GHz}$) can be simulated. To do this, enter the following command ($t \sim 5 \text{ min}$):

```
polaris /YOUR/POLARIS/PATH/projects/disk/example/line/POLARIS.cmd
```

In this simulation, the disk is observed edge-on and the Keplerian rotation around the central star is considered for the velocity field. You find the `'.fits'` files in the `projects/disk/example/line/data/` directory. The velocity channel map, integrated velocity channel map and spectrum should look like Fig. 7.5 (*top, middle*).

6.0.8 Spectral line emission (with Zeeman splitting)

Based on the gas temperature distribution, the Zeeman split spectral line emission of the OH transition at $\nu \sim 1665$ MHz can be simulated (see [Brauer et al. 2017a](#)). To do this, enter the following command ($t \sim 60$ min):

```
polaris /YOUR/POLARIS/PATH/projects/disk/example/zeeman/POLARIS.cmd
```

In this simulation, the disk is observed face-on and, therefore, the Keplerian rotation is not required. You find the `'.fits'` files in the `projects/disk/example/zeeman/data/` directory. The circular polarization spectrum should look like Fig. 7.5 (*bottom right*). Magnetic field maps calculated via the Zeeman analysis can be obtained with PolarisTools (see [7](#)).

7 PolarisTools

7.1 Introduction

PolarisTools is an optional toolkit written in `python` that offers a convenient way of using POLARIS and many tools to make the daily work with POLARIS easier. This toolkit started as a small `python` script collection created by Robert Brauer, who used it only for his own studies and simulations. After more than three years of development, PolarisTools improved similarly to the POLARIS code itself. In its current state, the toolkit can be used by almost every POLARIS user or those who want to become one. Nevertheless, it is fully optional and not every user of POLARIS is using it. The next sections show how to perform simulations with the toolkit (quickstart and full), how to create plots based on the results, how to define your own model environment, and how to use the other tools.

Copyright

PolarisTools is free software: you can redistribute it and/or modify it under the terms of the GNU General Public License as published by the Free Software Foundation, either version 3 of the License, or (at your option) any later version.

PolarisTools is distributed in the hope that it will be useful, but WITHOUT ANY WARRANTY; without even the implied warranty of MERCHANTABILITY or FITNESS FOR A PARTICULAR PURPOSE. See the GNU General Public License for more details.

You should have received a copy of the GNU General Public License along with PolarisTools. If not, see <http://www.gnu.org/licenses/>.

Units

For the PolarisTools other than `polaris-plot`, the options accept either the value in SI units or in various units by using the following appendix (e.g. `10au`). For `polaris-plot`, the values for the options are related to the units of the axes or colormap of the plot.

Length

`meter`: '`m`', astronomical unit: '`au`', parsec: '`pc`', solar radius: '`r_sun`'

Velocity

`meter per second`: '`m/s`', kilometer per second: '`km/s`', kilometer per hour: '`km/h`'

Mass

`kilogram`: '`kg`', solar mass: '`m_sun`', jupiter mass: '`m_jup`'

Luminosity

`watt`: '`w`', solar luminosity: '`l_sun`'

Angle

`degree`: '`degree`', radians: '`rad`', arcseconds: '`arcsec`'

7.2 The command `polaris-gen`

This tool can be used to create a grid based on a given model (`model_name`). To create a grid, enter the following command:

```
polaris-gen model_name grid_name.dat
```

See Sect. 7.7 for available model names.

Available options

The Tables 7.1 and 7.2 show an overview of the available options to modify the creation of a grid with `polaris-gen`.

7.3 The command `polaris-run`

This tool can be used to perform a simulation with POLARIS based on a given model (see Sect. 7.7 for available model names). By defining a name of the simulation (`simulation_name`), the results of different simulations will be saved in:

- `projects/model_name/simulation_name/simulation_type/`

Simulation types

The following commands give an overview of all available simulations that can be performed with POLARIS.

Dust temperature distribution

To calculate the dust temperature distribution based on the radiation field, enter the following command:

```
polaris-run model_name simulation_name temp
```

Use `--adj_tgas 1` to apply the dust temperature distribution also for the gas phase.

Radiative torque calculation

To calculate the necessary information to consider Radiative torque alignment, enter the following command:

```
polaris-run model_name simulation_name rat
```

The grid will be taken from a previous temperature calculation with the same simulation name.

Temperature and RAT calculation

The calculations of the dust temperature and radiative torque can be performed together by entering the following command:

```
polaris-run model_name simulation_name temp_rat
```

This simulation type behaves in terms of options the same as the temperature calculation.

Table 7.1: Available options and their default values of *polaris-gen*.

Command	Description
<i>Grid</i>	
--grid_type octree,spherical,cylindrical	Change the grid type (geometry) Default: defined by the model ('disk': spherical)
--max_level MAX_TREE_LEVEL	Change the maximum refinement level (only for octree grids) Default: defined by the model ('disk': not needed)
--variable_dust	Allow variations of the dust composition in the grid (see Sect. 7.8.1) Default: use a single dust composition in the whole grid
--gas_mass GAS_MASS	Define the total gas mass of grid (overwrites model value) Default: defined by the model ('disk': $10^{-4} M_{\odot}$)
--sidelength SIDELength	Define the sidelength of an OcTree grid (overwrites model value) Default: defined by the model ('disk': 600 au)
--inner_radius INNER_RADIUS	Define the inner radius of a spherical or cylindrical grid (overwrites model value) Default: defined by the model ('disk': 0.1 au)
--outer_radius OUTER_RADIUS	Define the outer radius of spherical or cylindrical grid (overwrites model value) Default: defined by the model ('disk': 300 au)
--z_max Z_MAX	Define the maximum vertical extent of cylindrical grid (overwrites model value) Default: defined by the model ('disk': 300 au)
--n_r N_RADIUS	Define the number of radial cells of spherical or cylindrical grid (overwrites model value) Default: defined by the model ('disk': 100 cells)
--n_ph N_PHI	Define the number of azimuthal cells of spherical or cylindrical grid (overwrites model value) Default: defined by the model ('disk': 1 cell)
--n_th N_THETA	Define the number of theta cells of spherical grid (overwrites model value) Default: defined by the model ('disk': 181 cells)
--n_z N_Z	Define the number of vertical cells of cylindrical grid (overwrites model value) Default: defined by the model ('disk': 181 cells)

Table 7.2: Available options and their default values of `polaris-gen` (continued).

Command	Description
<i>Grid (continued)</i>	
--sf_r SF_R	Define the step width factor in radial direction of spherical or cylindrical grid (overwrites model value) Default: defined by the model ('disk': 1.03)
--sf_th SF_TH	Define the step width factor in theta direction of spherical grid (overwrites model value) Default: defined by the model ('disk': 1.0 (sinus distribution))
--sf_z SF_Z	Define the step width factor in vertical direction of cylindrical grid (overwrites model value) Default: defined by the model ('disk': 1.0 (sinus distribution))
--extra EXTRA_PARAMETERS	Define additional parameter to vary model characteristics (multiple values possible) Default: defined by the model ('disk': $R_{\text{ref}}, h_0, a, b$, see Eq. 7.1)
--variable_dust VARIABLE_DUST	This allows the variation of the dust composition in the grid Default: defined by the model ('disk': disabled)
--variable_size_limits VARIABLE_SIZE_LIMITS	This allows the variation of the dust grain size limits in the grid Default: defined by the model ('disk': disabled)
<i>Source</i>	
--external EXTERNAL_INPUT_NAME	Select an ext_name to use an external model as input for the grid (experimental, see Sect. 7.8.9) Default: use <code>get_xyz()</code> functions that are defined in the model to generate the grid (see Sect. 7.8.1)
<i>Update</i>	
--update	Updates POLARIS v4.00 grids to newest version Default: The grid ' <code>grid_name.dat</code> ' will be created instead of updated
--revert	Revert POLARIS v4.XX grids to version 4.00.00 Default: The grid ' <code>grid_name.dat</code> ' will be created instead of reverted
--set_align ALIGN_RADIUS	Set the minimum alignment radius for the RAT theory in the grid Default: The grid ' <code>grid_name.dat</code> ' will be created instead of modified

Thermal dust emission

To calculate the thermal dust emission, enter the following command:

```
polaris-run model_name simulation_name dust
```

The grid will be taken from a previous temperature calculation with the same simulation name. Consider alignment of non-spherical dust grains by adding `_pa`, `_rat`, `_internal`, or `_idg` to `dust` (multiple choices are possible).

Scattered stellar emission

To calculate the stellar emission scattered at spherical dust grains, enter the following command:

```
polaris-run model_name simulation_name dust_mc
```

The grid can be taken from a previous temperature calculation or from a grid made with `polaris-gen`. To consider the self-scattering of the dust grain emission, define `--photons_dust` and disable stellar radiation by setting `--photons` to zero.

Thermal emission and scattered stellar emission

The stellar emission scattered at spherical dust grains can also be included in the thermal emission calculation. Since it is using the raytracing technique, it is much faster than the Monte-Carlo approach (see above). To take advantage of this technique, calculate the temperature distribution and save the radiation field by entering the following command:

```
polaris-run model_name simulation_name temp --radiation_field
```

After that, calculate the thermal emission and the scattered stellar emission by entering the following command:

```
polaris-run model_name simulation_name dust
```

Spectral line emission

To calculate the spectral line emission, enter the following command:

```
polaris-run model_name simulation_name line
```

The grid will be taken from a previous temperature calculation with the same simulation name (gas temperature is required). Zeeman splitting can be considered by changing `line` to `zeeman` as long as the transition of the gas species supports Zeeman splitting.

Available options

The Tables 7.3 to 7.7 show an overview of the available options to modify the execution of POLARIS simulations with `polaris-run`. The red names in brackets show for which simulation types the option can be used.

7.4 The command `polaris-plot`

This tool can be used to create plots from results of a simulation with POLARIS. The results are taken from the simulation defined by `model_name`, `simulation_name`, and `simulation_type`. Each plot command has the following structure:

```
polaris-plot model_name simulation_name simulation_type visualization_type
    ↳ visualization_input
```

Each `simulation_type` has separate options (`visualization_type`) to create visualization plots.

Table 7.3: Available options and their default values of `polaris-run`. The red names in brackets show for which simulation types the option can be used.

Command	Description
<i>Grid</i>	
--grid GRID_FILENAME (all)	Define the grid that is used by POLARIS (filename is relative to the <code>model/</code> directory) Default: <code>'grid_rat.dat'</code> in <code>simulation_name/rat/</code> , else <code>'grid_temp.dat'</code> in <code>simulation_name/temp/</code> , else <code>'grid.dat'</code> in <code>model_name/</code>
--grid_cgs GRID_FILENAME (all)	Define the grid in cgs units that is used by POLARIS (filename is relative to the <code>model/</code> directory) Default: as --grid (in SI units)
<i>Source</i>	
--stellar_source STELLAR_SOURCE (temp, rat, dust_mc)	Define the blackbody radiation source that is used by POLARIS (see Sect 7.7 for available radiation sources) Default: defined by the model (<code>'disk': 't_tauri'</code> , typical T Tauri star in the center)
<i>Detector</i>	
--bg_source BG_SOURCE (dust, dust_mc, line)	Define the background source that is used by POLARIS (see Sect 7.7 for available background sources) Default: defined by the model (<code>'disk': 'bg_plane'</code> , default background plane without any emission offset)
--photons NR_PHOTONS (temp, rat, dust_mc)	Set the number of photons for the radiation sources (stars, isrf) Default: defined by the stellar source (<code>'t_tauri'</code> : 10^6)
--photons_dust NR_PHOTONS_DUST (dust_mc)	Set the number of photons for the dust source Default: no dust emission
<i>Detector</i>	
--detector DETECTOR (dust, dust_mc, line, zeeman)	Define the detector with preset parameters (see Sect 7.7 for available detectors) Default: defined by the model (<code>'disk': 'cartesian'</code>)
--wavelength WAVELENGTH or WL_MIN WL_MAX or WL_MIN WL_MAX NR_WL (dust, dust_mc)	Define the wavelength(s) for Raytrace and Monte-Carlo simulations (WAVELENGTH, WL_MIN and WL_MAX, or NR_WL wavelengths logarithmically distributed between WL_MIN and WL_MAX) Default: defined by the detector (<code>'cartesian'</code> : 1×10^{-6} m)
--pixel NR_PIXEL (dust, dust_mc, line, zeeman)	Define the number of detector pixel (in x- and y-direction, overwrites separate x and y choices) Default: defined by the detector (<code>'cartesian'</code> : 256)
--pixel_x NR_PIXEL_X (dust, dust_mc, line, zeeman)	Define the number of detector pixel (in x-direction) Default: defined by the detector (<code>'cartesian'</code> : 256)
--pixel_y NR_PIXEL_Y (dust, dust_mc, line, zeeman)	Define the number of detector pixel (in y-direction) Default: defined by the detector (<code>'cartesian'</code> : 256)
--sides NR_SIDES (dust, line, zeeman)	Define the number of sides for healpix detector (all-sky-map) Default: defined by the detector (<code>'allsky'</code> : 32)
--subpixel MAX_SUBPIXEL_LVL (dust, dust_mc, line, zeeman)	Set the maximum level of subpixeling of the detector Default: one level

Table 7.4: Available options and their default values of `polaris-run` (continued). The red names in brackets show for which simulation types the option can be used.

Command	Description
<i>Detector (continued)</i>	
--zoom SIDELENGTH_ZOOM	Define the zoom factor for the detector sidelengths (the model needs to have the correct extent of the grid!)
(dust, dust_mc, line, zeeman)	Default: no zoom
--zoom_x SIDELENGTH_ZOOM_X	Define the zoom factor for the detector sidelength in x-direction (the extent of the grid need to match the extent defined in <code>/model.py!</code>)
(dust, dust_mc, line, zeeman)	Default: no zoom
--zoom_y SIDELENGTH_ZOOM_Y	Define the zoom factor for the detector sidelength in y-direction (the model needs to have the correct extent of the grid!)
(dust, dust_mc, line, zeeman)	Default: no zoom
--shift_x MAP_SHIFT_X	Define the shift in y-direction of the detector map
(dust, dust_mc, line, zeeman)	Default: no zoom
--shift_y MAP_SHIFT_Y	Define the shift in x-direction of the detector map
(dust, dust_mc, line, zeeman)	Default: no zoom
--rot_1 ROT_ANGLE_1	Set the rotation angle around the first rotation axis
(dust, dust_mc, line, zeeman)	Default: defined by the detector ('cartesian': 0°)
--rot_2 ROT_ANGLE_2	Set the rotation angle around the second rotation axis
(dust, dust_mc, line, zeeman)	Default: defined by the detector ('cartesian': 0°)
--rot_axis_1 AXIS_X AXIS_Y AXIS_Z	Set the first rotation axis
(dust, dust_mc, line, zeeman)	Default: (1, 0, 0)
--rot_axis_2 AXIS_X AXIS_Y AXIS_Z	Set the second rotation axis
(dust, dust_mc, line, zeeman)	Default: (0, 1, 0)
--peel_off 1 (yes) or 0 (no)	Enables/Disables the peel-off technique (see Gordon et al., 2001; Zhu & Stone, 2014)
(dust_mc)	Default: peel-off technique is disabled (instead use an acceptance angle)
--ac_angle ACCEPTANCE_ANGLE	Set the maximum acceptance angle (only if peel-off technique is disabled)
(dust_mc)	Default: defined by the detector ('cartesian': 1°)
--rt_grid cart,polar,slice,healpix	Define the type of the background grid used for dust-tracing
(dust, line, zeeman)	Default: defined by the detector ('cartesian': 'cartesian')

Table 7.5: Available options and their default values of `polaris-run` (continued). The red names in brackets show for which simulation types the option can be used.

Command	Description	
<i>Radiation source</i>		
--stellar_temperature EFF_TEMP (<code>temp, rat, dust_mc</code>)	Set the effective temperature of the stellar radiation source (black body emission)	<code>Default:</code> defined by the radiation source (' <code>t_tauri</code> ': 4000 K)
<i>Dust component</i>		
--dust DUST_COMPOSITION (<code>all</code>)	Define the dust component that is used by POLARIS	<code>Default:</code> spherical MRN-dust grains ' <code>mrn_sp</code> ' (<code>temp, dust, dust_mc</code>), non-spherical MRN-dust grains ' <code>mrn</code> ' (<code>rat</code>) or no dust grains (<code>line, zeeman</code>)
--dust_size A_MIN A_MAX (<code>all</code>)	Set minimum and maximum dust grain size of the dust components	<code>Default:</code> defined by the dust component (' <code>mrn</code> ': $a_{\min} = 5 \text{ nm}$, $a_{\max} = 0.25 \mu\text{m}$)
--size_dist DIST_NAME PARAMETER ... (<code>all</code>)	Define the dust grain size distribution (see Sect. 4.6.5)	<code>Default:</code> defined by the dust component (' <code>mrn</code> ': ' <code>plaw</code> ' -3.5)
--scattering MIE,HG,ISO (<code>temp, dust_mc</code>)	Define method to calculate scattering	<code>Default:</code> defined by the dust component (' <code>mrn</code> ': Mie-scattering)
--sub_dust (<code>temp</code>)	Consider sublimation temperature of dust grains	<code>Default:</code> No upper limit of dust temperature
--radiation_field (<code>temp</code>)	Save the radiation field in the grid (required by --stochastic_heating)	<code>Default:</code> no radiation field saved
--full_dust_temp (<code>temp</code>)	Calculate the temperature distribution for each dust grain size	<code>Default:</code> use an average temperature distribution
--stochastic_heating TEMP_A_MAX (<code>dust</code>)	Calculate stochastic heating (up to TEMP_A_MAX, --full_dust_temp and --radiation_field options)	<code>Default:</code> use an average temperature distribution
--fhj F_HIGHJ (<code>dust</code>)	Set the $f_{high,j}$ value for the radiative torque mechanism	<code>Default:</code> 0.25
--fc F_C (<code>dust</code>)	Set the f_c value for the internal alignment correlation	<code>Default:</code> 0.6

Table 7.6: Available options and their default values of `polaris-run` (continued). The red names in brackets show for which simulation types the option can be used.

Command	Description
<i>Gas component</i>	
--gas GAS_SPECIES (<i>line, zeeman</i>)	Define the gas species that is used by POLARIS Default: ' <code>co</code> '
--transition TRANSITION_ID (<i>line, zeeman</i>)	Set the transition index which will be simulated with POLARIS Default: defined by the detector (' <code>cartesian</code> ': 1. transition)
--abundance ABUNDANCE (<i>line, zeeman</i>)	Set the global abundance of the chosen gas species Default: defined by the gas species (' <code>co</code> ': 1×10^{-4})
--lvl_pop LTE,FEP,LVG (<i>line, zeeman</i>)	Set the level population approximation method Default: LTE approximation
--max_vel MAX_VELOCITY (<i>line, zeeman</i>)	Set the maximum velocity relative to the line peak which will be considered for the simulations Default: defined by the gas species (' <code>co</code> ': 3000 m s^{-1})
--channels NR_VELOCITY_CHANNELS (<i>line, zeeman</i>)	Set the number of velocity channels inside of two times MAX_VELOCITY Default: defined by the gas species (' <code>co</code> ': 35)
--kepler (<i>line, zeeman</i>)	Calculate the velocity field with the assumption of a single star in the center that causes Keplerian rotation of the surrounding dust and gas Default: no Keplerian velocity field (use velocity field from grid)
--turbulence TURBULENT_VELOCITY (<i>line, zeeman</i>)	Set the turbulent velocity v_{turb} of the gas particles Default: 100 m s^{-1}
--adj_tgas ADJ_TGAS (<i>temp</i>)	Set the gas temperature distribution as ADJ_TGAS times the dust temperature distribution Default: do not change the input gas temperature distribution
<i>Visualization</i>	
--no_vel_maps (<i>line, zeeman</i>)	Disable creation of velocity channel maps Default: save velocity channel maps
--midplane MIDPLANE_POINTS (<i>all</i>)	Set the number of pixels per axis of the midplane cuts output (0 disables creation of midplane files) Default: 256 pixel per axis
-midplane_zoom MIDPLANE_ZOOM (<i>all</i>)	Enable zoom onto the center of the simulated object in the midplane cuts Default: no zoom
--midplane_3d PLANE or PLANE NR_SLICES or PLANE NR_SLICES Z_MIN, Z_MAX (<i>all</i>)	Enable 3D midplane fits files (PLANE: 1 -> xy, 2 -> xz, 3 -> yz; Z_MIN and Z_MAX are the limits of the axis which is not shown by the plane. If not set, use the grid extent) Default: standard midplane cuts

Table 7.7: Available options and their default values of `polaris-run` (continued). The red names in brackets show for which simulation types the option can be used.

Command	Description
<i>Conversion factors</i>	
--conv_dens CONV_DENS --conv_len CONV_LEN --conv_mag CONV_MAG --conv_vel CONV_VEL	Set conversion factors to convert the given quantity in the input grid (all) Default: no conversion of the input quantities
--mf MASS_FRACTION	Set the dust to gas mass ratio (all) Default: MASS_FRACTION = 0.01 (dust-to-gas mass ratio $M_{\text{dust}} : M_{\text{gas}} = 1 : 100$)
--mu MU	Set the average mass of a hydrogen particle (in atomic mass units) (all) Default: 2 u
<i>Processing</i>	
--threads NR_THREADS	Set the number of CPU cores that will be used by POLARIS (all) Default: as much as possible (local computer), defined by server/cluster ('nec': 16)
--ram RAM_USAGE	Set the maximum amount of RAM that POLARIS can use (all) Default: as much as required (local computer), defined by server/cluster ('nec': '16gb')
--queue	If executed on a cluster/server system, put the simulation onto the queue (see Sect. 7.7 for available servers/clusters and Sect. 7.8 to define your own server/cluster) (all) Default: execute the POLARIS simulation directly in the terminal
--short	Shorten the wall time of a simulation on a server (all) Default: defined by the server (detected by working machine)
--long	Extend the wall time of a simulation on a server (all) Default: defined by the server (detected by working machine)
--save_out	Save POLARIS console output to ' <code>POLARIS.out</code> ' in <code>model_name/simulation_name/simulation_type/</code> (all) Default: only console output is shown

Visualization types

The following commands give an overview of all available plots that can be created with PolarisTools.

Midplane cuts

To create midplane cut plots from the data written by POLARIS, enter the following command:

```
polaris-plot model_name simulation_name simulation_type midplane
    ↪ source quantity plane
```

For `source`, choose between the grid that was used by POLARIS (`'input'`) and the grid that was created by POLARIS (`'output'`). For `quantity`, choose from the following options:

- `'gas_number_density'` or `'gas_mass_density'`
- `'dust_number_density'` or `'dust_mass_density'`
- `'gas_temperature'`
- `'dust_temperature'`
- `'mag_field'`
- `'vel_field'`
- `'rat_aalig'` (minimum grain size that is aligned by RATs)
- `'delta'` (see [Reissl et al., 2016](#))
- `'mach'` (Mach number)
- `'larm'` (Limit due to Larmor radius)
- `'dust_choice'` (index of considered dust composition in cell)

For `plane` choose between `'xy'`, `'xz'`, and `'yz'`. Instead of these three parameters, you can use `'all'` as `quantity` to create plots for each available quantity.

Emission maps

To create an emission map from thermal dust emission (`dust`), scattered light emission (`dust_mc`) or both (`dust_full`), enter the following command:

```
polaris-plot model_name simulation_name simulation_type map index_combination
```

The `index_combination` can be one of the following index combinations:

- `detector`
- `detector + wavelength`
- `detector + min_wavelength + max_wavelength`
- `detector + min_wavelength + max_wavelength + min_quantity`
- `detector + min_wavelength + max_wavelength + min_quantity + max_quantity`

The `detector` is the index of the observing detector (1, if only one detector), the `wavelength` is the wavelength index related to the simulated wavelengths (1 for first wavelength, ...), and the `quantity` is related to various Stokes vector related quantities. 1 is for I , 2 for Q , 3 for U , 4 for V , 5 for PI , 6 for P_I , 7 and 8 are for e.g. the optical depth. If only a `min` value is set, the maximum value will be adapted to the amount of data. Simulations that considered aligned dust grains can be used by adding the corresponding appendix as shown in Sect. 7.3. With this command, plots from simulations with the `--rt_grid 'healpix'` will also be created.

Spectral energy distribution

To create a spectral energy distribution from thermal dust emission (dust) or scattered light (dust_mc) simulations, enter the following command:

```
polaris-plot model_name simulation_name simulation_type sed index_combination
```

The index_combination is the same as for emission maps.

Velocity channel map

To create a velocity channel map, enter the following command:

```
polaris-plot model_name simulation_name line vel_map index_combination
```

The index_combination can be one of the following index combinations:

- spectral_line
- gas_species + spectral_line
- gas_species + spectral_line + min_quantity
- gas_species + spectral_line + min_quantity + max_quantity

The spectral_line is the index of the simulated spectral line (1, if only one spectral line was simulated), the gas_species is the index of the considered gas species (1, if only one gas species was considered), and the quantity is related to various Stokes vector related quantities. 1 is for I , 2 for Q , 3 for U , 4 for V , 5 for the optical depth, and 6 is for the column density.

Integrated velocity channel map

To create a integrated velocity channel map, enter the following command:

```
polaris-plot model_name simulation_name line int_map index_combination
```

The index_combination is the same as for velocity channel maps.

Spectral line spectrum

To create a spectral line spectrum, enter the following command:

```
polaris-plot model_name simulation_name line spectrum index_combination
```

The index_combination is the same as for velocity channel maps.

Average velocity map

To create a map of the average velocity derived from the position of the line peaks, enter the following command:

```
polaris-plot model_name simulation_name line velocity index_combination
```

The index_combination is the same as for velocity channel maps, but without an option to limit the quantity.

Zeeman magnetic field map

To create a magnetic field map, enter the following command:

```
polaris-plot model_name simulation_name zeeman mag_field index_combination
```

The `index_combination` is the same as for velocity channel maps. However, the quantity is related to various displays of the magnetic field strength. 1 is for estimated line-of-sight magnetic field strength for each pixel of the velocity channel map by creating the derivative of the intensity and comparing it to the circularly polarized fraction (see [Brauer et al., 2017a](#)). 2 is the intensity weighted magnetic field strength in the LOS direction. 3 is for the difference between both field strengths, 4 for the absolute difference, 5 for the relative difference between both field strengths, and 6 for the absolute relative difference.

Other plots

If your desired plot routine is not defined here, see Sect. [7.8](#) to create your own custom plot routines. To execute a given custom plot routine, enter the following command:

```
polaris-plot model_name simulation_name dust custom plot_routine_index
```

The `plot_routine_index` is the index of the plot routine (`plot_X()`).

Available options

The Tables [7.8](#) to [7.9](#) show an overview of the available options to modify the plotting of POLARIS results with `polaris-plot`. The red names in brackets show for which Visualization types the option can be used (`maps` stands for `midplane`, `map`, `vel_map`, `int_map`, `velocity`, and `mag_field`). If any number has to be given as a parameter, the exponential format can be used (e.g. `1.2e-3`). Furthermore, if not stated otherwise, the number is interpreted according to the units which are used in the plot

7.5 The command *polaris-remote*

With this tool, POLARIS and its results can be easily transferred between your local computer and a cluster/server. To use it, enter the following command:

```
polaris-remote server_name user_id --remote_command
```

The possible options (as `--remote_command`) to manage file transfer between your local computer and a cluster/server can be found in Table [7.11](#). Exactly one push or pull option has to be chosen and the red names in brackets show which option is required additionally to specify the project to push/pull. The `user_id` is your username/userid to login onto the server/cluster. See Sect. [7.7](#) for available server-/cluster and Sect. [7.8](#) to define your own server/cluster.

7.6 The command *polaris-extra*

With this tool, various input files for POLARIS can be created or converted. Each creation/conversion command has the following structure:

```
polaris-extra --creation_conversion_command
```

The possible options (as `--creation_conversion_command`) to create or convert various POLARIS input files can be found in Table [7.12](#).

Table 7.8: Available options and their default values of `polaris-plot`. The red names in brackets show for which Visualization types the option can be used (`maps` stands for `midplane`, `map`, `vel_map`, `int_map`, `velocity`, and `mag_field`).

Command	Description	
<i>Plot modification</i>		
--cut PARAMETER		Create a cut of a map plot (rotation angle [$^{\circ}$], optional: center position [x, y], not for ' <code>healpix</code> ') (<code>maps</code>) Default: normal map plot
--radial PARAMETER		Create an azimuthally averaged radial profile of a map plot (center position [x, y], not for ' <code>healpix</code> ') (<code>maps</code>) Default: normal map plot
--beam SIZE		Set a beam size to convolve raytrace outputs ["] (<code>maps</code>)
--title		Add explaining title above/into map plots (<code>midplane, map, vel_map</code>) Default: no title plotted
--vel_map_plots NUMBER		Set the max number of images that are on one <code>vel_map</code> plot (<code>vel_map</code>) Default: 8
<i>Zooming and scaling</i>		
--zoom FACTOR		Enable zoom onto the center of the map (<code>maps</code>) Default: no zoom
--zoom_x FACTOR		Enable zoom onto the center of the simulated object (only the x-axis is zoomed) (<code>maps</code>) Default: no zoom
--zoom_y FACTOR		Enable zoom onto the center of the simulated object (only the y-axis is zoomed) (<code>maps</code>) Default: no zoom
--xscaling SCALING		Plot x-axis with ' <code>linear</code> ' or ' <code>log</code> ' scaling (<code>all</code>) Default: ' <code>linear</code> ' scaling
--yscaling SCALING		Plot y-axis with ' <code>linear</code> ' or ' <code>log</code> ' scaling (<code>all</code>) Default: ' <code>linear</code> ' scaling
--cmap_scaling SCALING (+ PARAM)		Plot colormap with ' <code>linear</code> ', ' <code>log</code> ', ' <code>symlog</code> ', (+ linthreshold), or ' <code>power</code> ' (+ exponent) scaling (<code>all</code>) Default: ' <code>linear</code> ' scaling
<i>Units</i>		
--ax_unit UNIT		Unit used for axis and positioning in plots (' <code>arcsec</code> ', ' <code>au</code> ', ' <code>pc</code> ', ' <code>m</code> ', ' <code>arb_units</code> ') (<code>maps</code>) Default: ' <code>au</code> ' (astronomical unit)
--cmap_unit UNIT		Select unit for intensity (' <code>arcsec</code> ': Jy/as ² , ' <code>px</code> ': Jy/px, or ' <code>nuF</code> ': vF _v). ' <code>nuF</code> ' can also be used for <code>spectrum</code> (<code>map, vel_map, int_map</code>) Default: ' <code>arcsec</code> '

Table 7.9: Available options and their default values of *polaris-plot* (continued). The red names in brackets show for which Visualization types the option can be used (*maps* stands for *midplane*, *map*, *vel_map*, *int_map*, *velocity*, and *mag_field*).

<i>Colorbar</i>	
--extend EXTEND	Set colorbar extends ('min', 'max', 'both', 'neither', or automatic if not set)
(<i>maps</i>)	Default: 'neither'
--cmap CMAP_NAME	Set the used colormap via its name
(<i>maps</i>)	Default: 'neither'
--bad_to_min	Set the bad color of the colormap to the minimum color
(<i>maps</i>)	Default: 'neither'
--vmin VMIN	Set the minimum value of the colorbar (extend of the colorbar will be adjusted)
(<i>maps</i>)	Default: minimum value of the plot
--vmax VMAX	Set the maximum value of the colorbar (extend of the colorbar will be adjusted)
(<i>maps</i>)	Default: maximum value of the plot
--xmin XMIN	Set the minimum value of the x-axis in any plot
(<i>all</i>)	Default: minimum value of the x-axis in plot
--xmax XMAX	Set the maximum value of the x-axis in any plot
(<i>all</i>)	Default: maximum value of the x-axis in plot
--ymin YMIN	Set the minimum value of the y-axis in any plot
(<i>all</i>)	Default: minimum value of the y-axis in plot
--ymax YMAX	Set the maximum value of the y-axis in any plot
(<i>all</i>)	Default: maximum value of the y-axis in plot
<i>Vector plot</i>	
--vec_size VEC_FIELD_SIZE	Set the number of pixels per axis that are combined to create vector arrows
(<i>midplane, map</i>)	Default: 16 pixel per axis
--vec_color VEC_COLOR	Set the color of all plotted vectors
(<i>midplane, map</i>)	Default: choose color automatically from colormap to achieve high contrast
--no_vec	Disable the plotting of vectors
(<i>midplane, map</i>)	Default: plot vectors for magnetic field, velocity field and polarization

Table 7.10: Available options and their default values of `polaris-plot` (continued). The red names in brackets show for which Visualization types the option can be used (`maps` stands for `midplane`, `map`, `vel_map`, `int_map`, `velocity`, and `mag_field`).

Font and color	
--font_env ENVIRONMENT	Set the fontsize of the plots (smallest to largest: ' <code>paper</code> ', ' <code>notebook</code> ', ' <code>beamer</code> ', ' <code>poster</code> ')
(all)	<code>Default: 'notebook'</code>
Other	
--beam BEAM_SIZE	Set a beam size in arcseconds to convolve the map plots
(<code>map</code> , <code>vel_map</code> , <code>int_map</code>)	<code>Default: no convolution</code>
--tex, -t	Save the plots as a pgfplot source code (latex file)
(all)	<code>Default: save PDF file</code>
--visual, -v	Show the plot directly
(all)	<code>Default: save PDF file</code>

7.7 Available choices

The following sections provide an overview of all available choices for the PolarisTools commands (models, radiation sources, ...). This collection will not cover any possible model/object. However, it is straightforward to create any model as necessary which is described in Sect. 7.8.

Models

The available models can be found in Table 7.13 and include basic astrophysical objects. Each available model is briefly described. However, for more information about the models take a look at [/model.py](#).

Gas species

The available gas species can be found in Table 7.14 and include typical molecules and atoms (see Sect. 7.8.2 how to add new gas species). Each available gas species is briefly described. However, for more information about the gas species take a look at [/gas.py](#).

Dust components

The available dust choices can be found in Table 7.15 and include typical dust grain compositions (see Sect. 7.8.3 how to add new dust components). Each available dust component is briefly described. However, for more information about the dust components take a look at [/dust.py](#). The red names in brackets show which temperature calculation option can be used (using a single effective dust grain size (`default`), considering each dust grain size separately, or considering stochastic heating).

Detectors

The available detectors can be found in Table 7.16 and should work for most simulations (see Sect. 7.8.4 how to add new detectors). Each available detector is briefly described. However, for more information

Table 7.11: Available options and their default values of `polaris-remote`. Exactly one push or pull option has to be chosen and the red names in brackets show which option is required additionally to specify the project to push/pull.

Command	Description
<i>Push to server</i>	
--push_polaris_package	Push the PolarisTools package to server/cluster (use this, if POLARIS does not exist on server/cluster)
<i>Pull from server</i>	
--pull	Pull POLARIS results of a simulation from the server/cluster (defined by <code>MODEL_NAME</code> and <code>SIMULATION_NAME</code>)
--pull_all	Pull POLARIS results of a model from the server/cluster (defined by <code>MODEL_NAME</code>)
<i>Paths</i>	
--model MODEL_NAME	Define the model you want to exchange between server and local computer
(<code>push</code> , <code>pull</code> , <code>push_all</code> , <code>pull_all</code>)	Default: no default name
--simulation SIMULATION_NAME	Define the simulation you want to exchange between server and local computer
(<code>push</code> , <code>pull</code>)	Default: no default name
<i>Other</i>	
--exclude EXCLUDE	Define what should be excluded from pull/push from/to server/cluster
(<code>all</code>)	Default: no files excluded

Table 7.12: Available options and their default values of `polaris-extra`.

Command	Description
<i>Creation</i>	
<code>--create_zeeman GAS_SPECIES</code>	Creates a Zeeman input file for the chosen GAS_SPECIES (each supported gas species has to be defined in /create_gas.py)
<code>--create_dust mc3d,themis</code>	Creates dust catalog input file(s) with the MC3D code or DUSTEM input files (requires code adjustments in /create_dust.py!)
<i>Conversion</i>	
<code>--convert_jpl JPL_INDEX</code>	Converts a JPL database file (with JPL_INDEX) to the LAMBDA database format (files need to be in polaris/input/jpl_catalog/)
<code>--convert_cdms CDMS_INDEX</code>	Converts a CDMS database file (with CDMS_CODE) to the LAMBDA database format (files need to be in polaris/input/cdms_catalog/)
<i>Visualization</i>	
<code>--info DUST_COMPOSITION</code>	Prints possible wavelengths and dust grain sizes for a chosen dust composition

Table 7.13: Available models and a brief description.

Model	Description
<code>'disk'</code>	A circumstellar disk with a Shakura & Sunyaev density distribution
<code>'globule'</code>	A Bok globule with a Bonnor-Ebert sphere density distribution
<code>'sphere'</code>	A sphere with a constant density distribution

Table 7.14: Available gas species and a brief description.

Gas species	Description
<code>'co'</code>	Carbon monoxide (no zeeman)
<code>'13co'</code>	Carbon monoxide (isotope of co, no zeeman)
<code>'c18o'</code>	Carbon monoxide (isotope of co, no zeeman)
<code>'hco'</code>	HCO molecules (no zeeman)
<code>'so'</code>	Sulfur monoxide (zeeman for levels 3, 8, 10, 28, and 34)
<code>'oh'</code>	Hydroxide (zeeman for levels 2 and 3)
<code>'cn'</code>	Cyanide (zeeman for levels 11 to 17)
<code>'h1'</code>	Neutral hydrogen atom (zeeman for level 1)

Table 7.15: Available dust compositions and a brief description. The red names show which temperature calculation option can be used (using one effective dust grain size ([default](#)), considering each dust grain size, or stochastic heating). The green names show which scattering method can be used with the dust composition.

Dust composition	Description
'graphite_obl'*	Oblate shaped graphite grains (optical data from Weingartner & Draine, 2001)
temperature:	effective size, full dust temp
scattering:	Heney-Greenstein
'silicate_obl'	Oblate shaped astro-silicate grains (optical data from Weingartner & Draine, 2001)
temperature:	effective size, full dust temp
scattering:	Heney-Greenstein
'mrn_obl'	Oblate shaped silicate & graphite grains (silicate: 62.5 %, graphite \vec{E} perpendicular to c-axis: 25 %, graphite \vec{E} parallel to c-axis: 12.5 %; optical data from Weingartner & Draine, 2001)
temperature:	effective size, full dust temp
scattering:	Heney-Greenstein
'graphite_perpend'	Spherical graphite grains (\vec{E} perpendicular to c-axis; optical data from Weingartner & Draine, 2001)
temperature:	effective_size, full dust temp
scattering:	Heney-Greenstein, Mie
'graphite_parallel'	Spherical graphite grains (\vec{E} parallel to c-axis; optical data from Weingartner & Draine, 2001)
temperature:	effective size, full dust temp
scattering:	Heney-Greenstein, Mie
'silicate'	Spherical astro-silicate grains (optical data from Weingartner & Draine, 2001)
temperature:	effective size, full dust temp
scattering:	Heney-Greenstein, Mie
'CM20_1'	Spherical PAH grains (Component of the Themis model Jones et al., 2017)
temperature:	effective size, full dust temp, stochastic heating
scattering:	Heney-Greenstein
'CM20_2'	Spherical carbon grains (Component of the Themis model Jones et al., 2017)
temperature:	effective size, full dust temp, stochastic heating
scattering:	Heney-Greenstein
'aPyM5'	Spherical amorphous pyroxene silicate grains (Component of the Themis model Jones et al., 2017)
temperature:	effective size, full dust temp, stochastic heating
scattering:	Heney-Greenstein
'aOlM5'	Spherical amorphous olivine silicate grains (Component of the Themis model Jones et al., 2014)
temperature:	effective size, full dust temp, stochastic heating
scattering:	Heney-Greenstein
'themis'	Combination of 'CM20_1', 'CM20_2', 'aPyM5' and 'aOlM5' as described by Jones et al. (2017)
temperature:	effective size, full dust temp, stochastic heating
scattering:	Heney-Greenstein

about the detectors see [/detector.py](#).

Table 7.16: Available detectors and a brief description.

Detectors	Description
'cartesian'	A detector using a cartesian ray-tracing grid
'polar'	A detector using a polar ray-tracing grid
'allsky'	A detector using a healpix distributed ray-tracing grid (creates all-sky-maps)

Radiation sources

The available radiation sources can be found in Table 7.17 and include basic stars (see Sect. 7.8.5 how to add new radiation sources). Each available radiation source is briefly described. However, for more information see [source.py](#).

Table 7.17: Available radiation sources and a brief description.

Radiation sources	Description
't_tauri'	A typical T Tauri star ($T = 4000\text{ K}$, $R = 0.9 R_{\odot}$, $M = 0.7 M_{\odot}$)
'herbig_ae'	A typical Herbig Ae star ($T = 8500\text{ K}$, $R = 2 R_{\odot}$, $M = 5 M_{\odot}$)
'sun'	Our sun in the center of the model ($T = 5778\text{ K}$, $R = 1 R_{\odot}$, $M = 1 M_{\odot}$)
'binary'	A binary star with components rotating at a distance of $r_{1,2} = 5\text{ au}$ around the center of the model ($T_{1,2} = 4500\text{ K}$, $R_{1,2} = 0.41 R_{\odot}$, $M_{1,2} = 0.5 M_{\odot}$)
'isrf'	The interstellar radiation field (spectral energy distribution from Evans et al., 2001)

Background radiation sources

The available background radiation sources include only the unpolarized background plane without offset radiation that is used for ray-tracing simulations (see Sect. 7.8.6 how to add a new background radiation source).

Server/cluster

The available server/cluster can be found in Table 7.18 and include those which are used in the working group of Prof. Dr. Sebastian Wolf (see Sect. 7.8.8 how to add new server/cluster). Each available server/cluster is briefly described. However, for more information see [server.py](#).

Table 7.18: Available server/cluster and a brief description.

Server/Cluster	Description
'nec'	The NEC HPC-linux-cluster at Kiel university
'rz_cluster'	The linux-cluster at Kiel university
'astro_cluster'	The astro-cluster at the astrophysics department at Kiel university

7.8 Create your own project

This section describes how additional options/choices can be created for PolarisTools. As described in Section. 2, to take advantage of any changes made to the source code files, the execution of the following command in the `polaris/` directory is required:

```
./install_polaris.sh -u
```

7.8.1 Creating a model

The custom class in the `/custom/model.py` file gives an example how the create your own model (see Listing 7.1). All available options and parameters can be found in the base classes in the `/modules/base.py` file. After creating a new model, add this model to the dictionary at the top of the `/custom/model.py` file:

```
def update_model_dict(dictionary):
    model_dict = {...,
        'custom': CustomModel,
    }
```

The name `'custom'` can now be used as the `model_name` for every PolarisTools usage. This means creating a grid with the distributions defined in the model, performing simulations with the correct conversion factors, and plotting images with the correct extent of the model.

7.8.2 Creating a gas species

The custom class in the `/custom/gas.py` file gives an example how the create your own gas species (see Listing 7.2). All available options and parameters can be found in the base classes in the `/modules/base.py` file. Then, add your gas species to the dictionary at the top of the `/custom/gas.py` file:

```
def update_gas_dict(dictionary):
    gas_dict = {...,
        'custom': MolCustom,
    }
```

The name `'custom'` can now be used as the `GAS_SPECIES` for every `polaris-run` usage to consider the emission of the defined gas species in `line` and `zeeman` simulations. To plot results (magnetic field strength) from Zeeman simulations, provide `shift_2_mag()` and `mag_2_shift()` definitions according to the Zeeman splitting of the gas species.

7.8.3 Creating a dust component

The custom class in the `/custom/dust.py` file gives an example how the create your own dust component (see Listing 7.3). All available options and parameters can be found in the base classes in the `/modules/base.py` file. Then, add your dust component to the dictionary at the top of the `/custom/dust.py` file:

```
def update_dust_dict(dictionary):
    dust_dict = {...,
        'custom': CustomDust,
    }
```

The name `'custom'` can now be used as the `DUST_COMPOSITION` for every `polaris-run` usage to consider the emission of the defined dust grains in `temp`, `rat`, `dust`, and `dust_mc` simulations.

Listing 7.1: CustomModel class in the `/custom/model.py` file

```

class CustomModel(Model):
    """Change this to the model you want to use.
    """

    def __init__(self):
        """Initialisation of the model parameters.
        """
        Model.__init__(self)

        # Set parameters of the custom model (see parent Model class for all available
        # → options)
        self.parameter['distance'] = 140.0 * self.math.const['pc']
        self.parameter['grid_type'] = 'spherical'
        self.parameter['inner_radius'] = 0.1 * self.math.const['au']
        self.parameter['outer_radius'] = 100.0 * self.math.const['au']
        self.parameter['gas_mass'] = 1e-2 * self.math.const['M_sun']
        # Define which other choise are default for this model
        self.parameter['background_source'] = 'bg_plane'
        self.parameter['stellar_source'] = 't_tauri'
        self.parameter['dust_composition'] = 'mrn'
        self.parameter['gas_species'] = 'oh'
        self.parameter['detector'] = 'cartesian'

    def use_extra_parameter(self, extra_parameter):
        """Use this function to set model parameter with the extra parameters.
        """
        # Use extra_parameter to adjust the model without changing the model.py file

    def gas_density_distribution(self):
        """Define here your routine to calculate the density at a given position
        in the model space.

    Notes:
        Use 'self.position' to calculate the quantity depending on position.

        Define also the following routines if necessary:
            dust_density_distribution(self), gas_temperature(self),
            dust_temperature(self), velocity_field(self), magnetic_field(self),
            dust_id(self), dust_min_size(self), dust_max_size(self)

        xyz_density_distribution can return a density or 2D list of densities.
        - The first dimension is used to define multiple density distributions
            for different dust compositions (see CustomDust in dust.py for
            → explanation)
        - With the second dimension, multiple regions of the density distribution
            of the same dust composition can be normalized individually to
            → different total masses.
        - The self.parameter['gas_mass'] needs to have the same dimension and size
            → as the return of this

    Returns:
        float: Gas density at a given position.
    """
    gas_density = 1.0 # Or a function that depends on the position!
    # See other models to find prewritten distributions (shakura & sunyaev, ...)
    return gas_density

```

Listing 7.2: GasCustom class in the /custom/gas.py file

```

class GasCustom(Gas):
    """Change this to the gas species you want to use.
    """

    def __init__(self, file_io, parse_args):
        """Initialisation of the gas parameters.

        Args:
            file_io : Handles file input/output and all
                      necessary paths.
        """
        Gas.__init__(self, file_io, parse_args)

        # Set parameters of the custom gas species
        # (see parent Gas class for available options)
        self.parameter['filename'] = 'gas_database_file.dat'
        self.parameter['abundance'] = 1e-4
        self.parameter['zeeman_usable'] = False

    def shift_2_mag(self, velocity_shift, f_0, i_trans):
        """Calculates the magnetic field strength related to a Zeeman shift of
           a given spectral line transition.

        Args:
            velocity_shift (float) : Zeeman shift in [m/s]
            f_0 (float) : Rest frequency of spectral line [Hz]
            i_trans (int) : transition index of spectral line

        Returns:
            float: Magnetic field strength in [T]
        """
        return 1.0

    def mag_2_shift(self, magnetic_field, f_0, i_trans):
        """Calculates the Zeeman frequency shift of a spectral line
           transition related to a given magnetic field strength.

        Args:
            magnetic_field (float) : Magnetic field strength [T]
            f_0 (float) : Rest frequency of spectral line [Hz]
            i_trans (int) : transition index of spectral line

        Returns:
            float: Zeeman shift in [m/s]
        """
        return 1.0

```

Listing 7.3: CustomDust class in the `/custom/dust.py` file

```

class CustomDust(Dust):
    """Change this to the dust component you want to use.
    """

    def __init__(self, file_io, parse_args):
        """Initialisation of the dust parameters.

        Args:
            file_io : Handles file input/output and all necessary paths.
        """
        Dust.__init__(self, file_io, parse_args)

        # Define the dust catalog file in the POLARIS standard file format
        # (relative to the polaris/input/ directory)
        self.parameter['dust_cat_file'] = 'custom.dat'
        # Relative fraction of this dust composition to mix multiple dust compositions
        self.parameter['fraction'] = 1.0
        # Material density of the custom composition [kg/m^3]
        self.parameter['material_density'] = 2500
        # Minimum dust grain size
        self.parameter['amin'] = 5e-9
        # Maximum dust grain size
        self.parameter['amax'] = 250e-9
        # Possible dust size distributions 'plaw', 'plaw-ed', 'logn'
        self.parameter['size_keyword'] = 'plaw'
        # List of size parameter for dust size distribution (plaw -> [exponent])
        self.parameter['size_parameter'] = [-3.5]

    def get_command(self):
        """Provides dust component command line for POLARIS .cmd file.

        Note:
            This demonstrates how to mix multiple dust components together.

        Returns:
            str: Command line to consider the custom dust component.
        """
        # This shows how to mix multiple dust components and use them as one
        new_command_line = str()
        dust = self.dust_chooser.get_module_from_name('silicate_oblate')
        dust.parameter['fraction'] = 0.625
        new_command_line += dust.get_command_line()
        dust = self.dust_chooser.get_module_from_name('graphite_oblate')
        dust.parameter['fraction'] = 0.375
        new_command_line += dust.get_command_line()
        return new_command_line

```

7.8.4 Creating a detector

The custom class in the `/custom/detector.py` file gives an example how to create your own detector (see Listing 7.4 and 7.5). All available options and parameters can be found in the base classes in the `/modules/base.py` file.

Then, add your detector to the dictionary at the top of the `/custom/detector.py` file:

```
def update_detector_dict(dictionary):
    detector_dict = {...,
        'custom': CustomDetector,
    }
```

The name `'custom'` can now be used as the DETECTOR for every `polaris-run` usage to consider observe the emission in `dust`, `dust_mc`, and `line` simulations.

7.8.5 Creating a stellar radiation source

The custom class in the `/custom/source.py` file gives an example how to create your own stellar radiation source (see Listing 7.6). All available options and parameters can be found in the base classes in the `/modules/base.py` file. Then, add your stellar radiation source to the dictionary at the top of the `/custom/source.py` file:

```
def update_sources_dict(dictionary):
    sources_dict = {...,
        'custom': CustomStar,
    }
```

The name `'custom'` can now be used as the STELLAR_SOURCE for every `polaris-run` usage to consider the emission of the defined stellar radiation source in `temp`, `rat`, and `dust_mc` simulations.

7.8.6 Creating a background radiation source

The custom class in the `/custom/bg_source.py` file gives an example how to create your own background radiation source (see Listing 7.7). All available options and parameters can be found in the base classes in the `/modules/base.py` file. Then, add your background radiation source to the dictionary at the top of the `/custom/bg_source.py` file:

```
def update_bg_source_dict(dictionary):
    bg_source_dict = {...,
        'custom': CustomBGsource,
    }
```

The name `'custom'` can now be used as the BG_SOURCE for every `polaris-run` usage to consider the emission of the defined background radiation source in `dust` and `line` simulations (ray-tracing).

7.8.7 Creating a custom plot routine

The custom function in the `/custom/plots.py` file gives an example how to create your own plotting routines (see Listing 7.8). Perform a custom plotting routine by executing the following command:

```
polaris-plot model_name simulation_name simulation_type custom X
```

The number `X` is the unique identifier for the custom plot routine `plot_X()`.

Listing 7.4: CustomDetector class in the `/custom/detector.py` file

```

class CustomDetector(Detector):
    """Change this to the detector you want to use.
    """

    def __init__(self, model, parse_args):
        """Initialisation of the detector configuration.

        Args:
            model: Handles the model space including various
                   quantities such as the density distribution.
        """
        Detector.__init__(self, model, parse_args)
        # First wavelength of the observing wavelengths
        self.parameter['wavelength_min'] = 1e-6
        # Last wavelength of the observing wavelengths
        self.parameter['wavelength_max'] = 1e-6
        # Number of logarithmically distributed wavelengths
        # between wavelength_min and wavelength_max
        self.parameter['nr_of_wavelength'] = 1
        # Rotation angle around the first rotation axis
        self.parameter['rot_angle_1'] = 0.
        # Rotation angle around the second rotation axis
        self.parameter['rot_angle_2'] = 0.
        # Number of pixel per axis of the detector
        self.parameter['nr_pixel_x'] = 256
        # Number of pixel per axis of the detector
        self.parameter['nr_pixel_y'] = 256
        # Index of the related background source (for dust/line simulations)
        self.parameter['source_id'] = 1
        # Index of the related gas_species (for line simulations)
        self.parameter['gas_species_id'] = 1
        # Index of the related transition (for line simulations)
        self.parameter['transition_id'] = 1
        # Factor to zoom onto the observing object
        self.parameter['sidelength_zoom_x'] = 1
        self.parameter['sidelength_zoom_y'] = 1
        # Offset of the detector in x- and y-direction
        self.parameter['map_shift_x'] = 0.
        self.parameter['map_shift_y'] = 0.
        # Acceptance angle for dust_mc simulations without peel-off technique
        self.parameter['acceptance_angle'] = 1.0
        # Detector shape (defining the background grid for ray-tracing simulations)
        self.parameter['shape'] = 'cartesian'

```

Listing 7.5: CustomDetector class in the `/custom/detector.py` file(continued)

```

def get_dust_scattering_command(self):
    """Provides detector configuration command line for Monte-Carlo
    simulations for POLARIS .cmd file.

    Returns:
        str: Command line to consider the detector configuration.
    """
    '''To add multiple detectors, use the following:
new_command_line = str()
self.parameter['rot_angle_1'] = 0.0
new_command_line += self.get_dust_scattering_command_line()
self.parameter['rot_angle_1'] = 90.0
new_command_line += self.get_dust_scattering_command_line()
return new_command_line
'''
    return self.get_dust_scattering_command_line()

def get_dust_emission_command(self):
    """Provides detector configuration command line for raytrace
    simulations for POLARIS .cmd file.

    Returns:
        str: Command line to consider the detector configuration.
    """
    '''To add multiple detectors, use the following:
new_command_line = str()
self.parameter['rot_angle_1'] = 0.0
new_command_line += self.get_dust_emission_command_line()
self.parameter['rot_angle_1'] = 90.0
new_command_line += self.get_dust_emission_command_line()
return new_command_line
'''
    return self.get_dust_emission_command_line()

def get_line_command(self):
    """Provides detector configuration command line for spectral line
    simulations for POLARIS .cmd file.

    Returns:
        str: Command line to consider the detector configuration.
    """
    '''To add multiple detectors, use the following:
new_command_line = str()
self.parameter['rot_angle_1'] = 0.0
new_command_line += self.get_line_command_line()
self.parameter['rot_angle_1'] = 90.0
new_command_line += self.get_line_command_line()
return new_command_line
'''
    return self.get_line_command_line()

```

Listing 7.6: CustomStar class in the `/custom/source.py` file

```

class CustomStar(StellarSource):
    """Change this to the star you want to use.
    """

    def __init__(self, file_io, parse_args):
        """Initialisation of the stellar source parameters.

        Args:
            file_io : Handles file input/output and all necessary paths.
        """
        StellarSource.__init__(self, file_io, parse_args)

        # Position of the star [m, m, m]
        self.parameter['position'] = [0, 0, 0]
        # Effective temperature of the star [K]
        self.parameter['temperature'] = 4000
        # Radius of the star [R_sun] or luminosity [L_sun]
        self.parameter['radius'] = 2.0
        # Number of photons if no number is chosen via --photons
        self.parameter['nr_photons'] = 1000000
        # Can the velocity field be calculated by only this star in the center?
        self.parameter['kepler_usable'] = True
        # Mass of the star [M_sun] (for Keplerian rotation)
        self.parameter['mass'] = 0.7

    def get_command(self):
        """Provides stellar source command line for POLARIS .cmd file.

        Returns:
            str: Command line to consider the stellar source.
        """
        """To add multiple stars, use the following:
        new_command_line = str()
        self.parameter['temperature'] = 8000
        self.parameter['radius'] = 4.0
        new_command_line += self.get_command_line()
        self.parameter['temperature'] = 5000
        self.parameter['radius'] = 3.0
        new_command_line += self.get_command_line()
        return new_command_line
        """
        return self.get_command_line()

```

Listing 7.7: CustomBGsource class in the /custom/bg_source.py file

```
class CustomBGsource(BGSource):
    """Change this to the background source you want to use.
    """

    def __init__(self, file_io, parse_args):
        """Initialisation of the background source parameters.

        Args:
            file_io : Handles file input/output and all
                      necessary paths.
        """

        BGSource.__init__(self, file_io, parse_args)

        #: dict: Parameters which are different to the default values
        bg_source_parameter = {
            'A': 1.0e-3,
            'T': 1000.,
            'Q': 1.,
            'U': 0.,
            'V': 0.,
        }

        # Updates the parameter dictionary
        self.parameter.update(bg_source_parameter)
```

Listing 7.8: plot_1 class in the /custom/plots.py file

```

def plot_1(self):
    """Plot line spectrum from POLARIS simulations.
    """
    # Set data input to Jy to calculate the total flux
    self.file_io.cmap_unit = 'total'
    # Read spectrum data
    plot_data, header = self.file_io.read_spectrum(
        'line_spectrum_species_0001_line_0001')
    # Create pdf file if show_plot is not chosen
    self.file_io.init_plot_output('line_spectrum_species_0001_line_0001')
    velocity = []
    for vch in range(header['nr_channels']):
        # Get velocity of current channel
        velocity.append(1e-3 * self.math.get_velocity(vch,
            header['nr_channels'], header['max_velocity']))
    for i_quantity in range(4):
        # Create Matplotlib figure
        plot = Plot(self.model, self.parse_args,
            xlabel=r'$\mathit{v}\,[\mathrm{kilo\,metre\,per\,second}]$',
            ylabel=self.file_io.get_quantity_labels(i_quantity),
            extent=[velocity[0], velocity[-1], None, None], with_cbar=False)
        # Plot spectrum as line
        plot.plot_line(velocity, plot_data[i_quantity, :], marker='.')
        # Save figure to pdf file or print it on screen
        plot.save_figure(self.file_io)

```

Listing 7.9: CustomServer class in the `/custom/server.py` file

```

class CustomServer(Server):
    """Change this to the server you want to use.
    """

    def __init__(self, parse_args):
        """Initialisation of the server/cluster parameters.
        """
        Server.__init__(self, parse_args)

        # To obtain the 'node_name', enter the following commands on the server/cluster:
        # python
        # import platform
        # platform.node()
        # -> 'custom_system' (e.g. 'nesh-fe2' -> use 'nesh' as 'node_name')
        self.parameter['node_name'] = 'custom_system'
        # This directory is defined as a relative path to your home dir on the server
        self.parameter['server_polaris_dir'] = 'the_polaris_directory'
        self.parameter['address'] = 'custom_server.de:~/'
        self.parameter['queue_system'] = 'PBS'
        self.parameter['short_walltime'] = '2:00:00'
        self.parameter['short_batch_class'] = 'clexpress'
        self.parameter['medium_walltime'] = '48:00:00'
        self.parameter['medium_batch_class'] = 'clmedium'
        self.parameter['long_walltime'] = '100:00:00'
        self.parameter['long_batch_class'] = 'cllong'
        self.parameter['nr_threads'] = 16

    def get_command_line(self):
        """Provides server/cluster command line for POLARIS .cmd file. The syntax depends
           ↪ on the used queue system.

        Returns:
            str: Command line to consider a server/cluster.
        """
        new_command_line = str()
        new_command_line += '#' + self.parameter['queue_system'] + '-o' + \
                           + self.parameter['simulation_directory'] + 'POLARIS.out' + '\n'
        new_command_line += '#' + self.parameter['queue_system'] + '-j\n',
        new_command_line += '#' + self.parameter['queue_system'] + \
                           + '-l elapstim_req=' + self.parameter['walltime'] + '\n'
        new_command_line += '#' + self.parameter['queue_system'] + \
                           + '-l memsz_job=' + self.parameter['ram_usage'] + '\n'
        new_command_line += '#' + self.parameter['queue_system'] + \
                           + '-b' + self.parameter['node_number'] + '\n'
        new_command_line += '#' + self.parameter['queue_system'] + \
                           + '-l cpunum_job=' + str(self.parameter['nr_threads']) + '\n'
        new_command_line += '#' + self.parameter['queue_system'] + \
                           + '-q' + self.parameter['batch_class'] + '\n'
        new_command_line += '#' + self.parameter['queue_system'] + \
                           + '-N' + self.parse_args.simulation_name[0:15] + '\n'

        return new_command_line

```

7.8.8 Adding a server/cluster

The custom class in the `/custom/server.py` file gives an example how to create your own server/cluster (see Listing 7.9). All available options and parameters can be found in the base classes in the `/modules/base.py` file. Then, add your server/cluster to the dictionary at the top of the `/custom/server.py` file:

```
def update_server_dict(dictionary):
    server_dict = {...,
        'custom': CustomServer,
    }
```

The name `'custom'` can now be used as the `server_name` for every `polaris-remote` usage to move POLARIS related files between your local computer and the server/cluster. In addition, PolarisTools knows on which machine it runs and is able to prepare the shell scripts for queue usage.

7.8.9 Creating an external input

The custom class in the `/custom/ext_input.py` file gives an example how to create your own external input (see Listing 7.10). All available options and parameters can be found in the base classes in the `/modules/base.py` file. Then, add your external input data to the dictionary at the top of the `/custom/ext_input.py` file:

```
def update_ext_input_dict(dictionary):
    ext_input_dict = {...,
        'custom': CustomInput,
    }
```

The name `'custom'` can now be used as the `EXTERNAL_INPUT_NAME` for every `polaris-gen` usage to read the model/grid data from external files instead of calculating them analytically.

Listing 7.10: CustomInput class in the /custom/ext_input.py file

```

class CustomInput(ExternalInput):
    """Change this to the external input you want to use.
    """

    def __init__(self, file_io, parse_args):
        """Initialisation of the external input parameters.

        Args:
            file_io : Handles file input/output and all
                      necessary paths.
        """
        ExternalInput.__init__(self, file_io, parse_args)

        # Index of the MHD simulation
        self.model_index = 320

    def init_data(self):
        """Reads the data of e.g. an MHD simulation
        """

        # Save the data in this list
        self.data = [1.0]

    def gas_density_distribution(self):
        """Define here your routine to get the density at a given position
        in the model space from your read input data.

        Notes:
            Define also the following routines if necessary:
            - dust_density_distribution(self)
            - gas_temperature(self)
            - dust_temperature(self)
            - velocity_field(self)
            - magnetic_field(self)
            - dust_id(self)

        Returns:
            float: Gas density at a given position.
        """
        return self.data[0]

```

7.9 Quickstart guide

To try out the main capabilities of POLARIS, use the following step-by-step instruction. The example simulations are based on a model of a circumstellar disk with characteristics shown in Table 7.19. In this model, we assume compact, homogeneous, and spherical dust grains with a composition of 62.5% silicate and 37.5% graphite (MRN-dust, Mathis et al. 1977; optical properties from Weingartner & Draine 2001).

We consider furthermore a density distribution with a radial decrease based on the work of Hayashi (1981) for the minimum mass solar nebula. Combined with a vertical distribution due to hydrostatic equilibrium similar to the work of Shakura & Sunyaev (1973), we obtain the following equation:

$$\rho_{\text{disk}} = \rho_0 \left(\frac{R_{\text{ref}}}{\bar{\omega}} \right)^a \exp \left(-\frac{1}{2} \left[\frac{z}{H(\bar{\omega})} \right]^2 \right). \quad (7.1)$$

Here, $\bar{\omega}$ is the radial distance from the central star in the disk midplane, z is the distance from the midplane of the disk, R_{ref} is a reference radius, and $H(\bar{\omega})$ is the scale height. The density ρ_0 is derived from the disk (gas) mass. The scale height is a function of $\bar{\omega}$ as follows:

$$H(\bar{\omega}) = h_0 \left(\frac{\bar{\omega}}{R_{\text{ref}}} \right)^b. \quad (7.2)$$

The parameters a and b set the radial density profile and the disk flaring, respectively.

7.9.1 Create a grid

The first step is the creation of a grid, based on the chosen model. To do this, enter the following command ($t \sim 1$ s):

```
polaris-gen disk grid.dat
```

Now, you have a binary file named '`grid.dat`' in your `projects/disk/` directory that contains a grid with cells that have physical quantities like density and temperature that are defined by the chosen model.

7.9.2 Dust temperature distribution

The dust temperature distribution can be simulated by assuming that the dust grains are in equilibrium with the radiation field. To do this, enter the following command ($t \sim 1$ min):

```
polaris-run disk example temp --grid grid.dat --adj_tgas 1
```

The temperature distribution can easily be visualized by entering the following commands:

```
polaris-plot disk example temp midplane output dust_temperature xy  
polaris-plot disk example temp midplane output dust_temperature xz
```

You will find the resulting PDF files in the `projects/disk/example/temp/plots/` directory. The temperature distributions should look like those in Fig. 7.1.

7.9.3 Dust thermal emission

Based on the dust temperature distribution, the thermal emission of the dust grains at $\lambda = 850 \mu\text{m}$ can be simulated. To do this, enter the following command ($t \sim 1$ min):

```
polaris-run disk example dust --wavelength 850e-6
```

The thermal emission can easily be visualized by entering the following command:

```
polaris-plot disk example dust map 1 --cmap_scaling power 0.5
```

You will find the resulting PDF file in the `projects/disk/example/dust/plots/` directory. The intensity map is scaled by the power of 0.5 and should look like Fig. 7.2.

Table 7.19: Characteristics and default parameters of the considered circumstellar disk model ('disk').

<i>Central star</i>		
Radiation source		't_tauri'
Effective temperature	T_{star}	4000 K
Stellar radius	R_{star}	$0.9 R_{\odot}$
Stellar mass	M_{star}	$0.7 M_{\odot}$
<i>Disk model</i>		
Distance to star/disk	d	140 pc
Inner radius	R_{in}	0.1 au
Outer radius	R_{ou}	300 au
Scale height	h_0	10 au
Characteristic radius	R_{ref}	100 au
Radial density decrease	a	1.625
Disk flaring	b	1.125
Grid geometry		'spherical'
Cells in r -direction	n_r	100
Step width factor in r	sf_r	1.03
Cells in θ -direction	n_{θ}	91
Step width factor in θ	sf_{θ}	1.0 (sinus distribution)
Cells in ϕ -direction	n_{ϕ}	1
Inclination	i	0° (face-on), 90° (edge-on)
<i>Gas species</i>		
Gas species		'co'
Transitions frequency	ν_0	230.538 GHz
Abundance	CO/H	10^{-4}
Spectral resolution	$\Delta\nu_{\text{res}}$	132 MHz (171 m s ⁻¹)
Gas mass	M_{gas}	$10^{-4} M_{\odot}$
Gas-to-dust mass ratio	$M_{\text{gas}} : M_{\text{dust}}$	100 : 1
Turbulent velocity	v_{turb}	100 m s ⁻¹
Velocity field		Keplerian
<i>Dust grains</i>		
Dust grain composition		'mrn' (silicate, graphite)
Minimum dust grain size	a_{\min}	5 nm
Maximum dust grain size	a_{\max}	250 nm
Size exponent	a_{size}	-3.5
<i>Magnetic field</i>		
Magnetic field strength	B_z	1 mG

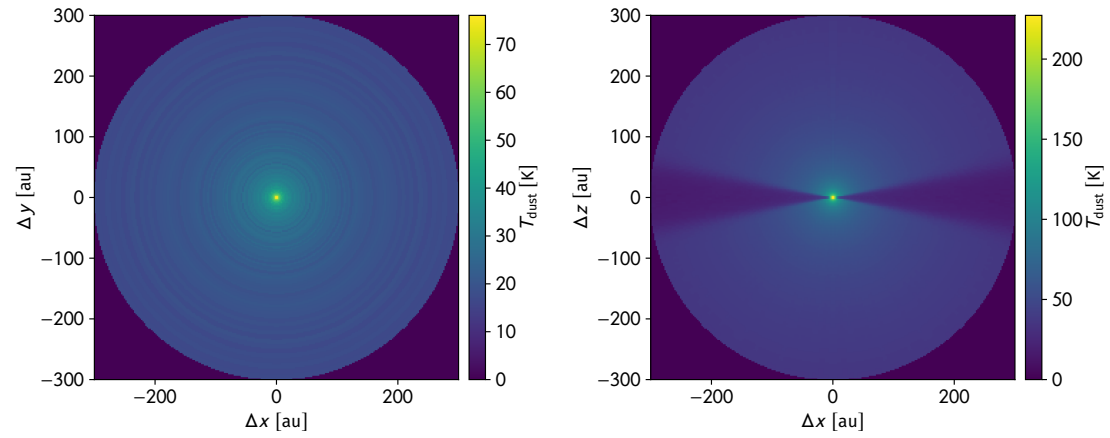


Figure 7.1: Dust temperature distribution in the disk midplane (*left*) and as a vertical cut through the disk (*right*).

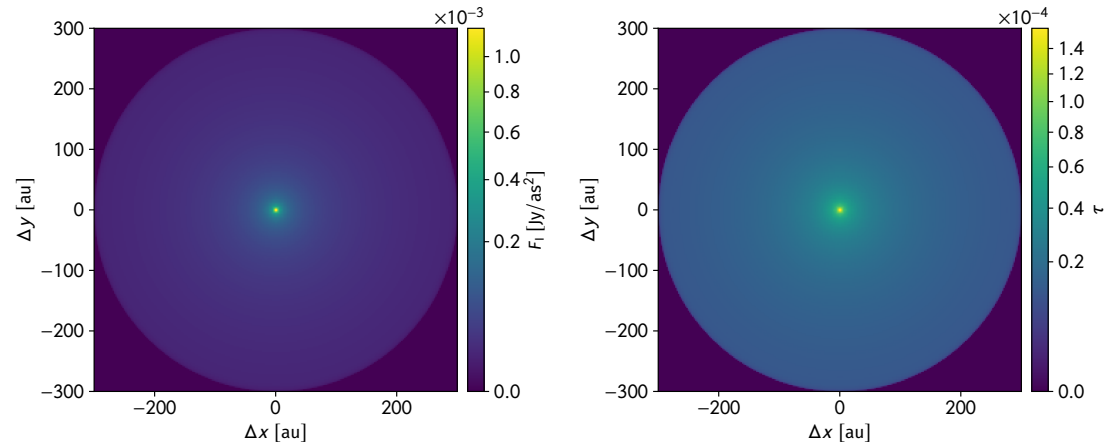


Figure 7.2: Thermal emission of the spherical dust grains at $\lambda = 850 \mu\text{m}$ (*left*) and optical depth along the line-of-sight (*right*).

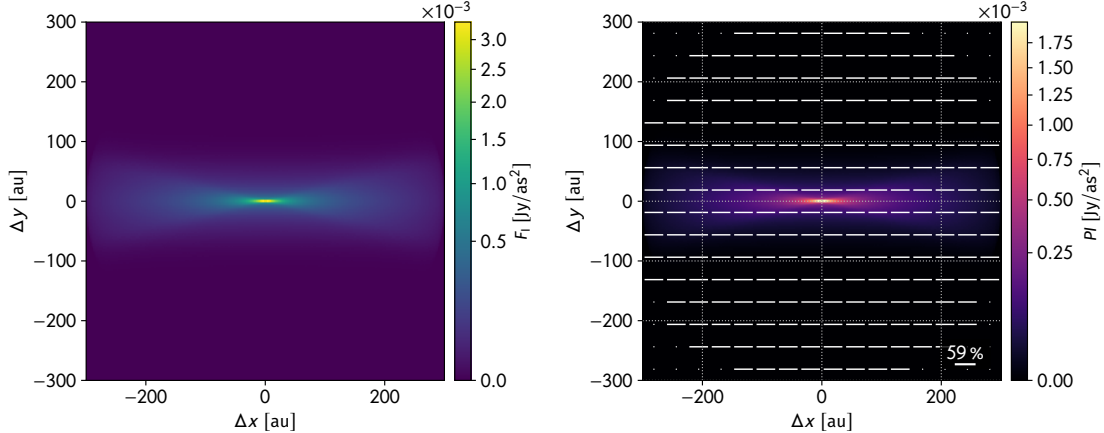


Figure 7.3: Thermal emission of the non-spherical dust grains at $\lambda = 850 \mu\text{m}$ (left) and the linearly polarized intensity overlapped with polarization vectors (right).

7.9.4 Dust thermal emission (with grain alignment)

Based on the dust temperature distribution, the thermal emission of aligned non-spherical dust grains at $\lambda = 850 \mu\text{m}$ can be simulated. To do this, enter the following command ($t \sim 2 \text{ min}$):

```
polaris-run disk example dust_pa --wavelength 850e-6 --rot_1 90 --dust mrn Oblate
```

In this simulation, the disk is observed edge-on (`--rot_1`) and the spherical dust grains will be replaced by oblate dust grains (`--dust`) which are perfectly perpendicular aligned with their longest axis to the magnetic field (`_pa`). Since this guide only shows the capabilities of POLARIS, it is sufficient to use the dust temperature distribution which was simulated with spherical dust grains. Otherwise, the temperature distribution needs to be calculated again with oblate dust grains (`--dust`). The thermal emission can easily be visualized by entering the following command:

```
polaris-plot disk example dust_pa map 1 --cmap_scaling power 0.5
```

You will find the resulting PDF file in the [projects/disk/example/dust_pa/plots/](#) directory. The polarized intensity map is scaled by the power of 0.5 and should look like Fig. 7.3.

7.9.5 Scattered stellar emission

Based on the dust density distribution, the stellar radiation at $\lambda = 1 \mu\text{m}$ scattered at the spherical dust grains can be simulated. To do this, enter the following command ($t \sim 5 \text{ min}$):

```
polaris-run disk example dust_mc --rot_1 60 --peel 1 --wavelength 1e-6 --photons 1e7
```

The disk is inclined by 60° (`--rot_1`) to achieve a better visual impression of the scattered light. The scattered stellar radiation can easily be visualized by entering the following command:

```
polaris-plot disk example dust_mc map 1 --cmap_scaling power 0.3
```

You will find the resulting PDF files in the [projects/disk/example/dust_mc/plots/](#) directory. The scattered light map should look like Fig. 7.4 (top).

7.9.6 Thermal emission and scattered stellar emission

The stellar emission scattered at spherical dust grains can also be included in the thermal emission calculation. To do this, the temperature calculation needs to be repeated with the `--radiation_field` option by entering the following command ($t \sim 2 \text{ min}$):

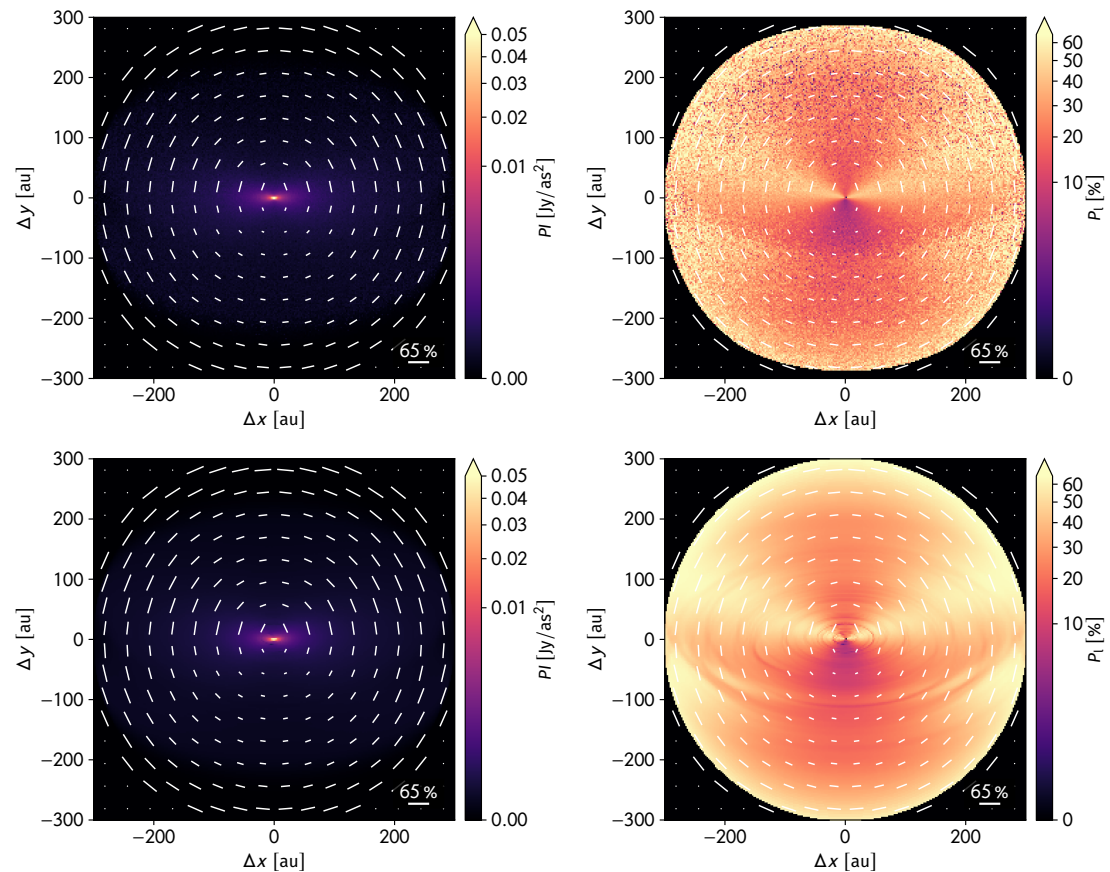


Figure 7.4: Polarized intensity map (*left*) and degree of polarisation (*right*) of the stellar emission at $\lambda = 1 \mu\text{m}$ scattered by spherical dust grains without (*top*) and with the thermal emission of the dust grains (*bottom*).

```
polaris-run disk example2 temp --grid grid.dat --adj_tgas 1 --radiation_field
```

Then, the thermal emission and scattered stellar emission of the dust grains at $\lambda = 1 \mu\text{m}$ can be simulated. To do this, enter the following command ($t \sim 5 \text{ min}$):

```
polaris-run disk example2 dust --rot_1 60 --wavelength 1e-6
```

The disk is inclined by 60° (`--rot_1`) to achieve a better visual impression of the scattered light. The scattered stellar radiation can easily be visualized by entering the following command:

```
polaris-plot disk example2 dust map 1 --cmap_scaling power 0.3
```

You will find the resulting PDF files in the [projects/disk/example/dust_mc/plots/](#) directory. The scattered light map should look like Fig. 7.4 (bottom).

7.9.7 Spectral line emission

Based on the gas temperature distribution (due to `--adj_tgas 1`), the spectral line emission of the C¹⁸O $J = 1 \rightarrow 0$ transition ($\nu \sim 109 \text{ GHz}$) can be simulated. To do this, enter the following command ($t \sim 5 \text{ min}$):

```
polaris-run disk example line --gas c18o --rot_1 90 --kepler
```

In this simulation, the disk is observed edge-on (`--rot_1`) and the Keplerian rotation around the central star is considered for the velocity field (`--kepler`).

The spectral line emission can easily be visualized by entering the following commands:

```
polaris-plot disk example line vel_map 1 1 1
polaris-plot disk example line int_map 1 1 1
polaris-plot disk example line spectrum 1 1 1
```

The results are limited to the first simulated transition of the first gas species and the first quantity (F_1). You will find the resulting PDF files in the [projects/disk/example/line/plots/](#) directory. The velocity channel map, integrated velocity channel map and spectrum should look like Fig. 7.5 (top, middle).

7.9.8 Spectral line emission (with Zeeman splitting)

Based on the gas temperature distribution (due to `--adj_tgas 1`), the Zeeman split spectral line emission of the OH transition at $\nu \sim 1665 \text{ MHz}$ can be simulated (see [Brauer et al. 2017a](#)). To do this, enter the following command ($t \sim 60 \text{ min}$):

```
polaris-run disk example zeeman --gas oh --transition 2 --max_vel 1000
```

In this simulation, the observed velocities are focused on the range between $v = \pm 1 \text{ km}$ and the disk is observed face-on (default) and, therefore, the Keplerian rotation is not required.

The spectral line emission can easily be visualized by entering the following commands:

```
polaris-plot disk example zeeman mag_field 1
polaris-plot disk example zeeman spectrum 1
```

You will find the resulting PDF files in the [projects/disk/example/line/plots/](#) directory. The integrated velocity map and circular polarization spectrum should look like Fig. 7.5 (bottom).

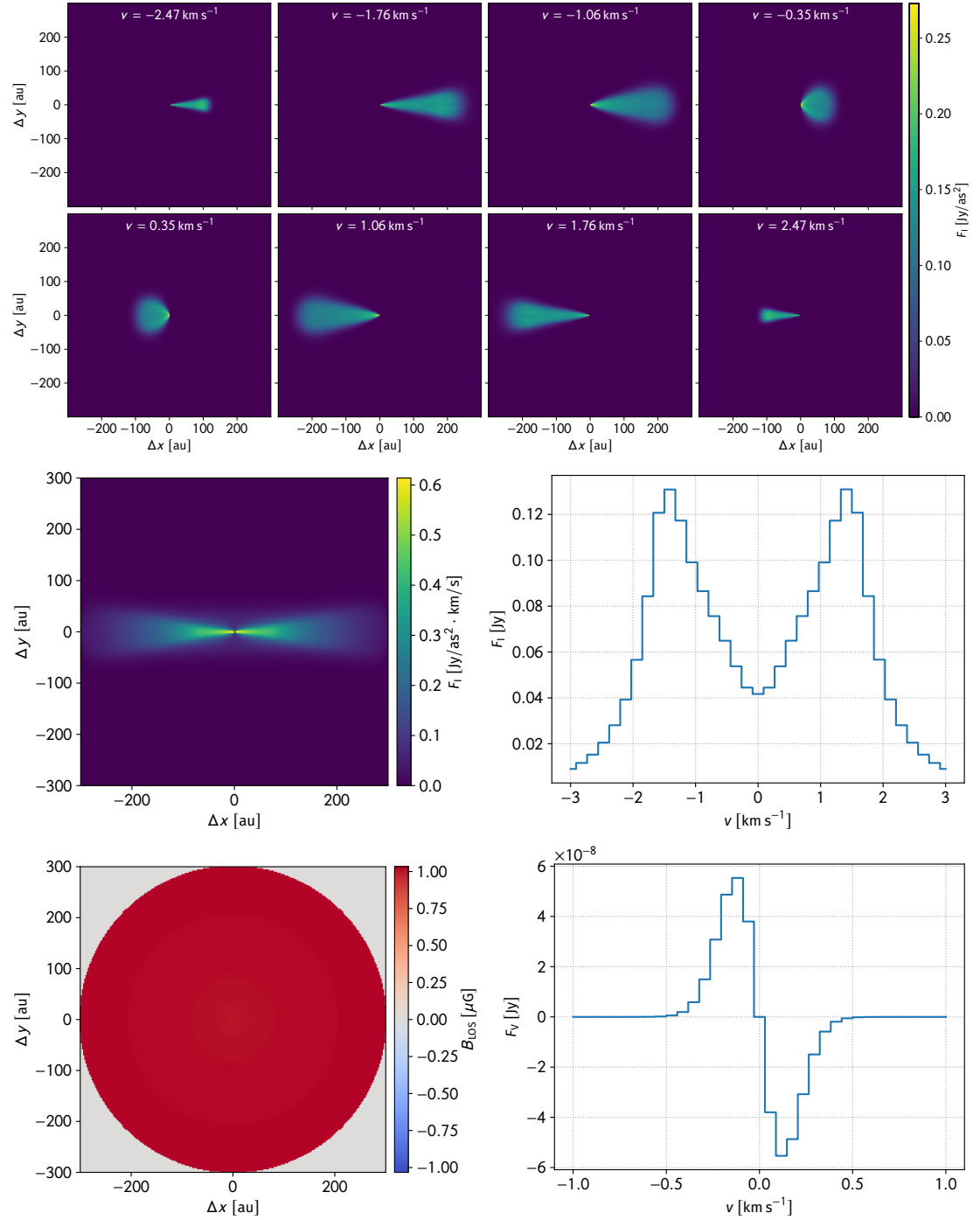


Figure 7.5: Velocity channel map (top), Integrated velocity channel map (middle left) and spectral line profile (middle right) of the CO $J = 1 \rightarrow 0$ transition ($v \sim 115 \text{ GHz}$). Estimated magnetic field strength (bottom left) and circular polarization profile (bottom right) of the OH transition at $v \sim 1665 \text{ MHz}$.

8 Files and directories

In the following, find an overview of all important files and directories that are used by POLARIS:

src/ ⇒ *Source files of the POLARIS code (c++)*
 /CommandParser[.cpp, .h] ⇒ *Parser for user inputs*
 /Cylindrical[.cpp, .h] ⇒ *Definition and handling of the cylindrical grid*
 /Detector.h ⇒ *Definition and handling of detector/output*
 /Dust[.cpp, .h] ⇒ *Definition and handling of dust grains*
 /Faddeeva[.cc, .hh] ⇒ *The Faddeeva package*
 /GasSpecies[.cpp, .h] ⇒ *Definition and handling of the gas species*
 /Grid[.cpp, .h] ⇒ *Definition and handling of the grid in general*
 /main.cpp ⇒ *Main file of POLARIS*
 /MathFunctions[.cpp, .h] ⇒ *Numerical calculations*
 /Matrix2D.h ⇒ *Definition and handling of matrices*
 /OcTree[.cpp, .h] ⇒ *Definition and handling of the OcTree grid*
 /OPIATE[.cpp, .h] ⇒ *Interface to the OPIATE code (currently disabled)*
 /Pipeline[.cpp, .h] ⇒ *Pipeline of POLARIS (handling of simulations)*
 /RadiativeTransfer[.cpp, .h] ⇒ *Solves the radiative transfer equation (various algorithms)*
 /Raytracing.h ⇒ *Definition and handling of the ray-tracing*
 /Source[.cpp, .h] ⇒ *Definition and handling of the radiation sources*
 /Spherical[.cpp, .h] ⇒ *Definition and handling of the spherical grid*
 /Stokes.h ⇒ *Definition and handling of the Stokes vector*
 /Synchrotron[.cpp, .h] ⇒ *Definition and handling of Synchrotron radiation*
 /typedefs.h ⇒ *Definition of various constants*
 /Vector.h ⇒ *Definition and handling of vectors*
 /Voronoi[.cpp, .h] ⇒ *Definition and handling of the voronoi grid*

input/ ⇒ *Input data used by POLARIS*
 /interstellar_radiation_field.dat ⇒ *Spectral energy distribution of the ISRF*
 /dust/xyz.dat ⇒ *Dust database files in the default POLARIS format*
 /gas/xyz.dat ⇒ *Gas database files in the LAMDA format (including Zeeman files)*

CCfits/ ⇒ *CCfits library used for handling fits files*
cfitsio/ ⇒ *Cfitsio library required by CCfits*

bin/ ⇒ *Executables to use systemwide (added to the PATH variable in the bashrc)*

lib/ ⇒ *Libraries to use systemwide (added to the PATH variable in the bashrc)*

projects/ ⇒ All simulations created with PolarisTools
 /model_name/ ⇒ Simulations related to a certain model
 /simulation_name/ ⇒ Simulations related to a simulation name
 /simulation_type/ ⇒ Simulations related to a simulation type
 /data/ ⇒ Output data files from POLARIS
 /plots/ ⇒ Plots from POLARIS or PolarisTools

tools/ ⇒ PolarisTools main directory
 /src/ ⇒ Source files of PolarisTools (python)
 /polaris-extra.in ⇒ Source file for the polaris-extra tool
 /polaris-gen.in ⇒ Source file for the polaris-gen tool
 /polaris-plot.in ⇒ Source file for the polaris-plot tool
 /polaris-remote.in ⇒ Source file for the polaris-remote tool
 /polaris-run.in ⇒ Source file for the polaris-run tool
 /polaris-test.in ⇒ Source file for the polaris-test tool (developer only)
 /modules/ ⇒ Modules for the PolarisTools
 /base.py ⇒ Definition of base classes for inheritance
 /bg_source.py ⇒ Definition of available background sources
 /command.py ⇒ Creates POLARIS command files
 /create_dust.py ⇒ Create dust catalog input files
 /create_gas.py ⇒ Create gas species input files
 /detector.py ⇒ Definition of available detectors
 /dust_source.py ⇒ Definition to use dust grains as a source
 /dust.py ⇒ Definition of available dust compositions
 /ext_input.py ⇒ Definition of available external data inputs
 /file.py ⇒ Handles file input/output
 /gas.py ⇒ Definition of available gas species
 /grid.py ⇒ Creates grids for POLARIS
 /math.py ⇒ Various calculations
 /model.py ⇒ Definition of available models
 /server.py ⇒ Definition of available servers (file exchange and queue usage)
 /source.py ⇒ Definition of available radiation sources
 /visual.py ⇒ Plot engine
 /custom/ ⇒ User-definable modules for the PolarisTools
 /bg_source.py ⇒ Definition of User-definable background sources
 /detector.py ⇒ Definition of User-definable detectors
 /dust.py ⇒ Definition of User-definable dust compositions
 /ext_input.py ⇒ Definition of User-definable external data inputs
 /gas.py ⇒ Definition of User-definable gas species
 /model.py ⇒ Definition of User-definable models
 /plots.py ⇒ Definition of User-definable plot routines
 /server.py ⇒ Definition of User-definable servers (file exchange and queue usage)
 /source.py ⇒ Definition of User-definable radiation sources

9 Changelog

The following list provides an overview of the fixed bugs and changes made in the last updates of POLARIS.

Version 4.02 \Rightarrow 4.03

- Added option to use the Mathis ISRF without SED file (see Sect. 4.2)
- Updated the use of the refractive index and Mie scattering calculation to the Wolf & Voshchinnikov approach (see Sect. 3.4.3).
- In addition to the grain alignment radius a_{alg} , the output midplane files of RAT simulations contain now also the average radiation field anisotropy and the average cosine between radiation field and magnetic field.
- In addition to other quantities, the output midplane files of TEMP and/or RAT simulations and the input midplane files of simulations that use the radiation field may include now also the radiation field and the Habing field G_0 value (see Table 3.8).
- The RAT alignment considers now also the influence of IR photons on the grain alignment.
- Fixed a wrong mixing of dust components to a dust mixture if the components have different size distributions (limits and shape) and bulk densities.

Version 4.01 \Rightarrow 4.02

- Cylindrical and spherical grids need now a value for the distribution of the φ -cells (f_φ) and have generally more options (see Sects. 3.3.2 and 3.3.3). The PolarisTools offer an option to update older grids (see Table 7.2).
- Optical properties for spherical dust grains can now be calculated from files containing the refractive index (see Sect. 3.4.3). Some of the shipped dust catalogs were updated accordingly (change for instance '`'silicate.dat'` \Rightarrow '`'silicate.nk'` in the command files). Even when not shipped anymore, the '`'.dat'` catalogs of the spherical dust grains are still working with POLARIS.
- Stochastic heating can be calculated with CMD_TEMP and CMD_TEMP_RAT simulations by simply defining the stochastic heating grain size limit (see Sect 4.6.2). The grid will contain an effective dust temperature for each grain lower than the stochastic heating size limit. This is only an approximation and will be less accurate than the usage of the radiation field, but will require much less hard drive space.
- Even without a saved radiation field, the scattered light can be considered in raytracing simulations, if any star and/or the dust source is defined (see Sect. 4.6.5). These sources will be used to calculate the radiation field before calculating the raytracing result.
- Added the `<path_grid_cgs>` option to set the conversion factor automatically for input grids in cgs (see Sect. 3.3.6).
- Fixed a unit problem with aligned radii calculation for RATs (affecting CMD_RAT and CMD_TEMP_RAT)
- Fixed several display errors.

9 Changelog

- Updated behavior of the polar RT grid.
- Fixed problems with mixing dust components with different grain size distributions.
- Fixed the emission/extinction of multiple dust/density distributions.
- Fixed adding direct emission of stars on healpix raytracing maps.
- Removed adding star direct emission of stars on slice raytracing maps.
- Fixed shift of raytracing detector to allow negative values.
- Updated hints for critical behavior.
- The scattering matrix elements S_{11} and S_{22} are saved as a gnuplot file in addition to the other dust plots (if the scattering matrix is available).

Version 4.00 ⇒ 4.01

- Improved SED calculation for polar raytracing grid.
- Fixed a bug that not correctly mixed multiple density distributions.
- Improved the stability of the Raytracer.

Index

<adj_tgas>, 43
<align>, 44
<axis1>, 37
<axis2>, 37
<common>, 7
<conv_dens>, 7, 18
<conv_len>, 18
<conv_mag>, 18
<conv_vel>, 18
<delta0>, 45
<detector_dust nr_pixel = ">, 38, 39
<detector_dust_healpix nr_sides = ">, 39, 40
<detector_dust_mc nr_bins = ">, 54
<detector_dust_mc nr_pixel = ">, 38
<detector_line nr_pixel = ">, 39
<detector_line_healpix nr_sides = ">, 40
<dust_component>, 7, 50
<dust_offset>, 42, 43
<enfsca>, 7, 36, 53
<f_c>, 44, 51
<f_highJ>, 47, 51
<gas_species vel_channels = "">, 55
<alarm_f>, 46
<mass_fraction>, 7, 18
<max_lines>, 7
<max_subpixel_lvl>, 36
<mu>, 18, 46
<nr_gnu_points>, 7
<nr_gnu_vectors>, 7
<nr_threads>, 7
<path_grid>, 7
<path_out>, 7
<phase_function>, 40, 53
<plot_out_midplanes>, 7
<source_background nr_photons = "">, 34
<source_dust nr_photons = "">, 35
<source_dust nr_photons = "">, 34
<source_isrf nr_photons = "">, 7, 34
<source_star nr_photons = "">, 7, 33
<source_starfield nr_photons = "">, 33
<task>, 7
<write_out_midplanes>, 7

abundance, 11
albedo, 31, 32
ALIG_GOLD, 45, 47

ALIG_IDG, 45, 47
ALIG_INTERNAL, 45, 47, 51
ALIG_RAT, 46, 47
alignment, angle, 42
alignment, anisotropy factor, energy density, 46, 47
alignment, anisotropy factor, gas stream, 46
alignment, correlation factor, 44
alignment, Gold, magneto mechanical, 45
alignment, Imperfect Davis – Greenstein (IDG), 45
alignment, imperfect internal, 45
alignment, Larmor limit, 46
alignment, Mach limit, 46
alignment, omega ratio, 46
alignment, Radiative torque (RAT), 46
alignment, Rayleigh reduction factor, 44
alignment, theories, 42
AMIRA, 75
anisotropic scattering, 41
argument, 7
attractor point, 47

Bohr magneton, 58
Boltzmann distribution, 45, 55

CMD_DUST_EMISSION, 50
CMD_DUST_SCATTERING, 53
CMD_RAT, 47
CMD_TEMP, 7
collision rate, 53
column density, 30
command file, 7
command file,old commands, new commands, changed commands, 9
comments, 7
common, 7
correlation factor, 44
cross sections matrix, 48
cylindrical grid, 14

Davis - Greenstein, 45
Davis - Greenstein effect, 45
DDSCAT, 18
degeneracy, 56
degree of circular polarization, 29

Index

degree of linear polarization, 29
detector, 38
detector, plane, 38
detector, spherical, 38
Doppler broadening, 60
dust grain alignment radius, 11, 46, 47
dust mass density, 11
dust number density, 11
dust temperature, 11, 41
dust, alignment theories, 42
dust, cross section file, 18
dust, description string, 19
dust, minimal grain radius, 11
dust, parameters file, 18
dust, radius, 19
dust, refractive index file, 20
dust, scattering matrix file, 19
dust, size exponent, 11

Einstein coefficient, 53
energy density, 46, 47
energy level, 53
enforced first scattering, 36

Fadeeva, function, 60
Fadeeva, package, 60
full escape probability (FEP), 56

gas mass density, 11
gas number density, 11
gas species, abundance, 11, 56
gas species, database, 21
gas species, excitation, 53
gas species, name, 22
gas species, number density, 11
gas species, parameters file, 21
gas species, polarization rotation matrices, 59
gas species, radius, 22
gas temperature, 11, 41
gas velocity, 11
gas, kinetic temperature, 55
Gaussian elimination, 55
Gnuplot, 71
gnuplot, 7
Gold, 45
grain alignment theories, 42
grid header, 9
grid physical parameters ID, 11
grid type ID, 10
grid types, 9
grid, cylindrical, 14
grid, octree, 15
grid, output, 65
grid, rotation, 37
grid, spherical, 10

grid, voronoi, 17
grid_rat.dat, 48

HEALPIX, 39
Heisenberg's uncertainty principle, 60
Henyey-Greenstein, 19, 41

input files, 7
interstellar radiation field (ISRF), 7, 34
isotropic scattering, 40
ISRF, 34

LAMDA, 21
Landè factor, 22, 60
large velocity gradient (LVG), 56
Larmor limit, 46
level populations, 55
line of sight magnetic field strength, 60
line radiative transfer, 21, 53
line strength, 59
Linux, 65
Local thermodynamic equilibrium (LTE), 31, 42
local thermodynamic equilibrium (LTE), 55

Mach number, 46
magnetic field, 11
magnetic quantum number, 56
magneto-optical effects, 59
maximal dust grain radius, 11
Mie scattering, 41
MIEX, 18
minimal dust grain radius, 11
modified black body spectrum, 32
Müller matrix, 19, 50

noise, 32
noise estimation, 32

octree grid, 15
optical depth, 30, 31, 36, 56
optical depth, statistical function, 31
optimization techniques, 35
optimization, enforced first scattering, 36
optimization, peel-off technique, 36
optimization, wavelength range selection, 37

peel-off technique, 36
PH_HG, 41
PH_ISO, 41
PH_MIE, 41, 53
phase function, Henyey-Greenstein (HG), 19, 41
phase functions, 40
photon emitting sources, 33
photon package, 29
photon, MC transfer, 31
photon, propagation, 29

plane detector, 38
 polarization by non-spherical dust grains, 48
 polarization, scattering, 50
 POP_FEP, 60
 POP_LTE, 56
 POP_LVG, 56
 position angle, 29
 pressure broadening, 60
 quantum numbers, 58
 radiation field, 11
 radiative pressure, 11
 ray-tracing, 32
 Rayleigh reduction factor, combination of, 47
 Rayleigh reduction factor, combined, 47
 Rayleigh reduction factor, definition, 44
 rotation, axis, 34, 37, 38
 rotation, grid, 37
 Runge-Kutta Fehlberg, 30
 scattering matrix, 19, 50
 scattering, anisotropic, 41
 scattering, Henyey-Greenstein, 41
 scattering, isotropic, 40
 scattering, Mie, 41
 scattering, phase function, 53
 scattering, relevance of, 32
 scattering, rotation, 53
 shape parameter, 10
 size exponent, 11
 skip cell in RT, 10
 source, dust, 34
 source, ISRF, 34
 source, star, 33
 source, starfield, 33
 sources, 33
 spectral energy distribution (SED), 7, 33, 37
 spherical detector, 38
 spherical grid, 10
 star, 33
 starfield, 33
 Stokes I, 29
 Stokes Q, 29
 Stokes U, 29
 Stokes V, 29
 Stokes vector, 29
 sub-level, 58
 sub-pixel level, 35
 sub-pixeling, 35
 synchrotron, 60
 task, 7
 temperature, dust, 11
 temperature, gas, 11
 temperature, sampling function, 32, 42
 temperatures, range, 41
 transition, 58
 turbulent velocity, 11
 typedefs.h, 31
 unit, cgs, 9, 18
 unit, conversion, 18
 unit, SI, 9, 18, 65
 velocity bins, 39
 velocity gradient, 56
 velocity range, 39
 velocity, gas, 11
 velocity, maximal observable, 39
 voronoi grid, 17
 wavelength range selection, 37
 Windows, 65
 Zeeman, parameters file, 22

Bibliography

- Bjorkman, J. E. & Wood, K. 2001, *The Astrophysical Journal*, 554, 615
- Bohren, C. F. & Huffman, D. R. 1983, *Absorption and scattering of light by small particles*
- Brauer, R., Wolf, S., & Flock, M. 2017a, *Astronomy and Astrophysics*, 607, A104
- Brauer, R., Wolf, S., & Reissl, S. 2016, *Astronomy & Astrophysics*, 588, A129
- Brauer, R., Wolf, S., Reissl, S., & Ober, F. 2017b, *Astronomy & Astrophysics*, 601, A90
- Camps, P., Misselt, K., Bianchi, S., et al. 2015, *Astronomy & Astrophysics*, 580, A87
- Cashwell, E. D. 1957, *A practical manual on the Monte Carlo method for random walk problems / (Los Alamos, N.M. :)*
- Davis, Jr., L. & Greenstein, J. L. 1951, *The Astrophysical Journal*, 114, 206
- Dexter, J. 2016, *Monthly Notices of the Royal Astronomical Society*, 462, 115
- Draine, B. T. & Flatau, P. J. 2013, ArXiv e-prints, 1305, arXiv:1305.6497
- Draine, B. T. & Weingartner, J. C. 1996, *\apj*, 470, 551, arXiv: astro-ph/9605046
- Draine, B. T. & Weingartner, J. C. 1997, *The Astrophysical Journal*, 480, 633
- Evans, II, N. J., Rawlings, J. M. C., Shirley, Y. L., & Mundy, L. G. 2001, *The Astrophysical Journal*, 557, 193
- Gold, T. 1952, *Monthly Notices of the Royal Astronomical Society*, 112, 215
- Gordon, K. D., Misselt, K. A., Witt, A. N., & Clayton, G. C. 2001, *The Astrophysical Journal*, 551, 269
- Habing, H. J. 1968, *Bulletin of the Astronomical Institutes of the Netherlands*, 19, 421
- Hayashi, C. 1981, *Progress of Theoretical Physics Supplement*, 70, 35
- Hoang, T., Nguyen-Quynh, L., Nguyen-Anh, V., & Kim, Y.-J. 2018, ArXiv e-prints
- Jones, A. P., Fanciullo, L., Koehler, M., et al. 2014, published; *A&A* 558, A62 (2013), 558, A62, arXiv: 1411.6293v1
- Jones, A. P., Koehler, M., Ysard, N., Bocchio, M., & Verstraete, L. 2017, *A&A* 602, A46 (2017), 602, A46, arXiv: 1703.00775v1
- Larsson, R., Buehler, S. A., Eriksson, P., & Mendrok, J. 2014, *Journal of Quantitative Spectroscopy and Radiative Transfer*, 133, 445
- Lazarian, A. 1995, *The Astrophysical Journal*, 451, 660
- Lazarian, A. & Efroimsky, M. 1996, *The Astrophysical Journal*, 466, 274
- Lazarian, A., Efroimsky, M., & Ozik, J. 1996, *The Astrophysical Journal*, 472, 240
- Lazarian, A. & Hoang, T. 2007, *Monthly Notices of the Royal Astronomical Society*, 378, 910
- Lazarian, A. & Roberge, W. G. 1997, *The Astrophysical Journal*, 484, 230
- Lucy, L. B. 1999, *Astronomy and Astrophysics*, 344, 282

Bibliography

- Mathis, J. S., Mezger, P. G., & Panagia, N. 1983, *Astronomy and Astrophysics*, 128, 212
- Mathis, J. S., Rumpl, W., & Nordsieck, K. H. 1977, *The Astrophysical Journal*, 217, 425
- Ober, F., Wolf, S., Uribe, A. L., & Klahr, H. H. 2015, *Astronomy & Astrophysics*, 579, A105
- Pandya, A., Zhang, Z., Chandra, M., & Gammie, C. F. 2016, *The Astrophysical Journal*, 822, 34
- Reissl, S., Seifried, D., Wolf, S., Banerjee, R., & Klessen, R. S. 2017, *Astronomy & Astrophysics*, 603, A71
- Reissl, S., Stutz, A. M., Brauer, R., et al. 2018, *Monthly Notices of the Royal Astronomical Society*, 481, 2507
- Reissl, S., Wolf, S., & Brauer, R. 2016, *Astronomy and Astrophysics*, 593, A87, arXiv: 1604.05305
- Reissl, S., Wolf, S., & Seifried, D. 2014, *Astronomy and Astrophysics*, 566, A65
- Shakura, N. I. & Sunyaev, R. A. 1973, *Astronomy & Astrophysics*, 24
- Spitzer, L. & McGlynn, T. A. 1979, *The Astrophysical Journal*, 231, 417
- Weingartner, J. C. & Draine, B. T. 2001, *The Astrophysical Journal*, 548, 296
- Weingartner, J. C. & Draine, B. T. 2003, *The Astrophysical Journal*, 589, 289
- Wolf, S. 2003, *Computer Physics Communications*, 150, 99
- Wolf, S. 2006, *Astrophysics Software Database*, 6
- Wolf, S., Henning, T., & Stecklum, B. 1999, *Astronomy and Astrophysics*, 349, 839
- Wolf, S. & Voshchinnikov, N. V. 2004, *Computer Physics Communications*, 162, 113
- Yusef-Zadeh, F., Morris, M., & White, R. L. 1984, *The Astrophysical Journal*, 278, 186
- Zhu, Z. & Stone, J. M. 2014, *The Astrophysical Journal*, 795, 53